Technical Report No. 19

DROUGHT ANALYSIS FOR THE UPPER-METUJE AND UPPER-SÁZAVA CATCHMENTS (CZECH REPUBLIC) USING THE HYDROLOGICAL MODEL HBV

Author names: Oldřich Rakovec, Anne F. van Loon, Stanislav Horáček, Ladislav Kašpárek, Henny A.J. van Lanen & Oldřich Novický

Date: 16 September 2009


WATCH is an Integrated Project Funded by the European Commission under the Sixth Framework Programme, Global Change and Ecosystems Thematic Priority Area (contract number: 036946). The WATCH project started 01/02/2007 and will continue for 4 years.

Title:	Drought analysis for the Upper-Metuje and Upper-Sázava catchments (Czech Republic) using the hydrological model HBV
Authors:	Oldřich Rakovec, Anne F. van Loon, Stanislav Horáček, Ladislav Kašpárek, Henny A.J. van Lanen & Oldřich Novický
Organisations:	Wageningen University, Wageningen, the Netherlands T.G. Masaryk Water Research Institute, Prague, Czech Republic.
Submission date:	16 September 2009
Function:	This report is an output from Work Block 4 Extremes: frequency, severity and scale, and will contribute to Task 4.1.1 Investigate processes controlling the propagation of drought, Task 4.1.2 Spatial and temporal scales and severity of droughts in 20 century, and Task 4.3.1 Frequency, severity and extent of droughts in 21 century.
Deliverable:	The report contributes to WATCH deliverable D.4.1.4 Report on the increased understanding of the propagation of drought in different hydro-climatological regions, physical catchment structures and different scales.

Preface

This study is based on the research done by Oldřich Rakovec for his MSc thesis Hydrology and Quantitative Water Management (HWM-80436) at the Wageningen University, the Netherlands, and for his Internship (HWM-70424) that has been done at the T.G. Masaryk Water Research Institute, Prague, Czech Republic. Both are obligations to obtain a MSc degree of Hydrology and Water Quality at the Wageningen University. He received input from his supervisors Anne F. van Loon, Stanislav Horáček, Ladislav Kašpárek, Henny A.J. van Lanen & Oldřich Novický. In the context of his Internship and MSc research, the first author spent several months at the T.G. Masaryk Water Research Institute in Prague. This stay was partially supported by the EU-FP6 project WATCH (WATer and global Change). The first author was invited to give an oral presentation on the UNESCO-FRIEND workshop on Low Flows and Drought in Bratislava, November 2008. The authors visited the Upper-Metuje and Upper-Sázava catchments in 2008 and 2009 to discuss preliminary outcome from the different hydrological models that are being developed and applied to study hydrological drought in the Upper-Nitra (WATCH test basin). The field trips and associated workshop was supported by the WATCH project.

Dr. Henny A.J. van Lanen, Wageningen, September 2009.

Legend for the pictures on the title page.

The Metuje River, river gauge MXII, 10 December 2008	Bučnice meteorological station Upper Metuje catchment 11 December 2008
The Sázava River, river gauge 1550, 12 January 2009	The Sázava River, river gauge 1550, 3 April 2009

Abstract

This study deals with the hydrological drought identification and the analysis of drought propagation through the hydrological system within two Czech catchments with contrasting hydrogeological conditions, the Upper Metuje and Upper Sázava. The conceptual hydrological model HBV was calibrated against observed streamflow. The advantage of HBV is that it simulates all variables that are needed for the investigation of hydrological drought, i.e. soil moisture storage, groundwater storage, and river discharge. The model performance was validated on an independent period using observed streamflow, groundwater heads and snow observations. Results were more satisfying for the Upper Metuje, as low flows in Upper Sázava are affected by anthropogenic influences. Drought is considered to be a below average water availability, which was defined using a smoothed monthly threshold. The drought signal in the Upper Metuje showed lag and attenuation when propagating through the hydrological system. Soil moisture drought still appears simultaneously with meteorological drought, but groundwater and streamflow droughts have developed after extensive soil moisture deficits. The analysis showed that high precipitation deficits do not always lead to severe hydrological droughts. It depends on the timing. Late summer is usually the most sensitive to lack of precipitation. The number of pronounced streamflow droughts within the Upper Metuje is larger in winter, but summer droughts have longer duration. Since no pooling of minor droughts was applied, droughts are often mutually dependent and, clearly, within a cluster of dependent droughts the drought intensity increases with duration. A similar drought analysis was performed for the Upper Sázava, but since the HBV results, in particular the low streamflow have a limited reliability, no conclusions regarding drought propagation were drawn. Therefore the comparison of drought propagation in the Upper Metuje and Upper Sázava catchments reflecting different hydrogeological conditions was not possible.

Keywords: Drought identification, drought propagation, HBV model, monthly threshold, Upper Metuje, Upper Sázava.

Acknowledgments

We thank Jan Seibert (Department of Geography, University of Zurich, Switzerland) for providing HBV light, including the automatic calibration module.

We also appreciate the support of Pavel Treml, Adam Vizina, Pavel Eckhardt, Jan Kašpárek, Anna Hrabánková and Jiří Dlabal, our colleagues from the Water Research Institute in Prague.

Our research was done in the context of the EU-funded Integrated Project WATCH (WATer and global CHange). We appreciate the financial support we got from this project to visit partner organisations in Prague and Bratislava.

Authors

September 2009

Contents

Abbreviations and symbols

Abbreviations

AET	Actual EvapoTranspiration
ArcGIS	Geographic Information System software product
BILAN	Water balance model developed by the T.G.Masaryk WRI in Prague
CHMI	Czech HydroMeteorological Institute
CORINE	European Commission programme to COoRdinate INformation on the Environment
DEM	Digital Elevation Model
EU	European Union
EZ	Elevation Zone
FAO	Food and Agriculture Organisation
HBV	Rainfall-runoff model Hydrologiska Byrans Vattenbalansavdelning
lnReff	Nash-Sutcliffe model efficiency using logarithmic discharges
LZ	Land cover Zone
PET	Potential EvapoTranspiration
PLA	Protected Landscape Area
P-M	Penman-Monteith method
R	Statistical software
Reff	Nash-Sutcliffe model efficiency
S-JTSK	Souřadný Systém Jednotné Trigonometrické Sítě Katastrální (Czech geodetic system)
VE	Volume Error
WATCH	WATer and global CHange

WGS 84	World Geodetic System 1984
WHO	World Health Organisation
WMO	World Meteorological Organisation
WRI	T. G. Masaryk Water Research Institute in Prague
WUR	Wageningen University and Research

Symbols

H	Groundwater Height [m a.m.s.l.]
m a.m.s.l	Meters above mean sea level [m]
P	Precipitation [mm.day^{-1}]
Q	Discharge [mm.day^{-1}]
T	Temperature [°C]

Chapter 1

Introduction

General

Water is a vital substance for human beings but it has two sides because water is a good servant but can be a bad master as well. The challenge is to have the right amount of it. If people have excess of water they are endangered, but if there is a lack of water they are threatened too. Both floods and droughts are very serious natural hazards, and are very important to be studied and understood to prevent harm to people.

In comparison with floods, droughts are often overlooked, since floods are more spectacular: more people suffer in shorter time. But the number of victims of droughts is higher than for floods. WHO (2008) reported that droughts accounted for half of the victims of natural disasters in total. Water shortage can also inflame social conflicts, including wars. In this research project we will describe and investigate droughts in Central Europe, where droughts are not as life threatening as in e.g. African arid regions, but regularly cause high losses. For example, Van Lanen and Tallaksen (2008) reported that the long term annual damage caused by drought in Europe is about three billion Euro and it is still increasing over last years. Further the authors mentioned that 15% of the EU total area and 17% of the EU total population experienced the impact of droughts over the period 2000--2006.

Drought is a natural phenomenon, which is caused by a meteorological anomaly and modified by the physical properties of a catchment. Drought can be defined (Tallaksen and Van Lanen, 2004) as *a sustained and regional extensive occurrence of below average natural water availability.* Deviations from normal conditions can be expressed in terms of a *meteorological drought* (deficit in precipitation) and a *hydrological drought* (deficit in soil moisture, groundwater and streamflow). The frequency, duration, severity and spatial extend are key aspects of droughts.

This study deals with the hydrological drought identification in two Czech river catchments

(Upper Metuje and Upper Sázava) and it contributes to the research, which is joint effort of the Wageningen University (WUR) in the Netherlands and T. G. Masaryk Water Research Institute (WRI) in Prague. This cooperation is coordinated by the European-funded project WATCH (Water and Global Change)[1], which has as one of the main objectives to advance the knowledge of the impact of global change on hydrological extremes.

Parallel to this study of Czech catchments, which are WATCH test basins (focal areas, Van Lanen et al., 2008) similar studies using the same conceptual model and drought analysis methods are applied to different climatic regions in Europe, i.e. Norway (Upper Glomma), Slovakia (Upper Nitra) and Spain (Upper Guadiana). The aim of this joint research is to study drought characteristics and propagation across Europe and to assess the performance of a simple conceptual hydrological model.

Objectives

The main objective of this report is to understand hydrological drought development under the Central European climate and compare the drought characterization of two geologically different catchments.

The sub-objectives are:

- Modelling of the Upper Metuje and Upper Sázava catchments by developing a hydrological model using HBV.
- Identification of drought in precipitation, soil moisture, groundwater, and streamflow in the Upper Metuje and Upper Sázava catchments.
- Comparing drought propagation in the Upper Metuje and Upper Sázava catchments, which reflect different hydrogeological conditions.

Outline

The second chapter introduces the study area. Chapter 3 continues with methods used in this study, including the calculation of potential evapotranspiration, a description of HBV model and a definition of drought and its characteristics. Results of hydrological modelling using HBV are reported in Chapter 4 and results of drought analysis are described in Chapter 5. Results and their credibility are discussed in Chapter 6. Finally Chapter 7 gives conclusions and recommendations.

[1] www.eu-watch.org

Chapter 2

Study areas

This chapter provides a brief characterisation of the study area. For a more detailed description, readers are reffered to Rakovec (2009).

The Upper Metuje and Upper Sázava catchments (Figures 2.1 and 2.2) are situated in the Czech Republic and have a Central European continental climate. The Upper Metuje catchment is located in the northeast on the border with Poland. The Metuje River joins the Elbe River, which flows into the North Sea. The Upper Metuje is an experimental catchment and is the headwater of the whole Metuje basin. The Upper Metuje has an area of 73.6 km^2 (12% of the whole Metuje basin). The Sázava River is situated in the centre of the Czech Republic. It flows into the Vltava River and finally into the Elbe River. The Upper Sázava catchment represents the headwater of the Sázava basin. It has an area of 131.3 km^2 (3% of the whole Sázava basin).

The reason why these two catchments were chosen is: (1) climatic similarity, and (2) geological differences. The Upper Metuje is a slowly responding catchment to precipitation due to groundwater storage in large aquifers and the Upper Sázava is a fast responding catchment because of impermeable rocks. This difference enables a study of the impact of hydrogeology on selected drought events.

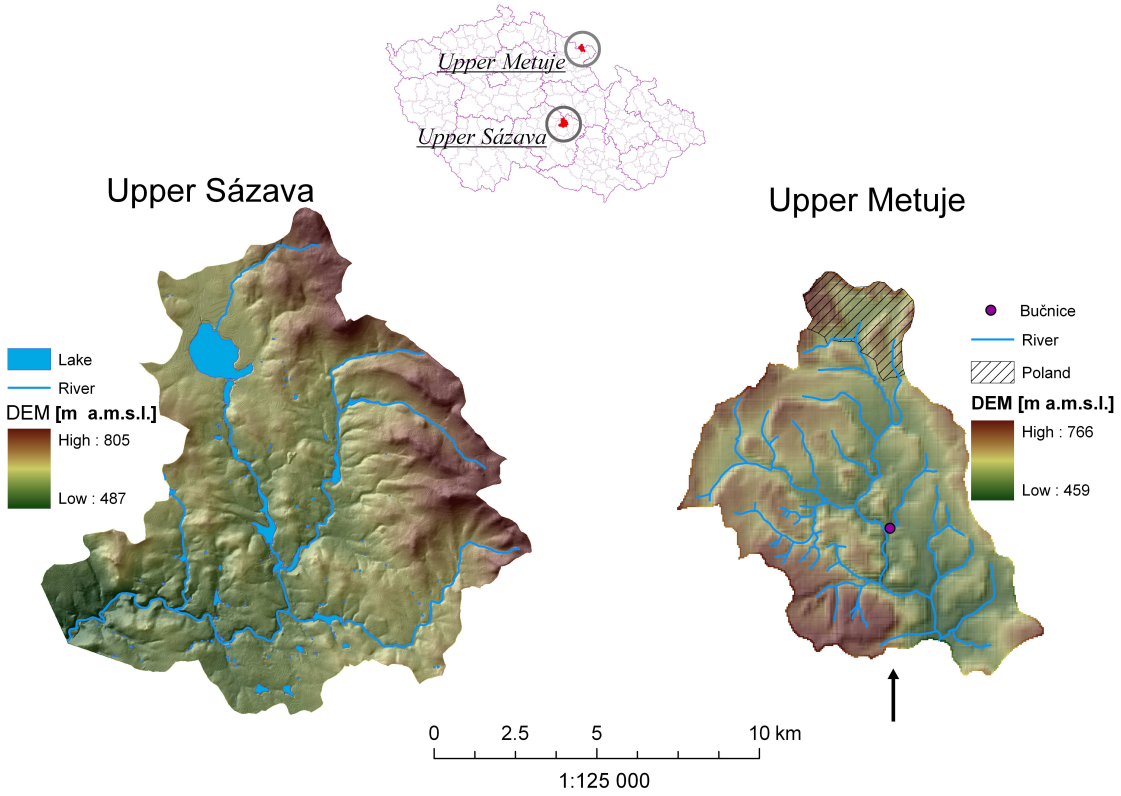

Figure 2.1: Location of the Upper Sázava and Upper Metuje catchments (top) and digital elevation model (bottom).

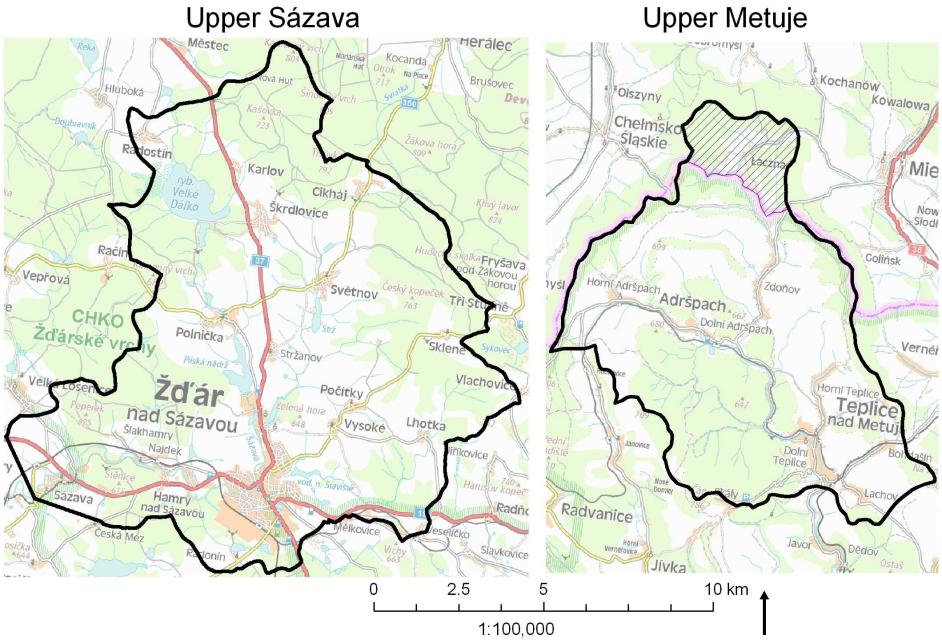

Figure 2.2: Topographical map of the Upper Sázava and Upper Metuje catchments, (derived from CENIA, 2008).

2.1 Upper Metuje catchment

2.1.1 Introdution

The location of Upper Metuje catchment is shown in Figures 2.1 and 2.2. The outlet where the discharge is measured, is named M XII (geographical coordinates, WGS 84: 50°34'46.58"N 16°10'26.09"E, or S-JTSK [1]: x=-612176 m, y=-1004265 m). The total area of the catchment is 73.6 km^2. Approximately 10% of catchment is located in Poland.

The data collection in the study area was initiated by the Water Research Institute in 1963. The main purposes of the observation are: (1) assessment of long term changes in water availability (presently due to global change), (2) investigation of the impact of groundwater abstraction on water resources and natural reserves, and (3) data collection for developing water balance models. To meet these objectives, different kinds of measurements were done: discharge measurements at three automatic gauging stations, three boreholes for groundwater level monitoring and meteorological data collection from the Bučnice station (WRI, 2008).

The Bučnice meteorological station is located at the altitude of 490 m a.m.s.l. and has geographical coordinates: WGS 84: 50°36'37.33"N, 16°8'57.56"E, or S-JTSK: x= -613521.03 m, y = -1000665.35 m (Figure 2.1). In addition to conventionally measured variables of air temperature, precipitation and relative humidity, also wind speed, wind direction and solar radiation have been measured since November 1998, when an automatic meteorological station has been installed. There were also attempts of snow height measurements, but they were stopped because of high errors of the measuring device. The actual weather situation with the history of two days can be checked on-line at CHMI (2009), where the Bučnice meteorological station can be found under the under the name Adršpach.

The Upper Metuje catchment has a mean altitude of 591 m a.m.s.l. and it varies between 459 and 780 m a.m.s.l. (Figure 2.1). The relief is formed by Adršpach-Teplické stěny Upland, which is very heterogeneous. It consists of deeply incised valleys, so called "rocky towns", table mountains and pseudokarst caves. The whole catchment is part of the Protected Landscape Area (PLA) Broumovsko and it is protected because of its unique Cretaceous sandstone relief, fluvial network, rare and protected plant and animal species, and local traditional architecture (Faltysová et al., 2002). The land cover consists predominantly of cropland and grass fields (51%), and forest (46%). The mean observed hydrometeorological variables for the period 1981--2006 are given in Table 2.1.

[1] S-JTSK = Czech projected coordinate system, ArcGIS name: Krovak East North

Table 2.1: Hydrometeorological characteristics of the Upper Metuje catchment (1981--2006).

Variable	Magnitude
Mean annual discharge (MXII)	0.85 m^3s^{-1}, or 365 $mm.year^{-1}$
Mean annual precipitation (Bučnice)	746 $mm.year^{-1}$
Mean annual temperature (Bučnice)	5.8°C

2.1.2 Spatial data

Geology

The Upper Metuje catchment is situated in the Police Basin which is part of the bigger Intra-Sudeten Basin. It is formed by Mesozoic sediments that are underlain by poorly permeable Permian and Carboniferous formations. The Police Basin is a syncline and has a clear NW-SE axis orientation. The schematic geological map and cross section are shown in Figures 2.3 and 2.4. The hydrogeological base of the area consists of formations from the Proterozoic - Lower Paleozoic era. These formations are slightly metamorphic sediments and volcanic rocks. The basin was created and it was filled with continental sediments (arkosian sandstone, conglomerate) and volcanics during the period between Lower Carboniferous and Lower Triassic (Variscan orogeny). Part of the basin became a sea during the Upper Cretaceous and new sediments were deposited, forming the top of the recent Police Basin (Kašpárek et al., 2006). This Upper Cretaceous layer is formed from the bottom by glauconite and clay sandstone (Cenomanian), sandy marlite with fillers of sandstone and siltstone (Cenomanian-Middle Turonian), and thick-bedded sandstone (Coniak) (Rees et al., 2004; Czech Geological Survey, 1995). The Quaternary geology is represented by deluvial sandy-loam and gravel-loam deposits along streams and by deluvial boulder - block sediments in the area around the thick bedded sandstone (Czech Geological Survey, 1995).

Hydrogeology

The Triassic formation (layer 1 in Figure 2.4) and the Cenomanian - Middle Turonian formation (layer 3 in Figure 2.4) are the most important layers because they form the main aquifers of the catchment [2]. The Triassic aquifer is confined. The unconfined Cenomanian - Middle Turonian aquifer lies above it. A regionally extensive layer of low permeable material is present in between. Both aquifers are drained along the Skalský Fault (Figure 2.3, SW-NE

[2]The Coniak formation does not represent an aquifer, because it is formed by eroded sandstone columns, see cross-section in Figure 2.4

direction), which has a very low permeability (Kašpárek et al., 2006).

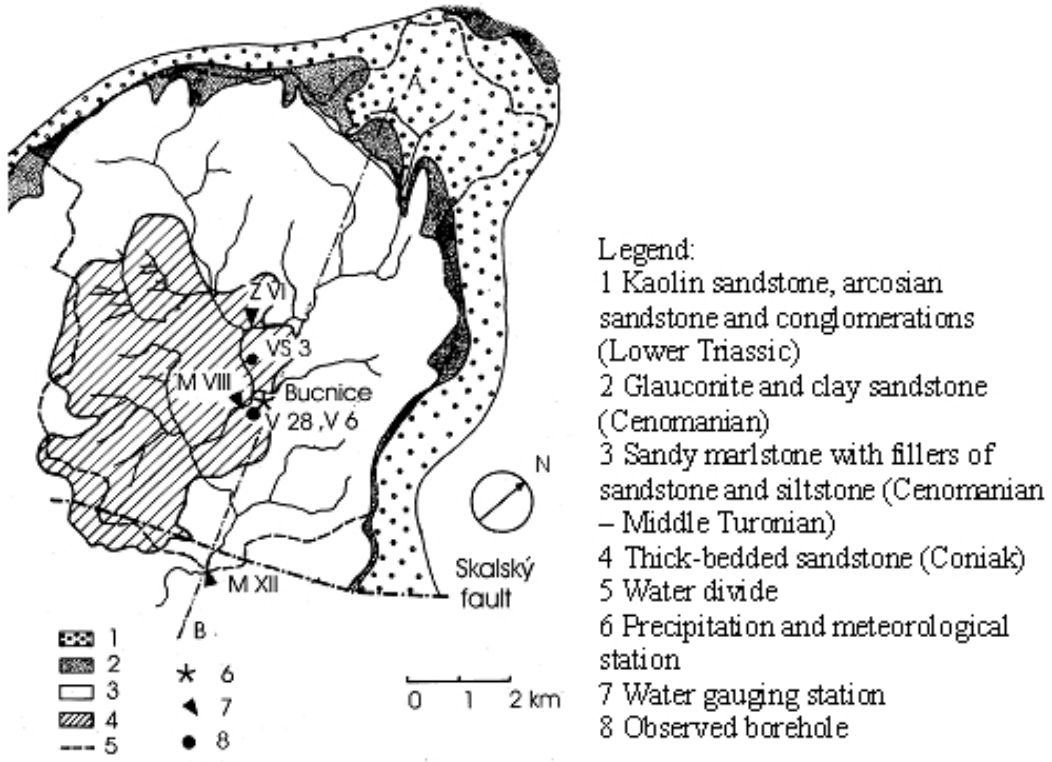

Figure 2.3: Detailed geological map of the Metuje Basin (Rees et al., 2004).

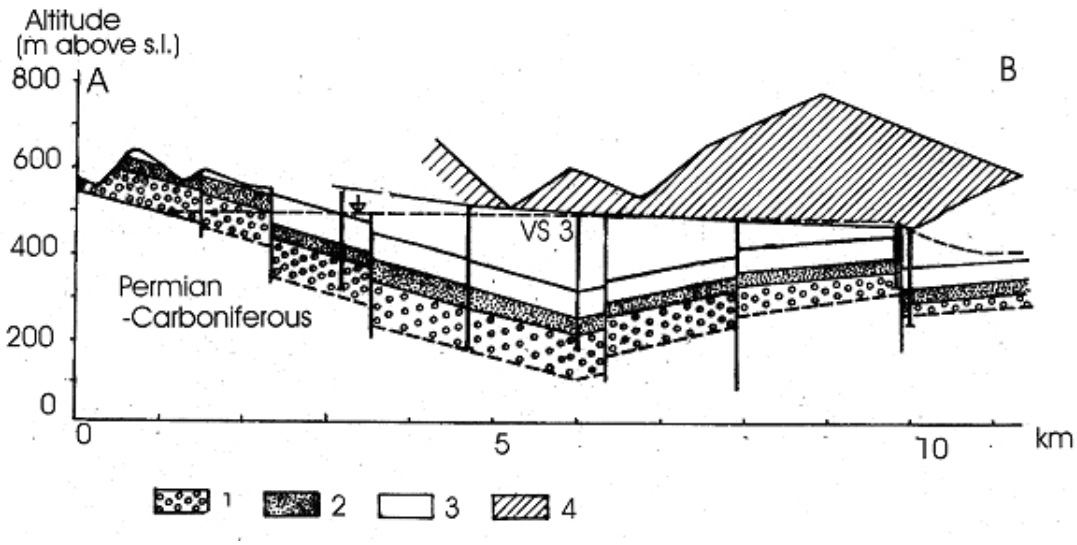

Figure 2.4: Geological cross-section of the Metuje Basin (Van Lanen et al., 2008), legend is identical to that in Figure 2.3.

Land cover

Land cover analysis for the Upper Metuje catchment is based on the CORINE 2000 database. We divided the land cover into 3 zones: agricultural areas (pastures and arable land), forest and semi natural areas (forests, scrub or herbaceous vegetation) and built-up (urban) areas for the use in the semi-distributed version of the HBV model. The proportion of each zone is given in Table A.1 and the land cover map is presented in Figure 2.5. Since we did not have data from the Polish part of the basin, we estimated and digitised the land use for this part from topographical maps (CENIA, 2008).

We also investigated the elevation pattern of our experimental catchment. We used a DEM with a quite low resolution (130 m x 130 m), because we wanted to include also the Polish part of the basin into our analysis, for which only low resolution DEM was available. We distinguished three elevation intervals represented by their mean values: 500 m, 600 m and 700 m (Table A.1 and Figure 2.5).

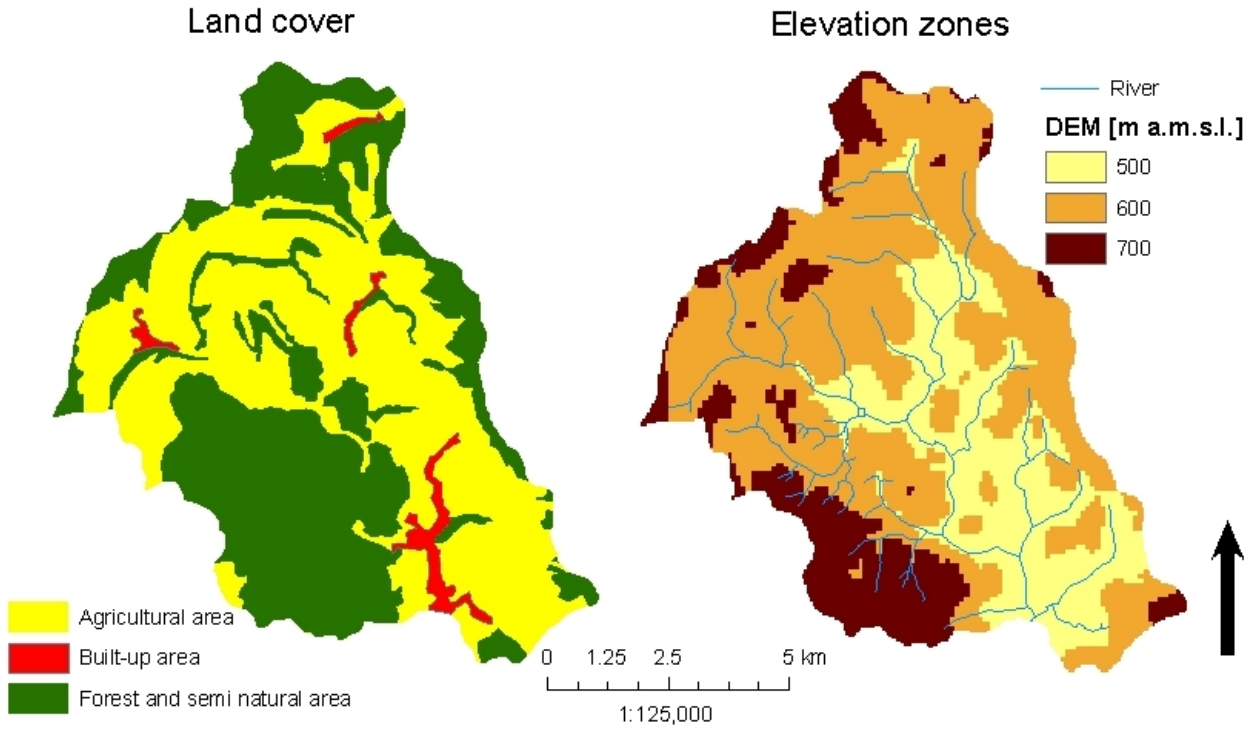

Figure 2.5: The Upper Metuje catchment, land cover zones and elevation zones (indicated by the mean elevation).

2.1.3 Time series data

Temperature

The long-term daily mean temperature measured at the Bučnice meteorological station is 5.8°C (1981--2006) (Table 2.1). The warmest month is July (15.5°C) and the coldest is January (-3.9°C).

Detailed monthly vertical temperature gradients with elevation were not calculated because there was no second temperature time series in the close neighbourhood. We assume that the vertical temperature gradient is 0.65°C/100 m, which corresponds to the wet adiabatic lapse rate (Salvato et al., 2003).

Precipitation

The long-term mean annual precipitation measured at the Bučnice meteorological station is 747 mm (1981--2006) (Table 2.1) with 1999 as the driest year (520 mm) and 1998 as the wettest year (972 mm). The wettest month is July with 93 mm. Surprisingly, the driest month is April with 42 mm. In general low precipitation amounts occur in winter season. The daily precipitation was manually measured till 1998 and afterwards by an automatic heated rain gauge, which ensures snow melting in winter season.

Detailed monthly vertical precipitation gradients with elevation were not calculated because no other precipitation time series close to the Upper Metuje catchment was available. The average vertical precipitation gradient was estimated to be 5%/100 m, which was derived from an old meteorological map (Dratva, 1943).

Groundwater

Groundwater observation wells are located in the centre of the catchment (Figure 2.6). They differ in depth. The wells VS-3 and V-28 are approximately 300 m deep with the base in Triassic sediments, whereas the wells V-6 and well NS are shallow (ca 5 m deep). The seasonal variation of groundwater heads is obvious from Figure 2.7. There is a clear and regular pattern of winter groundwater recharge (peaks) and summer recession (depressions). The time series of the groundwater records are not complete (Figure 2.7). Since V-6 and NS were not far apart and their records were almost identical, observations in NS were stopped in the beginning of 1990s. In this study we will use the well VS-3.

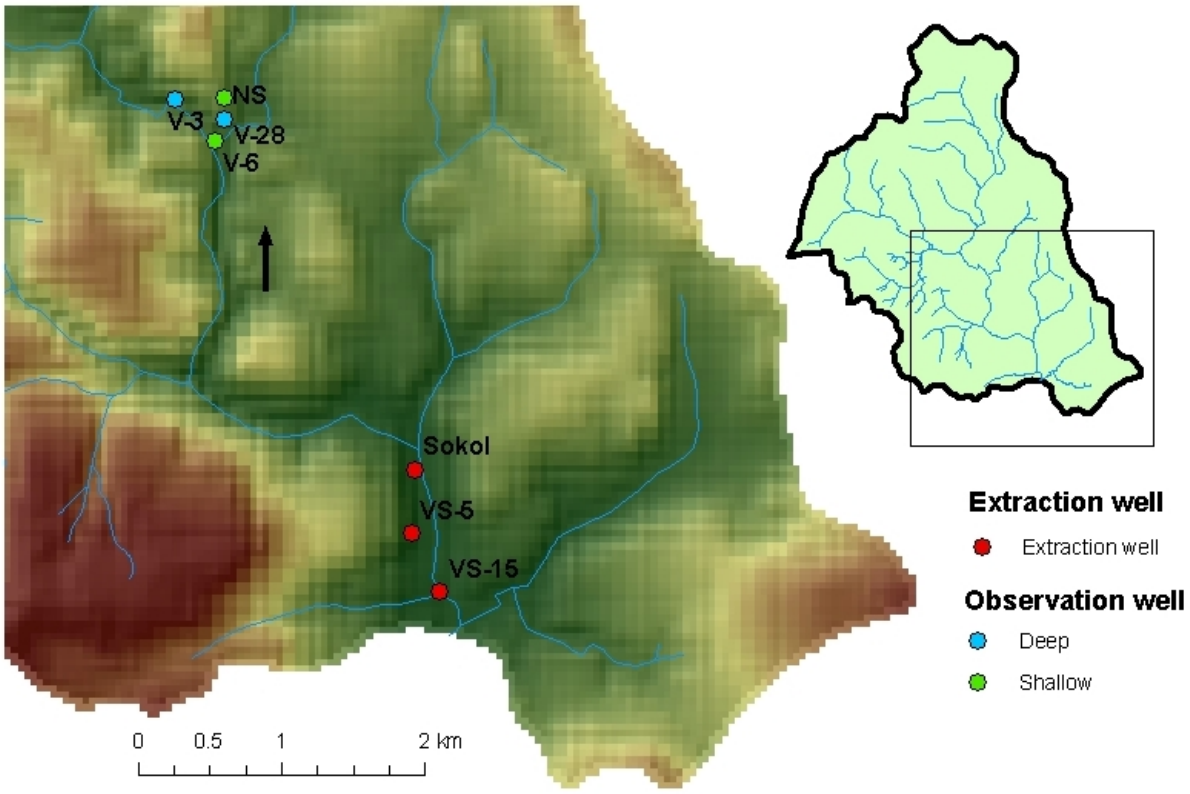

Figure 2.6: Location of groundwater observation and abstraction wells in the Upper Metuje catchment.

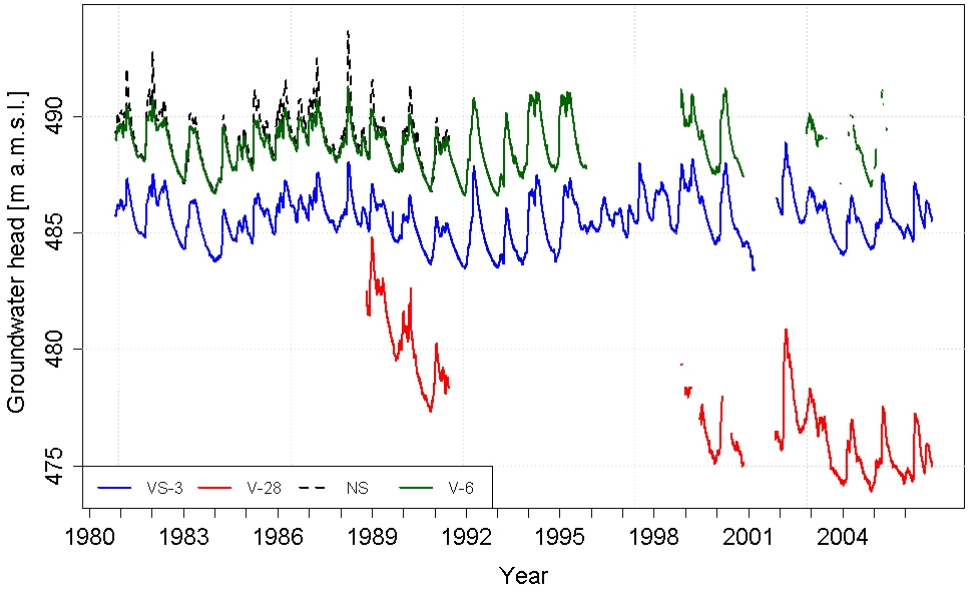

Figure 2.7: Groundwater heads in observation wells: VS-3, V-28, V-6 and NS.

River discharge

The mean annual discharge (1981--2006) for the gauging station MXII (Teplice nad Metují) gauging station is 365 mm or 0.85 $m^3.s^{-1}$. The highest discharges exceeded 21 $m^3.s^{-1}$ and the lowest dropped below 0.23 $m^3.s^{-1}$. Regular peaks caused by snowmelt can be observed in spring and low discharges predominantly in summer. This is also shown in Figure 2.8, where the mean monthly discharge is plotted.

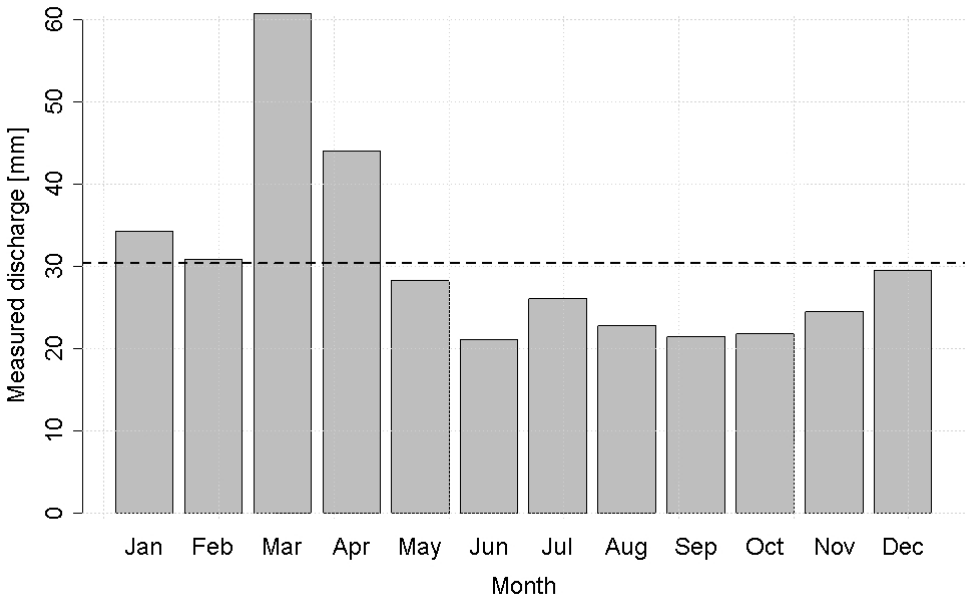

Figure 2.8: Mean monthly discharge for the Upper Metuje.

2.1.4 Human influences

The location of the groundwater extraction wells is also illustrated in Figure 2.6. They are concentrated close to the Skalský Fault (Figure 2.3), which drains large amounts of groundwater from the two aquifers. Monthly average extraction rates for the three biggest wells in Upper Metuje catchment are shown in Figure 2.9 (negative values). The location of the extraction wells and their codes are given in Figure 2.6. We can observe changes in groundwater abstraction since the changes amounts throughout last three decades. After a graduated increase in the 1980s from 20 to 50 $l.s^{-1}$, the extraction rates suddenly doubled in the beginning of the 1990s. Since the mid 1990s there is a slight decrease. Since 2004 the extraction from the Sokol well was substituted by that from VS-5. We must keep in mind that all these values are only available for registered wells, as stated in the Czech Act. No. 254/2001 Sb., i.e. extraction rates which

exceed 6000 $m^3.year^{-1}$ or 500 $m^3.month^{-1}$ must be registered. The real extraction amounts can be higher if not registered wells are included.

In addition to the extractions, there is also water directly recharged into the Metuje River, mainly from a sewage disposal plant in Teplice nad Metují. These rates do not exceed 20 $l.s^{-1}$. Their monthly averages are plotted in Figure 2.9 (positive values).

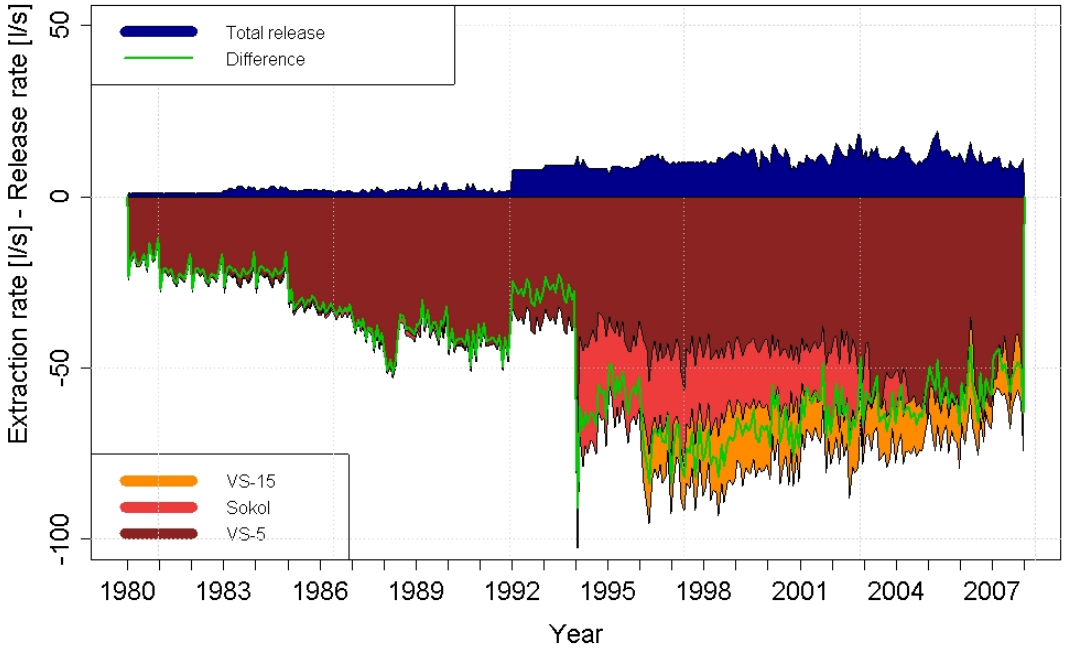

Figure 2.9: Average monthly groundwater extraction rates in the Upper Metuje catchment and average monthly water release rates directly into the Metuje River (WRI, 2009).

2.2 Upper Sázava catchment

2.2.1 Introduction

The location of the Upper Sázava catchment is illustrated in Figures 2.1 and 2.2. Meteorological and hydrological data from the Sázava catchment are collected by the Czech Hydrometeorological Institute (CHMI). Most of the time series are available from 1961 onwards. The catchment altitude varies between 487 and 805 m a.m.s.l., with a mean altitude of 628 m a.m.s.l. The river basin is located in the north-eastern part of the Českomoravská vrchovina (uplands) and it forms part of the Protected Landscape Area Žďárské vrchy which is a hilly region of gentle slopes and flat wide valleys. The land cover is dominated by cropland and forest. The mean values of the most important hydrometeorological variables for the Upper Sázava catchment are listed in Table 2.2. The streamflow gauging station is situated under the old bridge in the Sázava municipality with the code 1550 (geographical coordinates, WGS 84: 49°33'18.4"N, 15°50'57.1"E, or S-JTSK: x= -648531 m, y= -1114808 m).

Table 2.2: Hydrometeorological characteristics of the Upper Sázava catchment (1961--2006).

Variable	Magnitude
Mean annual discharge (1550)	1.25 m^3s^{-1}, or 303 $mm.year^{-1}$
Mean annual precipitation (Přibyslav)	679 $mm.year^{-1}$
Mean annual precipitation (Svratouch)	778 $mm.year^{-1}$
Mean annual temperature (Přibyslav)	6.9°C

2.2.2 Spatial data

Geology

The bedrock of Upper Sázava catchment consists predominantly of Proterozoic impermeable metamorphic rocks, which consists of black mica migmatite, gneiss and mica schist (see schematic geological structure shown in Figure 2.10). Furthermore, a ridge of granite is located in the south and a small area of diorite and gabbro occurs in the west of the catchment. In the north-western part we can also find Mesozoic sedimentary rocks of the Cretaceous period, consisting of siltstone and clay sandstone (Lower - Middle Turonian) overlying by quartzy sand, sandstone, claystone and conglomerate (Cenomanian). This interesting geological unit is called "Křída Dlouhé meze"

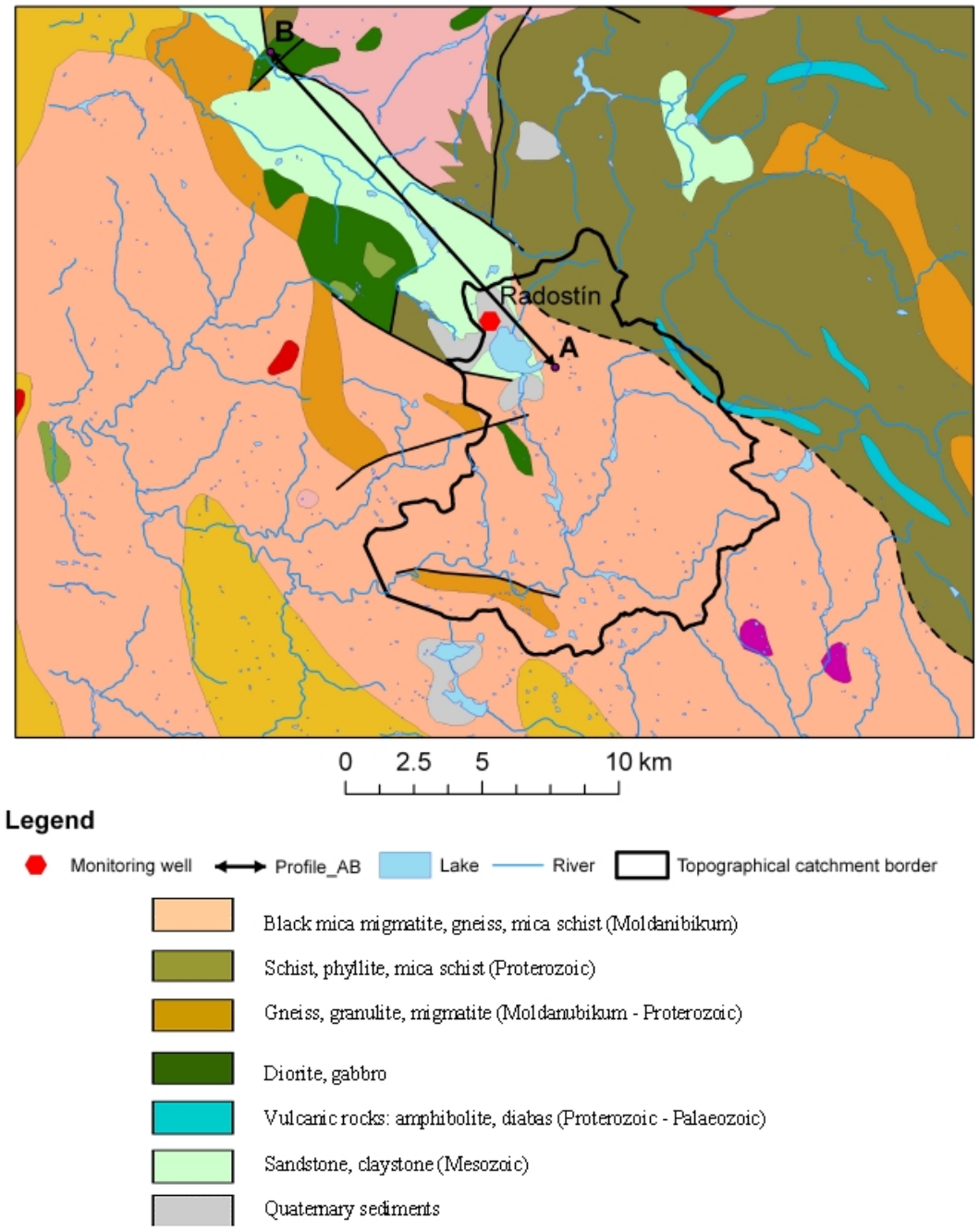

Figure 2.10: Detailed geological map of the Upper Sázava basin (CENIA, 2008) and location of the groundwater well Radostín.

which can freely be translated as "Cretaceous of Long Hedge". It is a narrow extension in north-western direction of the large Cretaceous Basin of the Bohemian Massif. The profile AB (see Figure 2.10 for location) illustrates the position of the geological layers (Figure 2.11). The Quaternary geology consists of peat which can be found in surroundings of the fish pond Velké Dářko (Figure 2.2). Fluvial deposits occur along rivers and streams, and other shallow Quaternary sediments lie on top of the bedrock. Their thickness does not exceed 6 m (Eckhardt, 1995).

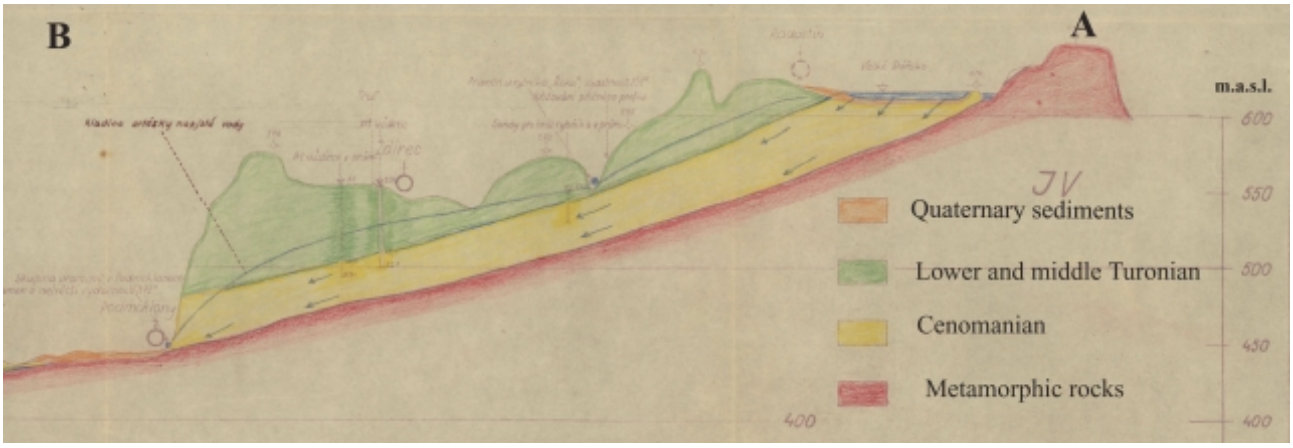

Figure 2.11: Cross-section of the Křída Dlouhé meze (Wallenfelsová, 1955).

Hydrogeology

The geological properties described in the previous subsection imply that there is no extensive groundwater storage in the Upper Sázava catchment in comparison with the Upper Metuje (Section 2.1.2). Nevertheless, two different kinds of aquifers and aquitards can be found in the Upper Sázava (Eckhardt, 1995). First, a shallow porous aquifer in Quaternary sediments. Second, a deeper aquitard in fractured bedrock caused by tectonics.

The water balance of Křída Dlouhé meze is also relevant. The groundwater and topographical divides do not coincide, they differ approximately by 5%. Potentially, some water can infiltrate from the fish pond Velké Dářko into the Cretaceous sediments and flow out of the topographic catchment in north-western direction because of the inclination of the geological layers. The potential flow direction is sketched with blue arrows in Figure 2.11.

Since the Velké Dářko is a very old reservoir, the exact hydraulic conductivity is difficult to derive from the geology. The reservoir was created in 15^{th} century and the bottom should have been sealed and very likely is not leaky (Kašpárek, 2009; Eckhardt, 2009). The field measurements (Section 2.2.3) do not confirm any significant losses of water. So, we assume that the water losses through the Křída Dlouhé meze are not significant.

Land cover

Land cover is derived, as in the Upper Metuje catchment from the Corine 2000 database (Figure 2.12). Agriculture areas cover half of the catchment followed by forest (42%). Built--up area cover 6%. Percentages of each elevation zone are listed in Table A.2. For hydrological modelling, water bodies like the Velké Dářko and the Pilská nádrž are important although they represent only 2% of the total area. For example, the Velké Dářko with an area of 205 ha has maximum water storage of 3.56 $10^6 m^3$ (Cech et al., 2002), which is dynamic and changes during the year according to the needs of fish pond management.

the assessment of the elevation zones was done with a higher resolution DEM (10 m x 10 m) than in the Upper Metuje catchment. We distinguished three elevation zones with representative mean values of 550 m, 650 m and 750 m (Figure 2.12), Table A.2).

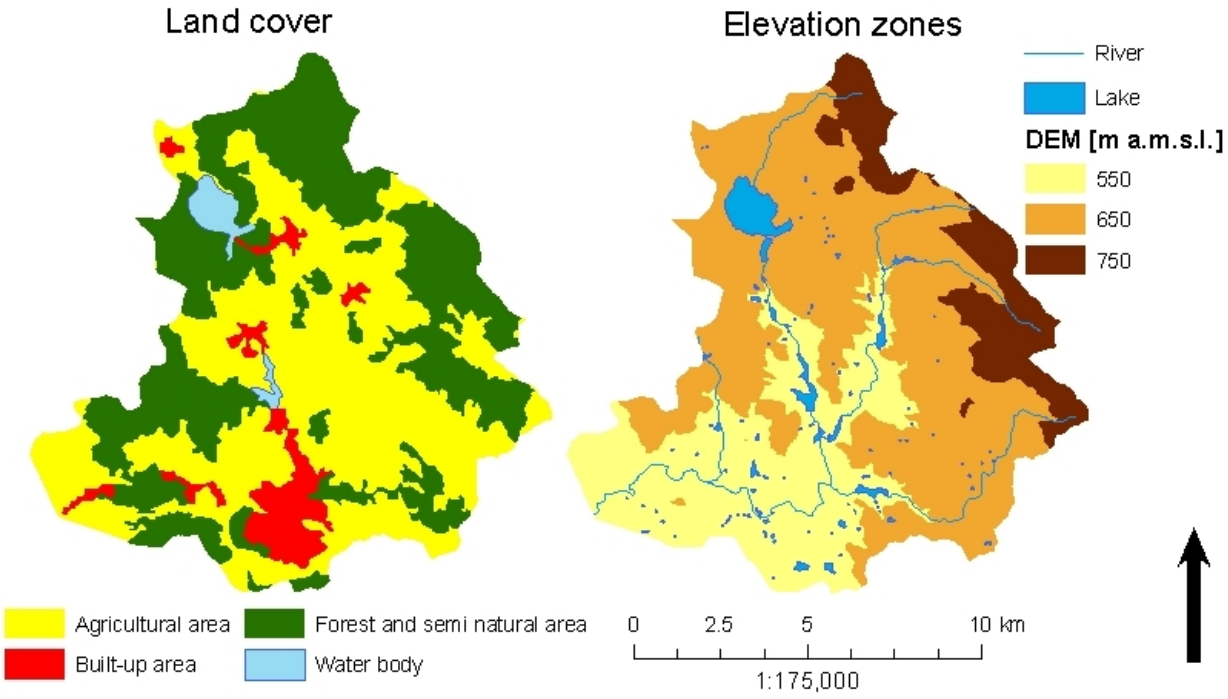

Figure 2.12: The Upper Sázava catchment, land cover zones and elevation zones.

2.2.3 Time series data

Location of stations

In comparison with the Upper Metuje there are meteorological data available from more stations in and around the Upper Sázava catchment which can be used for the hydrological modelling. Daily data of temperature, air humidity and precipitation are available from the

Přibyslav meteorological station. Furthermore, precipitation is recorded in Krucemburk, Žďár nad Sázavou - Stržanov (incl. snow height records), Křižánky and Kadov. Some weather data (minimum and maximum temperature, wind speed and solar radiation) are available from the Svratouch meteorological station. Although the Vatín meteorological station is located not far from the catchment border, we did not make an effort to obtain these data because of the short observation period, which started in the beginning of the 1990s. The location of the selected stations is shown in Figure 2.13.

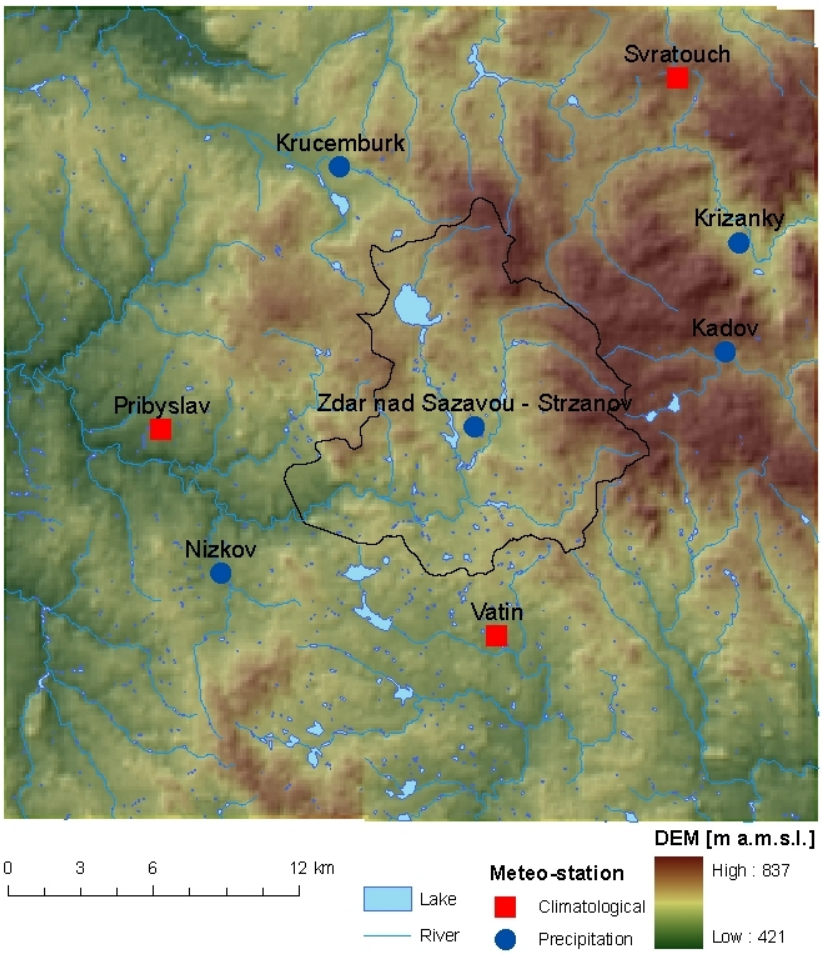

Figure 2.13: Location of climatological and precipitation stations in surroundings of the Upper Sázava catchment.

Temperature

The temperature records are available for two stations, i.e. daily temperature from Přibyslav (1961--2006) and daily minimum and maximum temperature from Svratouch (1984--2006). The long term mean daily temperature for the Přibyslav station is 6.9°C (Table 2.2). The warmest

month is July (16.4°C) and the coldest is January (-3.1°C). Similar as in the Upper Metuje catchment we assume that the vertical temperature gradient equals 0.65°C/100 m.

Precipitation

The network of precipitation gauging stations is rather dense (Figure 2.13). However, when we look at data availability since 1960 (Figure 2.14), not all gauging stations are useful for our analysis. Especially, Křižánky and Kadov have a short observation period.

Annual precipitation and the mean values for the four different rain gauges are given in Figure 2.15. Surprisingly, the highest annual precipitation was measured in Krucemburk (799 mm.year^{-1}), which altitude is about 180 m lower than from Svratouch (778 m.year^{-1}). This means for these two stations, that there is another overriding factor than the elevation difference. In general, the extremely wet years (i.e. 1965--67, 1987, 1995, 2001, 2005) and dry years (i.e. 1969, 1976, 1983--84, 1990--92, 2003--04) are identical for all stations.

Detailed monthly vertical precipitation gradients were calculated from the Přibyslav and Svratouch stations, considering only wet days (clearly, at dry days there is no precipitation gradient). The annual vertical precipitation gradient is 6.7%/100 m, with very low values in January and May (ca 3%/100 m) and high value in April (14%/100 m). The annual vertical precipitation gradient using the old meteorological map (Dratva, 1943) is 6%/100 m.

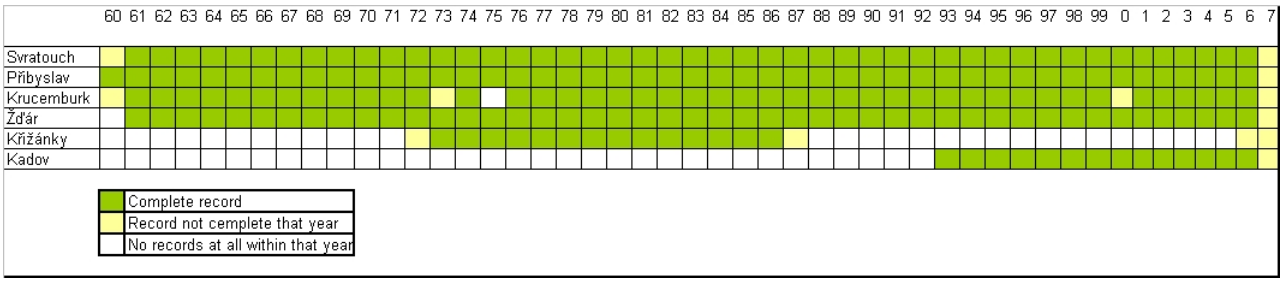

Figure 2.14: Availability of precipitation time series for the Upper Sázava catchment.

Snow

Snow pack is an important component of the hydrological cycle. Snow occurrence is the reason why the Czech hydrological year starts on 1 November. This date should guarantee that all the winter precipitation will be included in one winter to correctly evaluate the annual water balance. Although snow records are usually not an input for rainfall-runoff models, the data can be used it for validation of the snow simulation with the HBV model. For our research daily snow height and weekly snow water storage are available for Žďár nad Sázavou since 1961.

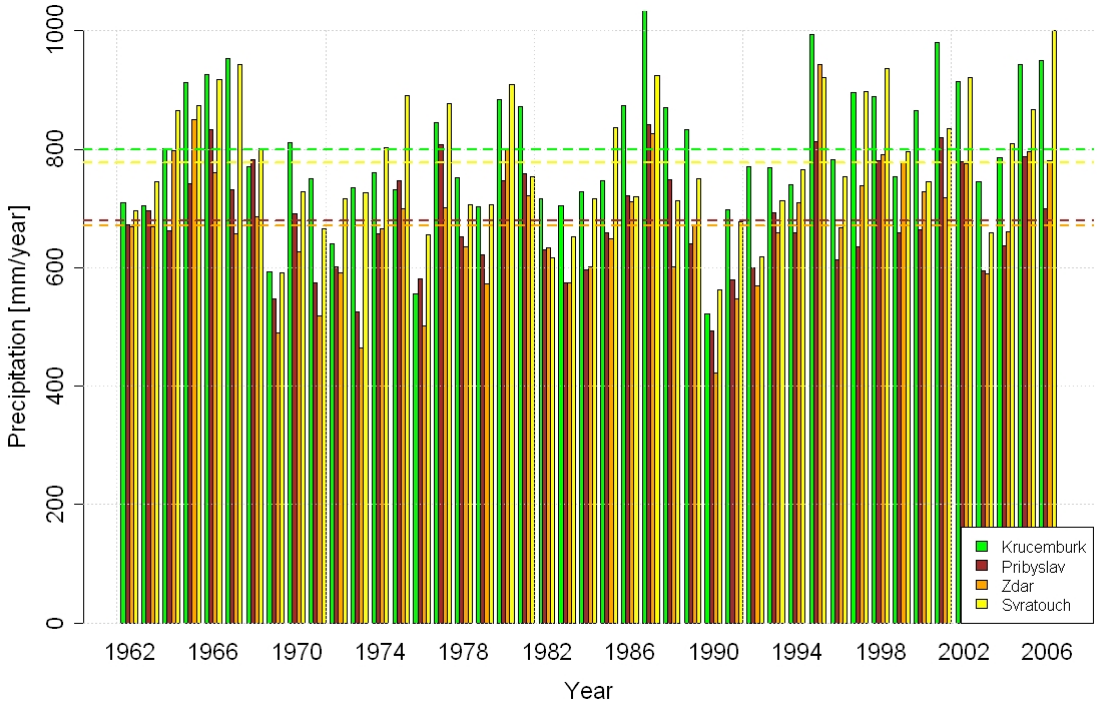

Figure 2.15: Annual precipitation for the Upper Sázava catchment (1961--2006).

Groundwater

For our research, weekly observations of groundwater heads are available from a well in Radostín (Figure 2.10). This shallow well is ca 9 m deep and it penetrates through the Quaternary sediments into the Cretaceous sediments. The groundwater heads are given in Figure 2.16. The mean head equals 617.5 m. A minimum value of 616.65 m was recorded in September 2007 and a maximum of 618.31 m in September 1967. A change in head behaviour occurs since 1990. The groundwater heads were suddenly lower and also the annual fluctuation decreased. There is also a strange pattern of constant values for the maximuma for the years 2000--2005. This can be caused by either frozen water in the well or by missing values, which are filled in by a constant value.

River discharge

The mean annual discharge (1962--2006) for the gauging station 1550 (Sázava u Žďáru nad Sázavou) is 303 mm or 1.25 $m^3.s^{-1}$. The highest discharges exceeded 34.6 $m^3.s^{-1}$ during a spring flood in 1981 and the lowest dropped slightly below 0.045 $m^3.s^{-1}$ in autumn 1989. Floods occur regularly in spring because of snowmelt and low discharges predominantly occur in summer and beginning of autumn. This is also shown in Figure 2.17, where the mean monthly discharges are plotted.

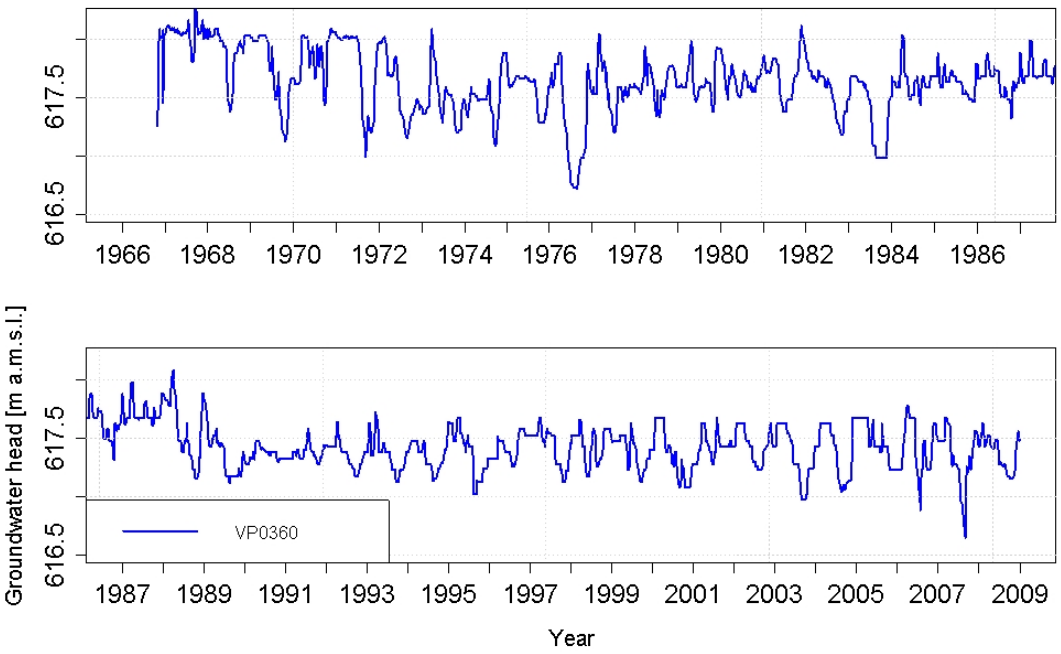

Figure 2.16: Groundwater heads in the observation well VP 0360 - Radostín.

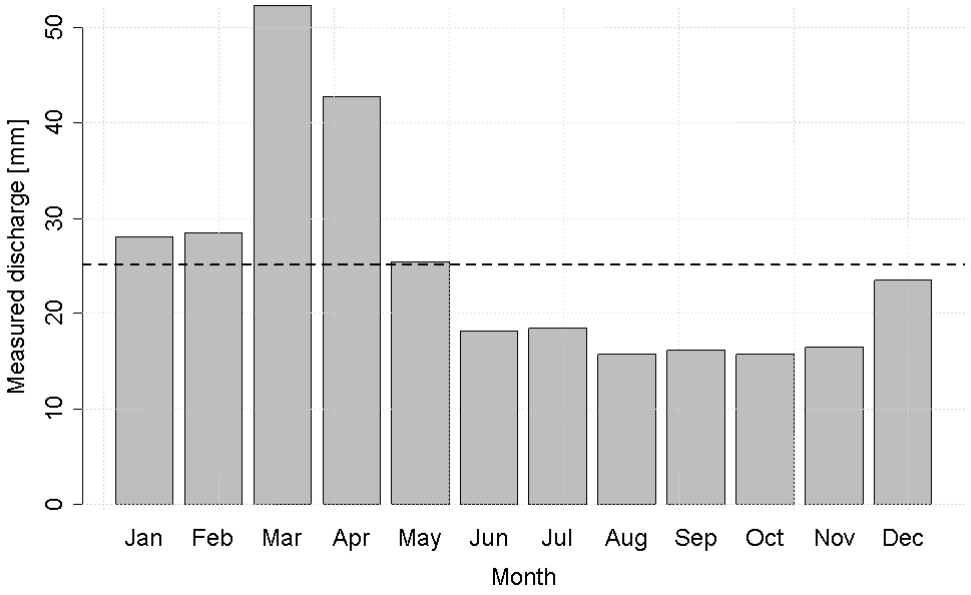

Figure 2.17: Mean monthly discharge for the Upper Sázava.

2.2.4 Human influences

The water balance of the Upper Sázava catchment is rather complicated for developing a rainfall-runoff model, because of the rather big city of Žďár nad Sázavou, which is located in the centre of the catchment along the Sázava River. The city has 23 000 inhabitants and well developed heavy industry. This must somehow influence the water balance of the whole catchment, especially in low flow situations. The drinking water for Žďár nad Sázavou is supplied from the Mostiště reservoir (Vodárenská, 2009), which is outside the catchment. The total supply capacity of the Mostiště reservoir is 220 $l.s^{-1}$, but only part is used for Žďár nad Sázavou. Using water from a resource outside the catchment indicates that there is water in the Sázava River which does not originate from inside the topographical catchment. It is water that is released from sewage disposal plants. For that reason we investigated the HEIS database (WRI, 2009) with monthly data of registered amounts of water release from sewage disposal plants. We also collected data on water abstraction rates from water bodies inside the Upper Sázava catchment, which is mainly used for the heavy industry.

The locations of the largest water releases and streamflow extractions are shown in Figure 2.18. Their rates for the period 1980--2007 are given in Figure 2.19. Except for the beginning of 1980s and 1990s, the water release is larger than the water extraction. In the last decade the average monthly surplus is approximately 100 $l.s^{-1}$, which is indicated by the green line in Figure 2.19.

Rakovec (2009) performed spot discharge measurements on the Sázava River and its main tributaries on 13 February 2009, when air temperature was -5°C and water temperature about 1°C to verify the above mentioned water surplus. The results of the hydrometrical measurements are shown in Figure 2.20 as specific runoff.

The spot measurements confirm our hypothesis that the effects of water releases and water abstractions in and near Žďár nad Sázavou are detectable in the discharge. The specific runoff of the Sázava River downstream of Žďár nad Sázavou was much higher than that of other sub-catchments. The discharge increased by ca 140 $l.s^{-1}$. This increase is more or less similar to the total release rates from the sewage disposal plants (Figure 2.19). Further Rakovec (2009) noticed the direct effect of water extraction from the Branský reservoir (sub-catchment in orange color in Figure 2.20). The calculated specific runoff from this sub-catchment derived from the observations was negative. The water deficit was ca 60 $l.s^{-1}$, which approximately corresponds with the extraction rate from the Branský reservoir (Figure 2.19).

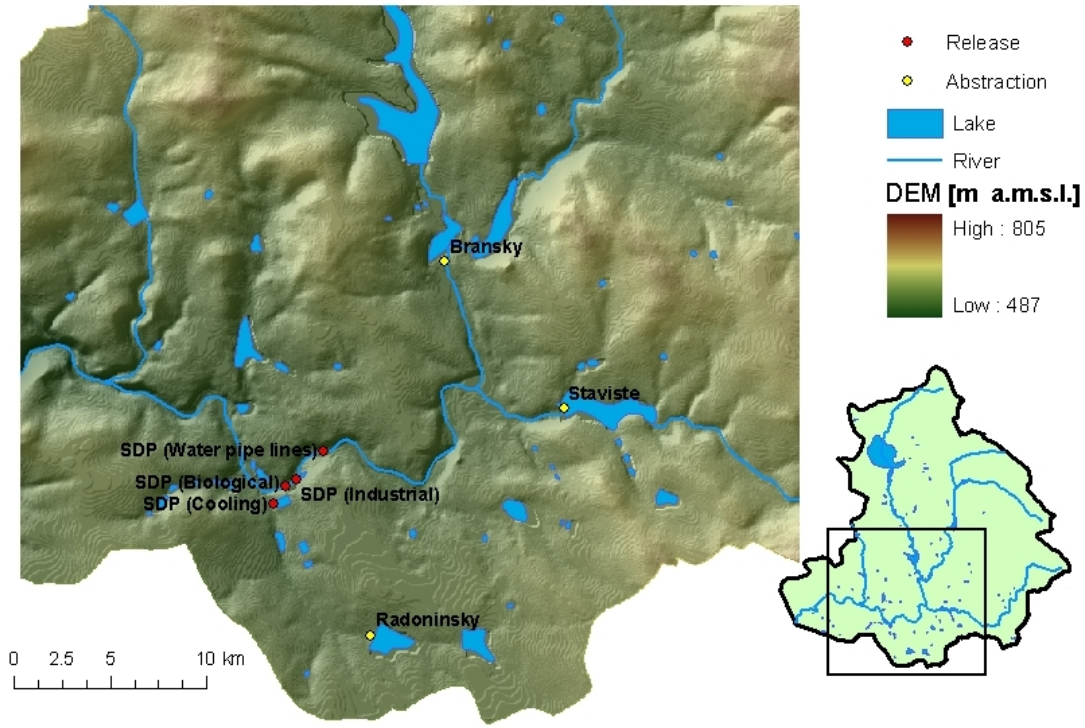

Figure 2.18: Location of streamflow extractions and water releases in the Upper Sázava catchment.

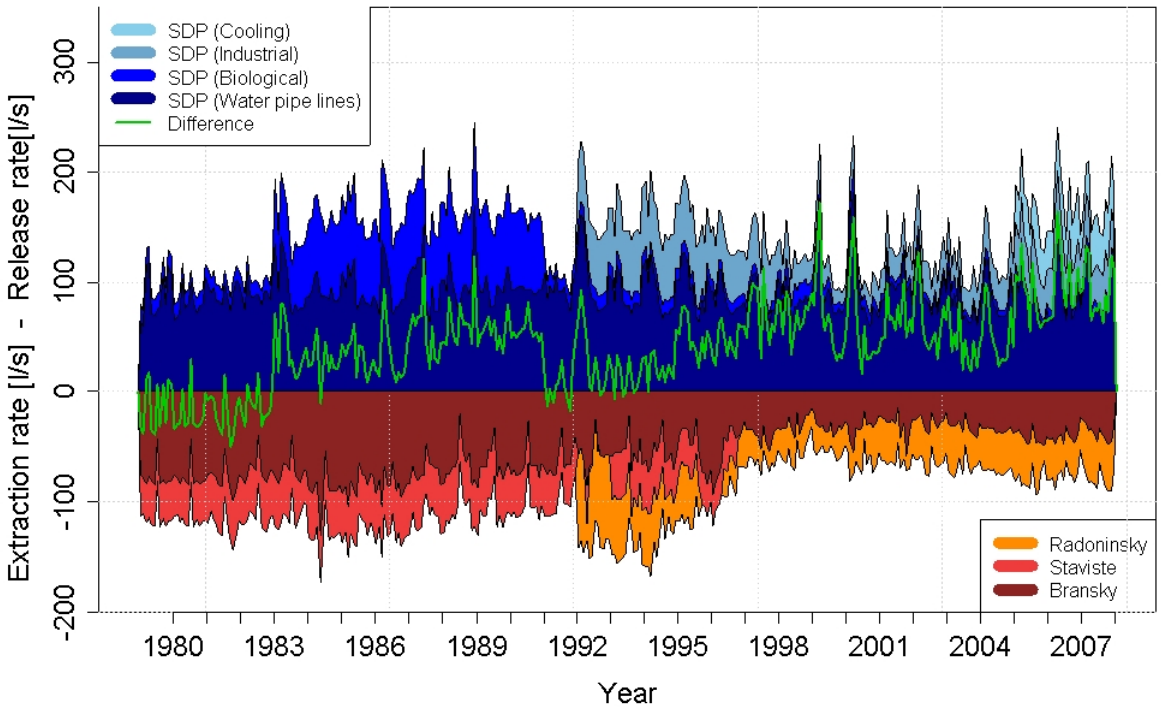

Figure 2.19: Release rates and extraction rates of open water within the Upper Sázava catchment (WRI, 2009).

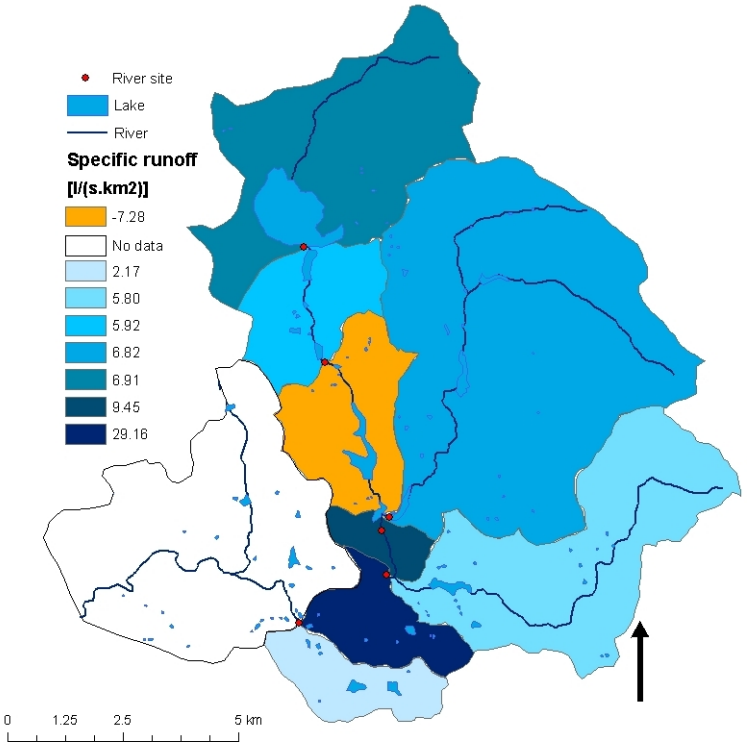

Figure 2.20: Specific runoff from spot measurements for the Upper Sázava sub-catchments, 13 February 2009.

Chapter 3

Methods

3.1 Potential evapotranspiration

Evapotranspiration is an important variable in rainfall-runoff modelling (Lu et al., 2005). It combines evaporation from the soil surface and transpiration from plants (Thornthwaite, 1948). It is an important component of the water balance. It can be measured either directly by lysimeters or indirectly, estimated by theoretical or empirical equations. Since the first option is inappropriate in most cases because of the high expenses, the latter is usually selected (Allen et al., 2006).

Penman-Monteith method

One of the most comprehensive indirect methods is the Penman-Monteith method (Allen et al., 2006). In 1948, Penman computed the evaporation from an open water surface from standard weather records of sunshine, temperature, humidity and wind speed. By further research the transpiration component of vegetation was also added. For our study, we will use the FAO Penman-Monteith method as defined by Allen et al. (2006) for a reference crop (crop height of 0.12 m, fixed surface resistance of 70 s.m^{-1} and an albedo of 0.23). The equation is as follows:

$$PET = \frac{0.408\Delta(R_n - G) + \gamma \frac{900}{T+273} u_2 (e_s - e_a)}{\Delta + \gamma(1 + 0.34u_2)} \tag{3.1}$$

PET potential evapotranspiration [mm.day^{-1}]

R_n net radiation at the crop surface [MJ.m^{-2}.day^{-1}]

G soil heat flux density [MJ.m^{-2}.day^{-1}]

T mean daily air temperature at 2 m height ($T = (T_{min} + T_{max})/2$) [°C]

u_2 wind speed at 2 m height [m.s^{-1}]

e_s saturation vapour pressure [kPa]

e_a actual vapour pressure [kPa]

e_s-e_a saturation vapour pressure deficit [kPa]

Δ slope vapour pressure curve [kPa.°C^{-1}]

γ psychrometric constant [kPa.°C^{-1}]

A detailed description of all input parameters is given by Allen et al. (2006). Here we will only describe our assumptions and simplifications, which we were forced to make due to limited data availability. The most important input variables into Equation 3.1 are mean daily temperature, solar radiation, actual vapour pressure and wind speed. In fact, only time series of temperature were available for the Upper Metuje. We followed recommendations made by Allen et al. (2006) to substitute missing or incorrect data as follows. Solar radiation (R_s) was estimated using Hargreaves radiation formula (Allen et al., 2006, p. 60):

$$R_s = 0.16\sqrt{T_{max} - T_{min}}R_a \tag{3.2}$$

where Ra is extraterrestrial radiation [MJ.m^{-2}.day^{-1}]. Wind speed was set to a constant value of 2 m.s^{-1} (Allen et al., 2006, p. 63) and actual vapour pressure was approached by another empirical equation based on daily minimum temperature (Allen et al., 2006, p. 58):

$$e_a = 0.611exp(\frac{17.27T_{min}}{T_{min} + 237.3}) \tag{3.3}$$

For the Upper Sázava catchment, wind speed and solar radiation data were available.

Thornthwaite method

We decided also to use the Thornthwaite method (Thornthwaite, 1948) to assess the effect of different indirect methods to calculate potential evapotranspiration. The Thornthwaite method is based only on temperature (Equation 3.4, [cm.month^{-1}]).

$$PET = 1.6(\frac{10T}{I})^a \tag{3.4}$$

where:

$$I = \sum_{j=1}^{12} i_j \tag{3.5}$$

$$i_j = (\frac{T_j}{5})^{1.514} \tag{3.6}$$

$$a = (0.0675I^3 - 7.71I^2 - 1792I + 49239)10^{-5} \tag{3.7}$$

T_j mean monthly temperature [°C].

Equation 3.4 can be transformed into Equation 3.8 [mm.day^{-1}]:

$$PET = 16\frac{N}{12}\frac{1}{30}(\frac{10T}{I})^a \tag{3.8}$$

where:
N length of day light [hours].

Results

Rakovec (2009) calculated daily potential evapotranspiration by the FAO Penman-Monteith and Thornthwaite methods for the Upper Metuje. The results are given in Figure 3.1. Clearly, results from two methods differ throughout the year. From December to August the Penman-Monteith method produces the highest values. In March and April, for example, these values are almost twice as high as for the Thornthwaite method. However, in autumn (September-November), the Penman-Monteith potential evapotranspiration is below the Thornthwaite results.

Potential evapotranspiration for the Upper Sázava was calculated using the same methods, but since daily data of solar radiation, minimum and maximum temperature and wind speed from the Svratouch station were available for the period 1985--2006, Rakovec (2009) calculated potential evapotranspiration using Penman-Monteith method twice. First, using the measured solar radiation and second, using the solar radiation calculated by Equation 3.2. The monthly averages of the potential evapotranspiration according to the three different approaches are shown in Figure 3.2. The differences between both versions of the Penman-Monteith methods are minor in comparison to the Thornthwaite method. From November to April the values of the Penman methods are twice as high than that of the Thornthwaite method.

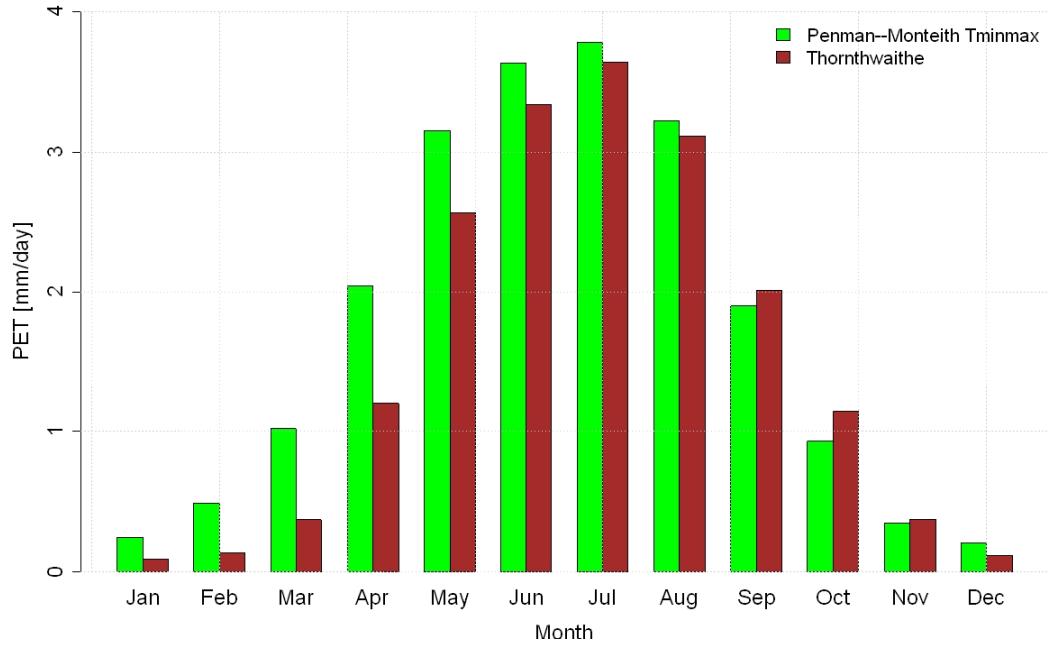

Figure 3.1: Long term monthly averages of potential evapotranspiration derived for the Bučnice meteorological station, (1981--2006).

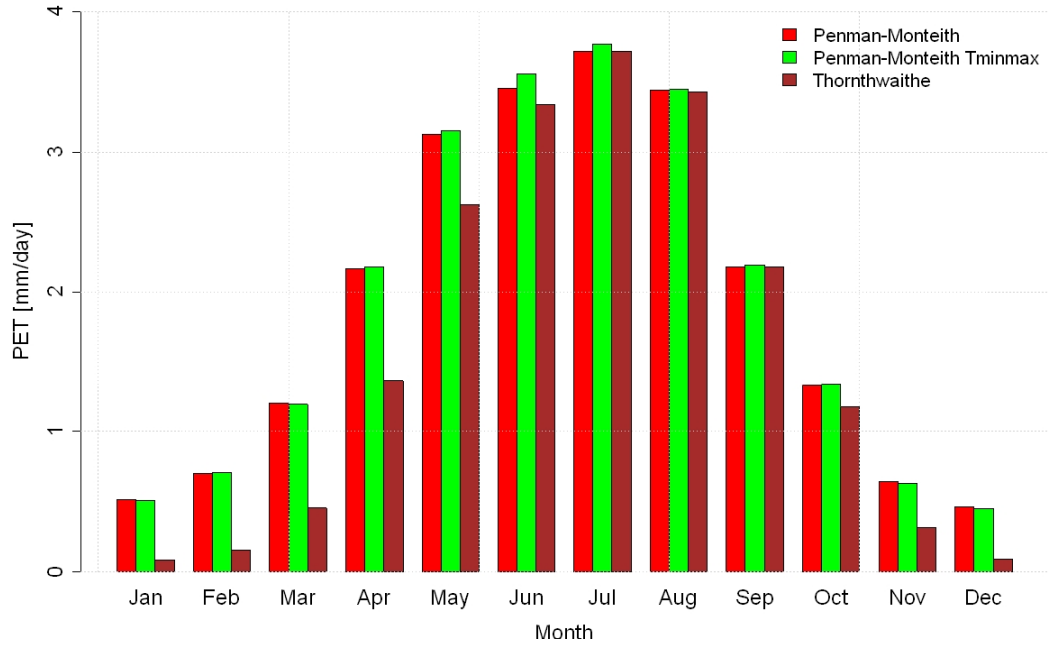

Figure 3.2: Long term monthly averages of potential evapotranspiration derived for the Svratouch meteorological station, (1985--2006).

3.2 HBV model

3.2.1 Introduction

HBV (Hydrologiska Byrans Vattenbalansavdelning) is a conceptual model for rainfall-runoff simulation, which was developed by Sten Bergstrom at the Swedish Meteorological and Hydrological Institute (Seibert, 2005). We decided to use HBV for the hydrological modelling and consequently its results for drought analysis, because: (1) it is a simple model that is based on water storages, (2) it is applied all over the world, and (3) it simulates all variables that are needed for the investigation of hydrological drought, i.e. snow, soil moisture storage, groundwater storage, and river discharge.

The HBV model applied for research purposes, but also for water engineering and operational hydrology, for example to forecast streamflow in Sweden (SMHI, 2009) or Norway (NVE, 2009). The various HBV model structures, concepts and applications are described in many papers. Bergstrom and Sandberg (1983) investigated the use of the lumped HBV model for different types of aquifer in Sweden. Braun and Renner (1992) described goodness of HBV for runoff modelling of different physiographic regions in Switzerland. Lindstrom et al. (1997) introduced HBV 96, which is a spatially-distributed version and they compared it with a lumped HBV model for Swedish catchments. Furthermore, Liden and Harlin (2000) investigated HBV 96 performance for climatologically different river basins in Europe, Africa and South America. Another small-scale HBV application, a fully spatially-distributed version of the HBV model with a more process-based runoff generation routine, was developed and tested on an Austrian mountainous catchment by Johst et al. (2008), where snow depth and trace concentration were used to evaluate model performance.

The HBV model was also used to investigate the impact of climate change scenarios, e.g. in Germany (Menzel and Burger, 2002), Ireland (Steele-Dunne et al., 2008) and the Hindukush-Karakorum-Himalaya region (Akhtar et al., 2008). Furthermore, it is applied to improve the hydrological representation in GCMs, namely HBV Baltic (Graham, 1999), which involves the whole Baltic Sea Basin with a total area of 1.6 10^6 km^2. The applicability of this macro-scale concept was evaluated by Bergstrom and Graham (1998).

3.2.2 HBV light

In this report we will use the HBV light version (Seibert, 2005). This model version was used and examined in many papers. For example, investigation of parameter uncertainty (Seibert,

1997), regionalisation of model parameters (Seibert, 1999), performance of different HBV model structure (Uhlenbrook et al., 1999), effects of spatial scale on model fit (Seibert et al., 2000), comparison of single- and multi-criteria calibration techniques (Seibert, 2000), reliability of model parameters outside calibration period focusing on floods (Seibert, 2003) or investigation of model performance for droughts (Hohenrainer, 2008).

Model structure

The structure of HBV light used in this report is illustrated in Figure 3.3. The model consists of four components: lumped or distributed snow and soil routines, a lumped response function and a lumped routing routine. Seibert (2005) comprehensively describes all model equations and parameters. We will give here only a brief summary.

The *snow routine* simulates precipitation either as snow or rain depending on the threshold temperature (TT). Below this temperature the precipitation is assumed to be snow and it is accumulated in the snow pack. To correct for aerodynamic losses at the rain gauge and winter evaporation, the snow fall correction factor (SFCF) is introduced. Snow melt is calculated using the degree-day factor (CFMAX) and rain and melt water are retained in the snow pack until it exceeds a certain fraction, the water holding capacity (CWH). Liquid water in snow refreezes according to the refreezing coefficient (CFR).

The *soil routine* determines the volume of rain and snow melt, which is stored in the soil box or directly recharged to the groundwater box. A non-linear relation is used for that separation, which is determined by the power of the shape coefficient (BETA) and depends on the actual water content of the soil box and the maximum soil moisture storage in soil box (FC). The amount of actual evaporation depends on the evaporation threshold (LP). If the soil moisture exceeds LP, the actual evaporation equals potential, otherwise there is a linear reduction of the potential evaporation. Furthermore, the potential evapotranspiration correction factor (CET) is used to calculate daily potential evapotranspiration from mean monthly values of potential evapotranspiration and temperature, if time series of daily potential evapotranspiration are not used as input.

The *response routine* consists of two groundwater boxes, that are represented by simple linear reservoirs. There are two or three outflows from these groundwater boxes depending on the threshold value (UZL), as shown in Figure 3.3. Each outflow is linearly dependent on the recession coefficient (K0, K1, K2) and actual groundwater storage. Water can also percolate from the upper groundwater box to the lower one, depending on the percolation rate (PERC).

The *routing routine* is based on a triangular weighting function defined by the parameter MAXBAS.

HBV can be run either as a lumped or as a semi-distributed model. The catchment can be divided in up to 20 elevation zones and three vegetation zones (i.e. tiles). The first option makes it possible to adjust precipitation and temperature due to vertical elevation gradients and the latter ensures a unique parameter set for each land cover class reflecting its different physical properties. Every tile obtains a weight that is proportional to the ratio between its area and the area of whole catchment.

There are more alternative model structures, as described by Seibert (2005). In this study we will also investigate a modified structure, which includes some delay in the response function. This concept uses two parallel groundwater boxes and it is described by Seibert (2000) within an application, that tries to model some delay caused by a thick unsaturated zone.

Input data

The HBV input data comprise time series of daily precipitation, temperature and observed streamflow. Precipitation and temperature are corrected for each elevation zone using the vertical precipitation gradient (PCALT) and vertical temperature gradient (TCALT). Furthermore, HBV requires time series of potential evapotranspiration, either daily or monthly average. In the latter case, mean monthly temperature must be provided additionally.

Derivation of precipitation

To identify a meteorological drought, precipitation as simulated by HBV ($Psim$) is needed. $Psim$ represents catchment average precipitation calculated and used by HBV, as it is not given in the HBV output file. The calculation of $Psim$ is based on the mass balance of the HBV snow and soil boxes which is:

$$Psim[i] = AET[i] + snow[i] - snow[i-1] + SM[i] - SM[i-1] + GW[i] \tag{3.9}$$

where i is the time step, AET stands for actual evapotranspiration, $snow$ represents the snow water storage, SM is the amount of water stored in soil box and GW is water entering the response routine.

Objective functions

The objective function is a measure to assess model performance. The objective functions, which are available for the calibration of the model parameters in the HBV light model are

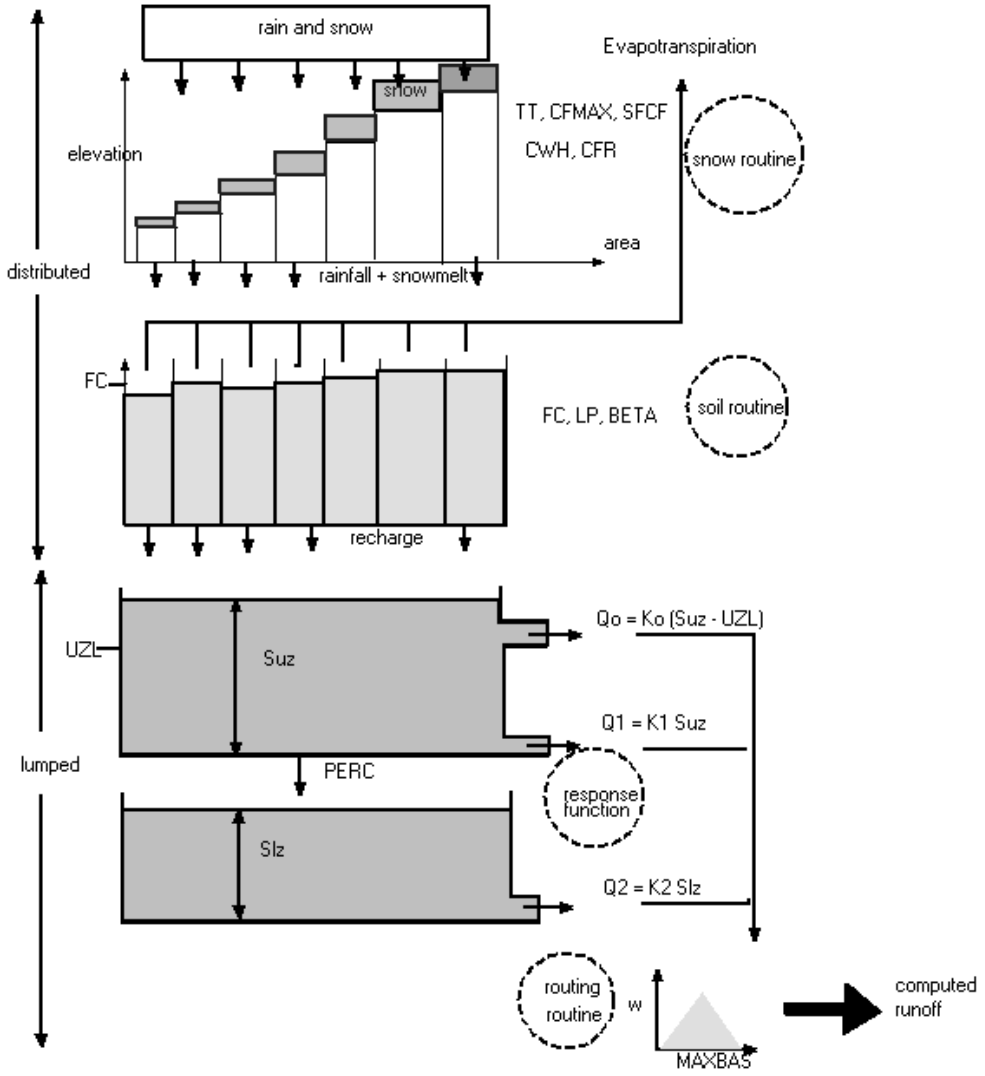

Figure 3.3: HBV model structure (Seibert, 2000).

described below. Nash and Sutcliffe (1970) defined the most common used criterion in hydrology to assess the agreement between observed and simulated discharge, which is called the efficiency of a model (Equation 3.10). An efficiency of 0 indicates that the model performance is equal to the observation mean and an efficiency of 1 represents a perfect fit, where observed and simulated discharge are equal. A modified version of this criterion is its logarithmic version (Equation 3.11), which gives more weight to low flow situations (Hohenrainer, 2008). Another objective function is the volume error (Equation 3.12). For the best fit the VE equals 0, in case the sum of simulated discharge equals the observed one. This criterion is applied to assess the model water balance. If it is positive then the model underestimates the observed conditions and vice versa.

$$R_{eff} = 1 - \frac{\sum_{i=1}^{n} (Q_{obs}(i) - Q_{sim}(i))^2}{\sum_{i=1}^{n} (Q_{obs}(i) - \overline{Q_{obs}(i)})^2} \tag{3.10}$$

$$lnR_{eff} = 1 - \frac{\sum_{i=1}^{n} (lnQ_{obs}(i) - lnQ_{sim}(i))^2}{\sum_{i=1}^{n} (lnQ_{obs}(i) - \overline{lnQ_{obs}(i)})^2} \tag{3.11}$$

$$VE = \frac{\sum_{i=1}^{n} (Q_{obs}(i) - Q_{sim}(i))}{\sum_{i=1}^{n} Q_{obs}(i)} \tag{3.12}$$

Calibration technique

Calibration aims to find the best parameter set for the model. Uhlenbrook et al. (1999) stated, that although some model parameters have a physical basis, they are effective only on the catchment scale, which indicates that they are hard to measure in the field. That makes model calibration necessary for almost all hydrological models. Since HBV light in its semi-distributed version requires altogether 31 parameters it is a hard to perform a manual calibration. In the past there was no other possibility than to do it by a trial and error, as for example Bergstrom and Sandberg (1983) and Braun and Renner (1992) did. The manual calibration, including a sensitivity analysis is useful to understand the effect of each parameter on model performance but it is very difficult to evaluate all possible combinations. Nowadays, there are many automatic calibration techniques available, which can help to find the optimum parameter set.

Among others, Monte Carlo is a procedure, which tests a huge number of random parameter sets within given parameter ranges. The best sets are selected according to a prescribed objective criterion. Monte Carlo is included in HBV light and it was applied, for example, by Seibert (1997), Seibert (1999), Uhlenbrook et al. (1999) and Liden and Harlin (2000).

Another calibration tool included in HBV light, is the automatic calibration based on the genetic algorithm, which is combined with the local optimisation. The whole technique is described by Seibert (2000), and a brief summary follows below. The optimal parameter set is found by its evolution using selection and recombination. The concept is sketched in Figure 3.4. An initial population of n parameter sets (default n is set to 50) is generated inside the given parameter space. The goodness of fit of each set is evaluated by the magnitude of the objective function. Two best sets are assumed to be parental (A, B) and subsequently a new population of n parameter sets is established randomly following four rules for each parameter. These rules have certain probabilities (p) and the new parameter is chosen either from parental set A or B (p = 0.41 for both cases), or randomly between values of A and B (p = 0.16). Small probability

(p = 0.02) is also kept for mutation, when the new value is selected randomly within the whole parameter space. This procedure of setting new populations is repeated until the maximum number of model runs (i) is reached. In case the new parameter set gives worse results than the previous one, the model returns to the best preceding parental parameter set.

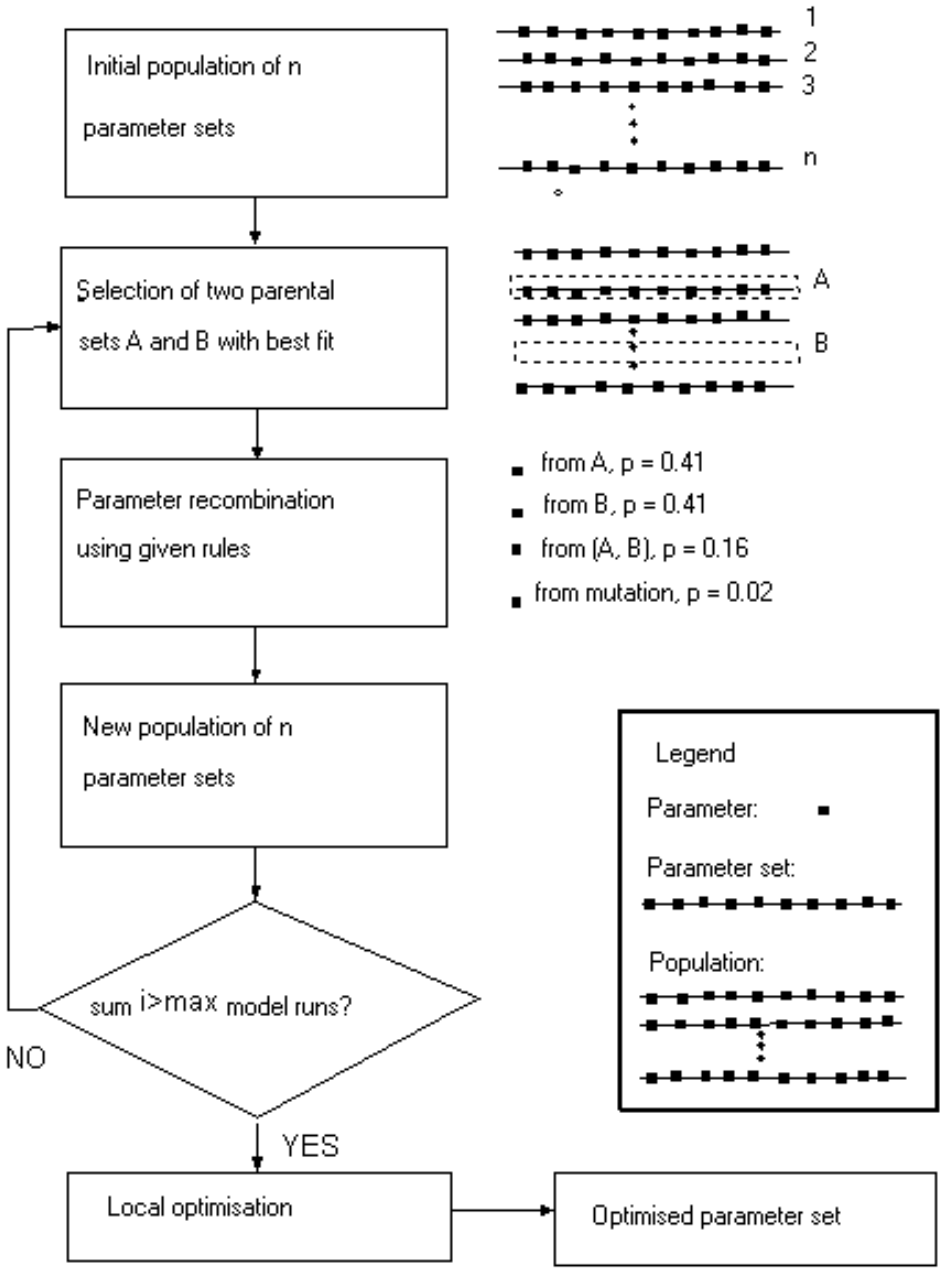

Figure 3.4: Automatic calibration using the genetic algorithm (Seibert, 2000).

3.3 Drought

3.3.1 Introduction

As mentioned in the introduction (Chapter 1), drought is an occurrence of below average water availability. According to Tallaksen and Van Lanen (2004), Dingman (2004) or Heim (2002) we can make a distinction between drought types.

A lack of precipitation over a large area and for a long period that is unusually extreme and prolonged in comparison with usual climatic conditions is called a *meteorological drought*. This water deficit influences the water balance of a given area and it propagates through the hydrological cycle. The lack of precipitation is often, but not always, accompanied by higher evaporations rates, higher temperature, higher solar radiation and lower air humidity. A meteorological drought may lead to different types of drought.

Hydrological drought is the most important one for our investigation and it is caused when soil water deficit occurs, and groundwater heads and streamflow stages are lowered below a certain level (*soil moisture drought, groundwater drought and streamflow drought*), however Tallaksen and Van Lanen (2004) does not include the *soil moisture drought* within the *hydrological drought*. Because of the connections between the unsaturated zone, groundwater and open water, a meteorological drought propagates through the hydrological cycle. The hydrological drought signal shows lag and attenuation compared to the meteorological drought signal. This is influenced by the physical properties of the catchment.

Hydrological drought can be further divided into a *summer* drought which develops from a meteorological drought as described above or a *winter* drought. The latter occurs as a consequence of precipitation being stored as snow and ice (Fleig et al., 2006) or due to below average recharge. Both types of these seasonal droughts can influence each other, when e.g. a severe summer drought continues into a long winter drought (Fleig et al., 2006) or the other way, from winter to summer drought as a consequence of extensive overland flow of early snow melt on frozen topsoils. It causes low soil moisture and reduced groundwater recharge, and that can lead to the summer drought by the end of the hydrological year due to low base flow (Van Lanen et al., 2004).

Seen from a different point of view, *agricultural drought* is defined when soil moisture is too low to enable sufficient crop production. When stress on an ecosystem occurs, an ecological drought can be distinguished. During an *ecological drought* shortage of water affects plants and animals. When impacts of drought influence society and its economy we speak about

socio-economic drought. Another term *green drought* is mentioned e.g. by Trnka et al. (2009) which is associated with relatively high annual precipitation, but low agricultural productivity due to poorly rain timing. An example from Ethiopia can be found in BBC (2009), which describes vibrant green fields but no food.

We should also be aware of some possible misunderstandings in terms related to droughts, e.g.: *aridity*, which is a permanent feature of a dry climate or *water scarcity*, which is an imbalance between water demand and water availability (Van Lanen and Tallaksen, 2008). Another term is *desertification*, which is the outcome of a series of drought events and human activities, which irreversibly degrades the land, e.g. high cattle grazing (Tallaksen and Van Lanen, 2004).

3.3.2 Low flow and drought characteristics

An investigation of hydrological drought requires quantitative criteria. There are many different approaches how to evaluate drought events. We should keep in mind that various methods can lead to different results and we should always consider the environment we are analysing. In the following part we will briefly describe the drought characteristics as proposed by Hisdal et al. (2004): *low flow characteristics* and *deficit characteristics*.

Low flow characteristics can be derived from time series and indices of hydrological variables (e.g. daily streamflow, groundwater levels or recharge):

- Percentile from the Flow Duration Curve (FDC). The FDC gives an empirical relation between streamflow discharge and the percentage of time that this discharge was reached or exceeded. An index of flow exceedance is often expressed as a percentile, which represents the magnitude of discharge that was exceeded for given percentage of time of record.

- Annual minimum flow, AM(n). This characteristics is derived from streamflow data, which are smoothed by a moving average of n-days (the previous n/2 days and the n/2 coming days). AM(n, i) represents a time series for i years.

- Base flow index (BFI). The BFI is the ratio of the base flow to the total flow that is calculated from hydrograph smoothing and separation procedures using daily discharges. The BFI represents a ratio between runoff originating from groundwater storage and runoff originating from quick flow. BFI ranges between 0.9 for permeable catchments with high groundwater storage, and 0.15--0.2 for impermeable flashy catchments without groundwater storage. BFI (i) represents a time series of BFI for i years.

- Recession indices describe the shape of the falling limb of the hydrograph. Many indices are derived from hydrogeological, relief and climatic properties of a catchment.

Deficit characteristics are based on introducing a threshold level below which a streamflow or another hydrometeorological variable is assumed to be in a drought event. Every single drought can be easily defined by its total duration and its deficit volume.

- Threshold level method. This method is based on defining a threshold below which a drought is identified. Besides its duration and deficit volume, the minimum flow or intensity for each single drought event can be determined. For selection usually low flow indices are used, such as percentiles of FDC, e.g. Q70--Q90 for perennial rivers. The threshold value can vary during the year (on seasonal, monthly or daily base). The term drought is in that case more shifted to an anomaly. For a correct qualitative interpretation and drought analysis, the threshold method is often used in combination with pooling procedures, i.e. joining mutually dependent drought events and eliminating minor drought events. The threshold level method can in addition to streamflow also be used on other hydrological variables, like precipitation, soil moisture and groundwater.

- Sequent peak algorithm (SPA) is in fact a special kind of threshold level method that includes a pooling procedure. It is derived from cumulative storage deficits. This means that a drought event does not finish when reaching the threshold level, but after the refilling of the total drought deficit volume. This method is derived from reservoir management. SPA can not be applied to state variables, such as soil moisture or groundwater storage.

3.3.3 Drought analysis

In this section we give an overview of tools and methods, which we applied to the simulated and observed time series to perform drought analyses.

Low flow characteristics

Low flow indices are calculated to verify the model outcome against the observed time series and also to enable comparison of low flow properties between the Upper Metuje and Upper Sázava catchments, namely the shapes of the flow duration curves, annual values of base flow indices and annual minimum flows (Section 4.3).

Deficit characteristics

The *threshold method* is used for drought identification of meteorological and hydrological droughts. In this study we applied a monthly threshold derived from the 80-percentiles of duration curves, which is in the ranges of the 70--90 percentiles, as recommended for perennial rivers by Hisdal et al. (2004). Furthermore we smoothed the discrete monthly threshold values by applying a moving average of 30 days.

In addition, we used a minimum duration of 3 days to eliminate minor droughts. For the meteorological and streamflow drought, we also applied the *sequent peak algorithm* for better understanding of the drought propagation. This SPA method was based on the same values as for the threshold method.

For precipitation ($Psim$, Section 3.2.2) we used a moving average of 30 preceding days to pool. The identification of a meteorological drought is identical to a hydrological drought by using a monthly threshold with a moving average of 30 days. However, first a pooling procedure of a moving window of n days is applied on the precipitation data itself, because the number of days without precipitation would give a zero threshold, in case of $P80 = 0$. Moving averages of 10 and 30 days are investigated (Section 5.1).

Single drought events are characterised by their duration and deficit volume. For the whole time period, the total number of droughts, mean number of days, mean deficit and mean intensity are given.

3.4 Other methods

Boxplot

Boxplot (Figure 3.5) is a convenient way of graphical plotting of data through their five non-parametric summaries, (1) sample minimum (Q_{min}), (2) lower quartile (Q_{25}), (3) median (Q_{50}), (4) upper quartile (Q_{75}), and (5) sample maximum (Q_{max}) (Wikipedia, 2009). The interquartile range is defined as $Q_{75} - Q_{25}$. If the extreme value occurs further than the distance 1.5 times the interquartile range from the box, the outlier is indicated by a dot, as it is default in **R**. The less extreme values below Q_{25} and over Q_{75} are connected to the box by a whisker, if they are located less than 1.5 times the interquartile range from the box.

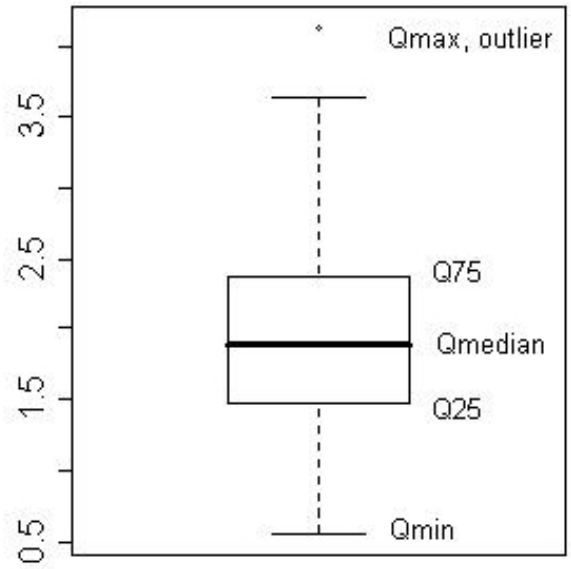

Figure 3.5: Description of a boxplot.

Groundwater storage conversion

Simulated groundwater storage can not be directly compared with observed groundwater heads. To enable comparison of the simulated groundwater storage with the observed groundwater head, we transformed the sum of the storages (SUZ and SLZ) into a groundwater head H_s [m a.m.s.l.] by using Equation 3.13 (Seibert, 2000). Coefficients m (slope) and c (offset) are derived by a linear regression which analysis the relationship between simulated groundwater storage and observed groundwater heads.

$$H_s = m(SUZ + SLZ) + c \tag{3.13}$$

Standardisation of model parameters

Standardisation of model parameters was derived according to Equation 3.14.

$$SV = \frac{OV - LL}{R} \tag{3.14}$$

where SV is the standardised value of parameter, OV is the original parameter value, LL is the lower limit of the parameter space and R is the range for the parameter space.

Chapter 4

Results of hydrological modelling (HBV)

The hydrological modelling with HBV is needed to obtain daily time series of hydrological cycle components (fluxes and state variables), since not all variables were measured, e.g. soil moisture, groundwater heads or water storage in snow. Using the conceptual HBV model, we simplify the catchment water balance into several interconnected reservoirs, which are changing their water storages. Once we have the time series of hydrological cycle components, we can identify droughts from these components and finally we can investigate the propagation of the drought. Since we have time series of streamflow, groundwater heads and water storage in snow (only for the Upper Sázava), we can compare the model performance with these observed time series.

4.1 Upper Metuje catchment

The hydrological system and available data for the Upper Metuje catchment are described in detail by Rakovec (2009) and a brief overview is given in Section 2.1. As discussed earlier, human influence can not be neglected (Section 2.1.4), which makes it difficult to simulate the whole hydrological system by using a simple model. The disturbances in water balance are caused by irregular groundwater abstractions, with the highest discontinuity (jump) in 1994 when the extraction rates suddenly doubled (Figure 2.9).

Considering the human influences it is a challenge to carefully select periods to calibrate the model, to validate it on discharge for an independent time period and to validate the groundwater storage data. The calibration and validation of the HBV model for the Upper

Metuje follows in Sections 4.1.1 and 4.1.2. The modelling setup is given in Figure 4.1.

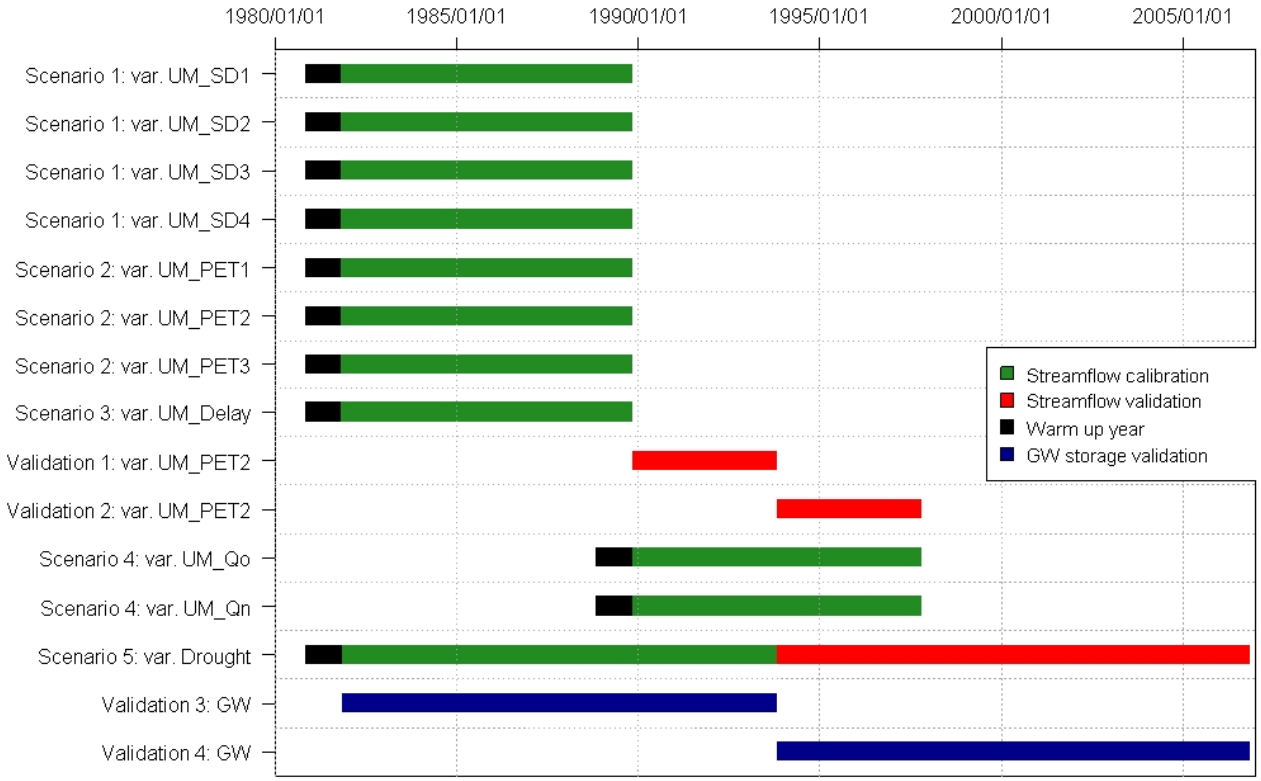

Figure 4.1: Hydrological modelling scheme for the Upper Metuje catchment.

4.1.1 Calibration

The HBV model was calibrated against observed daily streamflow using the automatic calibration based on the genetic algorithm (Section 3.2), with the logarithmic model efficiency (Equation 3.11) as an objective function. Each parameter set was derived through 3500 model runs and 1200 local optimisation runs. The parameter space was based on Seibert (2000), as shown in Table 4.1.

First, we investigated four scenarios (Scenarios 1--4) to derive the best HBV model for the following drought analysis (Scenario 5). Eight hydrological years starting from 1 November 1981 to 31 October 1989 with one warm up year as an initial condition (from 1 November 1980 to 31 October 1981) includes Scenarios 1--3, as shown in Figure 4.1. The aim of this analysis is to investigate:

1. the importance of model distributivity on model performance [4 variants (UM_SD1 to UM_SD4) based on different number of elevation zones (EZ) and land cover zones (LZ)];

Table 4.1: Range of model parameters (Seibert, 2000).

Parameter	Unit	Lower limit	Upper limit
Snow routine			
Threshold temperature (TT)	°C	-1.5	2.5
Degree-day factor (CFMAX)	mm.°C^{-1}.day^{-1}	1	10
Snowfall correction factor (SFCF)	--	0.5	1.2
Water holding capacity (CWH)	--	0	0.2
Refreezing coefficient (CFR)	--	0	0.1
Soil routine			
Maximum water storage in the soil (FC)	mm	50	500
Evaporation threshold (LP)	--	0.3	1
Shape coefficient (BETA)	--	1	6
Correction for PET (CET)	°C^{-1}	0.001	0.3
Response routine			
Recession coefficient (K0)	day^{-1}	0.1	0.5
Recession coefficient (K1)	day^{-1}	0.05	0.3
Recession coefficient (K2)	day^{-1}	0.001	0.1
Threshold for K0 outflow (UZL)	mm	0	50
Maximum percolation (PERC)	mm.day^{-1}	0	4
Weighting function (MAXBAS)	day	1	7

2. the effect of three different potential evaporation inputs (Section 3.1, variants UM_PET1 to UM_PET3) on the streamflow simulation [daily Penman-Monteith, mean monthly Penman-Monteith and mean monthly Thornthwaite);

3. the effect of applying a different HBV response function called *delay* (Section 3.2.2, variant UM_Delay).

The hydrological years 1982--1989 were selected because the groundwater abstraction rates were more or less constant during that time (Figure 2.9) and we still kept four more years (1990--1993) for streamflow validation within the undisturbed period.

The fourth calibration scenario uses data from 1 November 1989 to 31 October 1997 for two variants: observed and naturalised streamflow (UM_Qo and UM_Qn). We obtained the latter by correcting the observed streamflow for monthly groundwater abstraction rates and

water release rates from sewage disposal plants (Figure 2.9). We used this approach to try to eliminate human influences in the observed data.

Based on the results of the four scenarios, we developed a final model (Scenario 5) for drought analysis covering the period 1982 to 2006. The first half of the period is used for calibration (1982--1993) and the second half (1994--2006) for validation of the model on independent period to avoid the sudden change of human influence. However, one may argue about the term *validation*, because the observed streamflow could be affected.

Scenario 1: the effect of the HBV model structure zonation

We investigated, what the effect of the model setup on the objective function. We developed four variants of different number of elevation zones (EZ) and land cover zones (LZ), as follows: 3 EZ & 3 LZ, 3 EZ & 1 LZ, 1 EZ & 3 LZ and 1 EZ & 1 LZ. We assumed, that the semi-distributed HBV model made of three elevation zones and three land cover zones (3 EZ & 3 LZ) would provide the best results since it is the most complex as opposed to the fully lumped version (1 EZ & 1 LZ) which was anticipated to give the worse results. The volume error plotted against the calibration criteria ($lnReff$) is shown in Figure 4.2. Each sub-figure gives the outcome for one model structure variant for three different potential evaporation inputs (impact of the latter will be explained later). The best model performance is the one with the highest calibration criterion $lnReff$ and the lowest volume error, so it should be in the upper left corner.

As expected, the highest $lnReff$ with the lowest volume error was achieved by using the most distributed version (3 EZ & 3 LZ). Similar results with even smaller differences among potential evaporation inputs were found for the variant of three elevation zones and only one land cover zone (3 EZ & 1 LZ). Poorer results were obtained for variants based only on one elevation zone (1 EZ & 3 LZ and 1 EZ & 1 LZ), where the volume error for some cases exceeded 10% and $lnReff$ dropped below 0.6. The main conclusion for the Upper Metuje catchment is that the elevation zonation is more important than land cover zonation.

Scenario 2: the effect of different PET inputs

We showed the differences among different potential evapotranspiration inputs in Figure 4.2. A simple mean monthly Thornthwaite method (PET 3) for the potential evapotranspiration showed $lnReff$ values never dropping below 0.73, in comparison with the daily Penman-Monteith method (PET 1), which varied more and $lnReff$ values even dropped below 0.57.

In this scenario we also compared hydrographs for the three different potential evapotran-

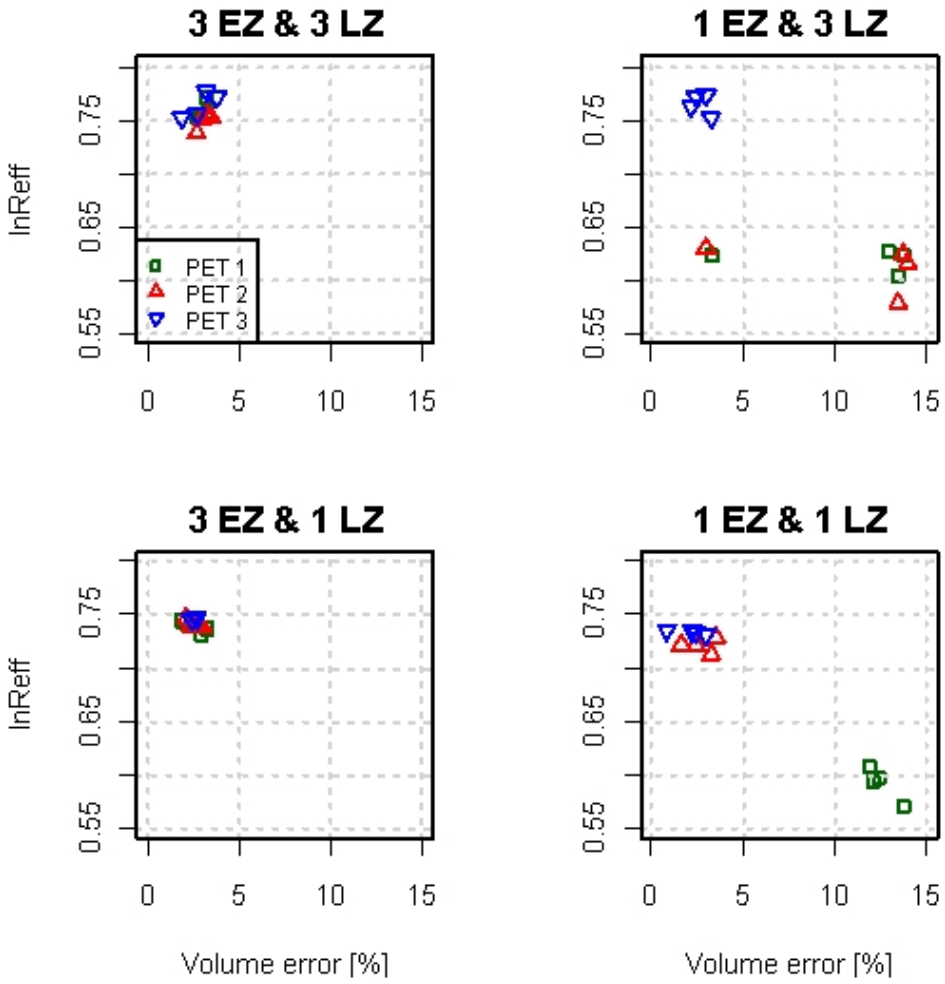

Figure 4.2: Objective functions vs. model setup, scenario 1 for the Upper Metuje catchment.

spiration inputs of the HBV model for variant 1 of scenario 1 (3 EZ & 3 LZ). The values for the objective functions are given in Table 4.2. The differences between simulated streamflow time series are negligible, although the differences between the different inputs are substantial, e.g. the mean monthly Penman-Monteith potential evapotranspiration is twice as high as the mean monthly Thornthwaite in winter and spring (Figure 3.1 and Rakovec, 2009).

Table 4.2: Objective functions of scenario 2 for the Upper Metuje catchment.

PET method	**lnReff**	**Reff**	**VE**
Penman-Monteith daily (PET 1)	0.76	0.67	3%
Penman-Monteith monthly (PET 2)	0.76	0.71	3%
Thornthwaite monthly (PET 3)	0.76	0.67	3%

The full hydrographs are shown in Figure B.1 and zoomed into low flows in Figure B.2. The first hydrograph covering the whole flow range (Figure B.1) shows the best run in terms of the objective functions (variant 017, based on 3 EZ & 3 LZ and PET 2) and the latter includes simulated streamflow for all three potential evaporation inputs (PET 1 to PET 3). Each of those variants is represented by four hydrographs based on four calibrated parameter sets. The dashed horizontal line shows the 80--percentile of the observed flow duration curve and the colour strip on the x-axis indicates whether the temperature is positive or negative, to provide information on the cause of the low flow (winter or summer). The timing of observed and simulated extremes coincide, only the magnitude of high flows differs, which agrees with the chosen calibrating criterion of $lnReff$ (Equation 3.11), which puts more weight on low flows. The flow recession is successfully captured. The values of the best parameter set (variant 017, black dashed in Figure B.2) are listed in Table A.4.

Scenario 3: delay response function

The objective functions for scenario 3, which uses the modified system of groundwater boxes (Section 3.2.2) are shown in Table 4.3. The input of potential evaporation is based on the long term mean monthly Penman-Monteith (PET 2). The results indicate that the model performance of the delay version is worse compared to the classical HBV model structure (Table 4.2). The calibration criterion ($lnReff$) dropped from 0.76 to 0.71 and the volume error increased from 3% to 11%. However, the simulated shape of the recession curve (Figure B.3) is interesting for low flows, because the falling limb of hydrographs shows higher sensitivity to recharge. Furthermore, there are no the sharp and sudden changes in the shape from steeper to more gentle slopes. The latter is caused by the missing component in the delay model structure of the fast responding outflow (Q0) from the upper groundwater box (Figure 3.3). Nevertheless, the delay version will not be used for drought analysis, because of the worse performance in objective criteria.

Table 4.3: Objective functions of scenario 3 for the Upper Metuje catchment.

Model setup	**lnReff**	**Reff**	**VE**
Delay	0.71	0.46	11%

Scenario 4: observed vs. naturalised runoff

The fourth scenario investigated whether river flow naturalisation helps to improve the

model goodness of fit. Table 4.4 shows, that flow naturalisation was not successful; all three objective functions were better for the observed variant. The reason for this could be temporal resolution we used. We had to derive the daily time series of human influence from monthly sums (Figure 2.9). Our temporal downscaling did not improve model performance.

Table 4.4: Objective functions of scenario 4 for the Upper Metuje catchment.

Streamflow input	**lnReff**	**Reff**	**VE**
Observed	0.70	0.60	1%
Naturalised	0.63	0.40	-10%

Scenario 5: reference model for drought analysis

This scenario is assumed to give the best possible model for drought identification and drought analysis. It is based on the findings from the scenarios 1--4. First, we built a semi-distributed HBV model of three elevation and three land cover zones (3 EZ & 3 LZ). The model was calibrated for 12 years (1982--1993) with a warm-up year of 1981 (Figure 4.1). The potential evapotranspiration was based on 12 mean monthly values of Penman-Monteith (PET 2). Figures B.4 and B.5 show the observed and simulated hydrographs. Table A.5 gives the parameter set.

Table 4.5: Objective functions of scenario 5 and its validation for the Upper Metuje catchment.

Period	**lnReff**	**Reff**	**VE**
Calibration (1982--1993)	0.77	0.63	2%
Validation (1994--2006)	0.65	0.44	0%

Model equifinality

Model equifinality represents a problem, which arises that many parameter combinations, often widely distributed over their individual feasible ranges, lead to acceptable model performance (Wagener et al., 2004). To get an impression about the model equifinality, we created Figure 4.3, which contains boxplots (Section 3.4, Figure 3.5) for the standardised ranges of model parameters (Section 3.4, Equation 3.14). The graph shows the magnitude of the parameters after the automatic calibration within the given boundaries (Table 4.1). The figure is based on total number of eight calibrated parameter sets for Scenario 2 and variant PET 2. The calibration criterion ($lnReff$) for all eight parameter sets varied between 0.74 and 0.77. The

upper three sub-figures show parameters of the distributed snow and soil routines for the three land cover classes (A, B, and C) separately. The lower graph (D) illustrates the standardised ranges of the lumped response function and routing routine. Parameter uncertainty is rather high, especially for the snow and soil boxes (CFMAX, CFR, CWH). The model is rather stable for the groundwater boxes, except for K0.

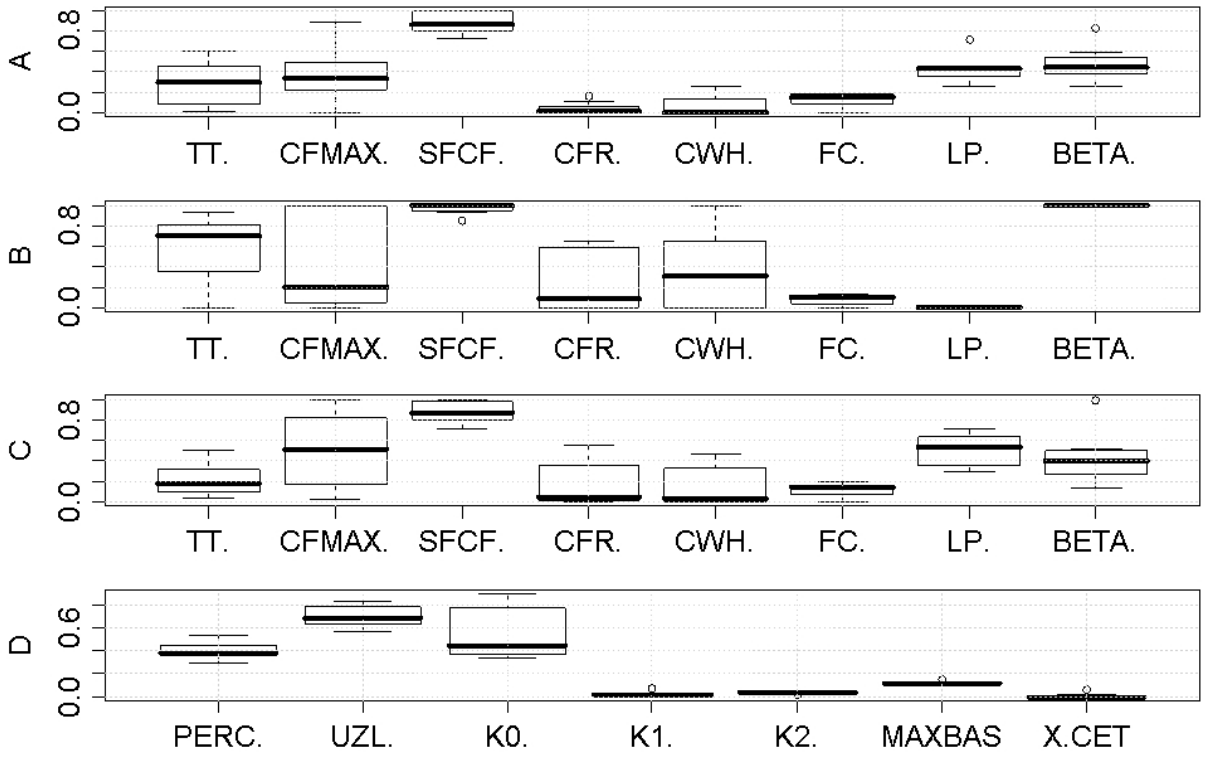

Figure 4.3: Standardised ranges of model parameters for distributed snow and soil routines (A: Agricultural area, B: Built-up area, C: Forest) and lumped response function and routing routine (D).

4.1.2 Validation

The HBV model validation is based on application of the calibrated model (Section 4.1.1) to simulate streamflow during an independent period from the calibration. We also will use the model to compare the observed groundwater heads with the simulated groundwater storage.

Streamflow

The first model validation uses parameters from scenario 2, variant PET 2 (017). Because

of the sudden temporal change in groundwater abstraction in 1994, we split the validation period into two parts (1990--1993) and (1994--1997), as it is shown in Figure 4.1 (Validation 1 and 2). The hydrograph for both validations is illustrated in Figure B.6 (whole flow range), with focus on low flows in Figure B.7. There is a general agreement between observed and simulated discharge. The timing of peaks coincides (except for the spring flood in 1995; the reason is likely an error in the temperature data, see x-axis), only the magnitude differs. This is acceptable because more weight have been put on low flows. The objective functions are written in Table 4.6. For $lnReff$ and $Reff$ there is an expected decrease in the objective functions from the first undisturbed period to the second disturbed one. In case of the volume error, the difference between simulated and observed discharge is higher for the first sub-period than for the second one, which was not expected.

Table 4.6: Objective functions, validation, Upper Metuje.

period	**lnReff**	**Reff**	**VE**
1990--1993	0.59	0.45	-21%
1994--1997	0.53	0.26	-11%

Second, we also validated the reference model (scenario 5) on the disturbed period (1994--2006). The values of objective functions are provided in Table 4.5. They show a better agreement than results of the previous model (Table 4.6), especially the zero volume error. The goodness of fit of the hydrographs for the validation period can be derived from Figures B.8 and B.9. In general, the observed and simulated low flows correspond rather well. However, in some cases there is a deviation. For example the magnitude of severe drought in 2004 was not simulated properly. The outcome from the reference model (scenario 5) will be used for drought identification and analysis (Chapter 5).

Groundwater storage

Simulated groundwater storage can not directly be compared with observed groundwater heads. The HBV simulated groundwater storage was recalculated into simulated groundwater head by Equation 3.13 for each period separately. The observed groundwater data were those from the observation well VS-3 (Section 2.1.3).

The observed groundwater heads from the well VS-3 and the converted groundwater storages are shown in Figure B.10 for the undisturbed period (1981--1993) and in Figure B.11 for

the disturbed period (1994--2006), as indicated in Figure 4.1 (Validation 3 and 4, GW). The correlation coefficient ($r^2 = 0.76$) agrees rather well for the first one including extreme values. The recession also looks realistic. The goodness of fit decreased for the second period, in which r^2 dropped to 0.54. For example, the observed low groundwater heads in the autumns of 1993[1] and 1994 did not match with simulated storage at all and the differences between extreme values are higher than during the undisturbed period (1982--1993).

4.2 Upper Sázava catchment

The hydrological system and available data for the Upper Sázava catchment are described in detail by Rakovec (2009) and a brief overview is given in Section 2.2. Similarly to the Upper Metuje, human influence complicates the modelling of catchment water balance. Contrary to the Upper Metuje, effluent water from industrial and municipal sources exceeds water abstractions in the Upper Sázava. On average, the water surplus is about 40 $l.s^{-1}$ for the period 1980--2008 (Figure 2.19).

The HBV modelling scheme with the different calibration and validation periods is presented in Figure 4.4. A comprehensive explanation of the calibration and validation is given in Sections 4.2.1 and 4.2.2.

4.2.1 Calibration

The experiences from the calibration of the HBV model for the Upper Metuje were used for the Upper Sázava, in addition, we investigated two scenarios and their impact on the model goodness of fit:

- different precipitation input (scenario 1);
- length of the calibration periods (scenario 2).

The scenarios were made of 3 elevation zones and 3 land cover classes according to Table A.2. Temperature was used from the Přibyslav station (Section 2.2.3) and the potential evapotranspiration was based on the Penman-Monteith method, calculated for the Svratouch station (Figure 3.2).

[1] Autumn 1993 belongs to the Czech hydrological year 1994.

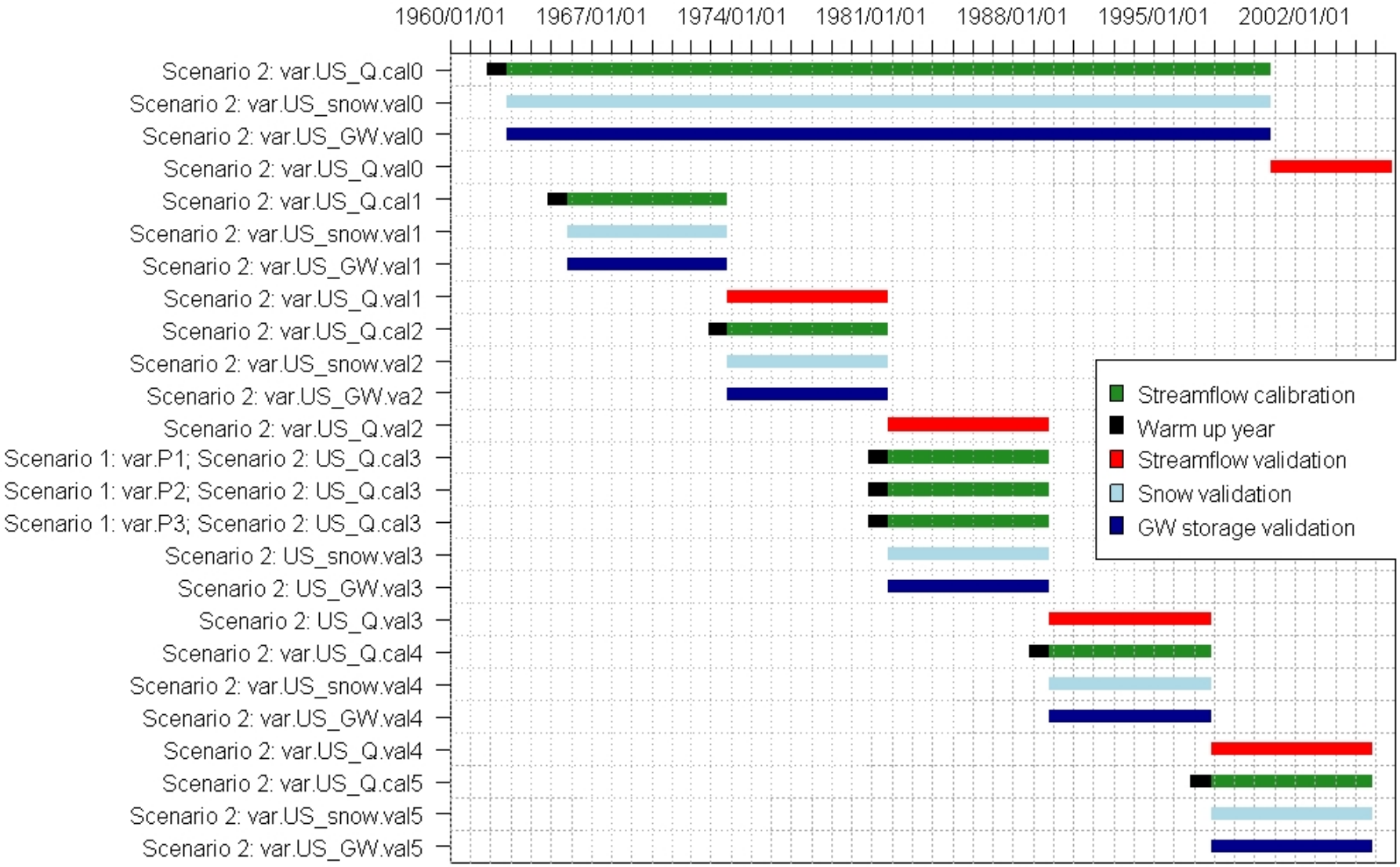

Figure 4.4: Hydrological modelling scheme for the Upper Sázava catchment.

Scenario 1: the effect of precipitation input

Since more precipitation records were available in and near the Upper Sázava, we defined three precipitation variants as proposed by Rakovec (2009). The model rainfall inputs are based on (Section 2.2.3):

- records only from the two professional meteorological stations in Přibyslav and Svratouch near the catchment with the weight based on Thiessen polygons ($var.P1$);
- record only from one non-professional station in Žďár nad Sázavou, Stržanov, which is located in the middle of the catchment ($var.P2$);
- precipitation derived as an arithmetic mean from the four stations in Přibyslav, Svratouch, Krucemburk and Přibyslav ($var.P3$).

The calibration period for scenario 1 was set at 1 November 1981 to 31 October 1989 (Scenario 1 $var.P1$ to $var.P3$), to enable comparison with the Upper Metuje. Hydrographs for the three variants and the observed one are plotted in Figure B.12. The timing of observed and simulated high flows is identical in most of the cases, only the magnitude differs sometimes. Figure B.13 provides only the low flow range. There are no major differences in simulated streamflow among the precipitation variants. However, in general the pattern between the observed hydrograph and the simulated hydrographs differs. A reason for this can be the already mentioned human influence, which is more relevant in drier periods, when the ratio of the effluent water in the streamflow is higher.

Table 4.7 shows the objective functions for the precipitation variants (Scenario 1 $var.P1$ to $var.P3$). All HBV models underestimate the streamflow volume (positive volume error). The best model performance was achieved using the precipitation input $var.P1$. For that case, the calibration criterion of lnReff reached 0.75 which could be classified as sufficient, but the volume error was too high (13%). Objective functions become worse from $var.P1$ to $var.P3$, implying that the data from the two professional meteorological stations are most representative for Upper Sázava, even though the stations are situated outside the catchment. The precipitation input of var 2 which is based on one rain gauge in the middle of Upper Sázava shows poorer performance than using data from professional stations outside the catchment. The last approach using a simple average of four rain gauges without considering the weight associated with the area failed with a lnReff of 0.63 and a volume error 19%.

Table 4.7: Objective functions of scenario 1 for the Upper Sázava catchment.

Precipitation variant	**lnReff**	**Reff**	**VE**
$var.P1$	0.75	0.70	13%
$var.P2$	0.72	0.60	14%
$var.P3$	0.63	0.40	19%

Scenario 2: length of the calibration period

In this scenario, the values of objective functions for different lengths of calibration periods (Scenario 2, $var.US\_Q.cal0$ to $var.US\_Q.cal5$) are compared. We distinguished five independent eight year periods, with an overlap of only one warm-up year. We can compare objective functions for the short eight years calibrations ($var.US\_Q.cal1$ to $var.US\_Q.cal5$) with the one from the long calibration of 37 years (1963--2000, $var.US\_Q.cal0$). The time periods were selected according to the approach of Klemeš (1986), which was also used by Perrin et al. (2001). The precipitation input is identical to $var.P1$ of scenario 1, which is from the professional stations in Přibyslav and Svratouch.

In Table 4.8, the highest values for the objective functions are given for the long calibration period 1963--2000 and for the five eight year sub-periods. On average the models calibrated for shorter periods give a slightly better lnReff than the model calibrated for long period of 37 years. The differences in the low flow range of the hydrograph can be significant, as illustrated for the low flows in 1975 and 1976 in Figure 4.5. While the results of short-term calibration ($var.US\_Q.cal2$) do follow the major observed low flow, the long-term calibration ($var.US\_Q.cal0$) does not identify severe extremes.

Two reference models were classified for drought analyses. First one covers the period from 1963 to 2000 ($var.US\_Qcal0$) for the long term evaluation of droughts (Section 5.3), the values of the parameter set are listed in Table A.6. Second one includes a model which was additionally calibrated from 1982 to 1993 according to scenario 1 ($var.P1$) to enable a comparison with the Upper Metuje catchment by using the same time window of twelve years (Section 5.4).

4.2.2 Validation

Besides validation of HBV models against streamflow and groundwater storage as for the Upper Metuje catchment, we could also check the performance of the snow routine. Groundwater and snow validation is done for the calibration periods (Figure 4.4), while streamflow validation

Table 4.8: Objective functions of scenario 2 for the Upper Sázava catchment.

Length of calibration	**Code**	**lnReff**	**Reff**	**VE**
1963--2000	$var.US\_Q.cal0$	0.63	0.61	15%
1966--1973	$var.US\_Q.cal1$	0.67	0.60	18%
1974--1981	$var.US\_Q.cal2$	0.62	0.62	11%
1982--1989	$var.US\_Q.cal3$	0.75	0.70	13%
1990--1997	$var.US\_Q.cal4$	0.67	0.64	14%
1998--2005	$var.US\_Q.cal5$	0.62	0.51	5%
average of $var.US\_Q.cal1$ to $var.US\_Q.cal5$		0.67	0.61	12%

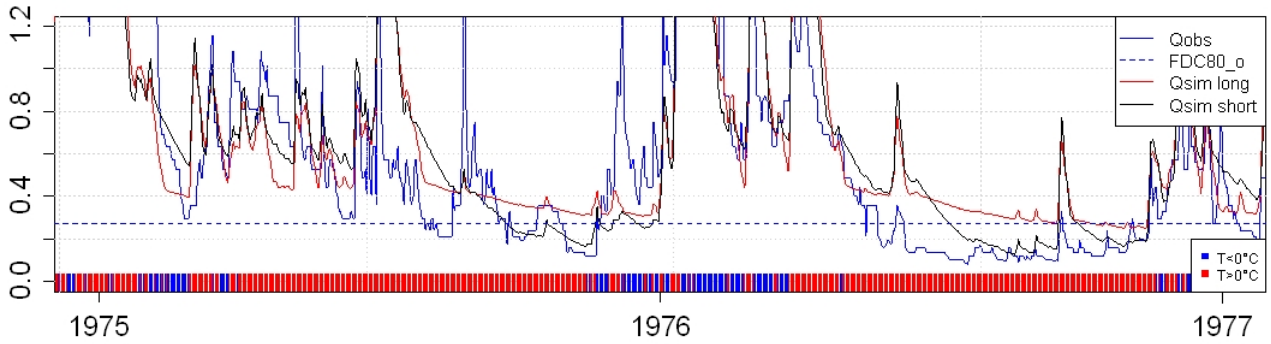

Figure 4.5: Observed and simulated hydrographs from a model based on a short calibration period (1974--1981, $var.US\_Qcal2$) and a model based on a long calibration period (1963--2000, $var.US\_Qcal0$) for low flows in 1975 and 1976 (Upper Sázava catchment).

is done for the period which follows the calibration. The over-all scheme is sketched in Figure 4.4.

Streamflow

The streamflow validation is expressed by values of objectives functions in Table A.7. The lnReff varies around 0.50 and similar to the calibration, the HBV underestimates the flow according to the volume error (VE).

The full and zoomed to low flow hydrographs for validation ($US\_Q.val0$) of calibrated parameters ($US\_Q.cal0$, Table A.6) and observed streamflow are shown in Figure B.14. The overall agreement is rather good, however the simulated low flows did not capture the fluctuations, as happened in the calibration.

Groundwater storage

In spite of lack of well developed aquifers in the Upper Sázava catchment, we tried to make a link between the groundwater observations from the Radostín well (Section 2.2) and the HBV simulated groundwater storage. We applied the same approach as described in Equation 3.13. Results for the calibration period 1963--2000 are shown in Figure B.15. The correlation coefficient ($r^2 = 0.21$) indicates a weak agreement between the measured heads and the modelled groundwater storage. The very different geology might be the reason, because the major part of the catchment consists of hard rock as opposed to the area where the shallow Radostín well is located where Mesozoic sediments outcrop. Another reason for the disagreement could be the uncertainty in the observed data. CHMI could not provide information on the sudden change in the groundwater regime from 1989 onwards.

Correlation coefficients for the validation sub-periods ($var.US\_GWval0$ to $var.US\_GWval5$ in Figure 4.4) are given in Table A.8. No relationship was found between the simulated and observed time series in the sub-period 1982--1984, but contrary to it, some agreement occurs in the sub-period 1998--2005 ($r^2 = 0.43$). The average correlation coefficient for the five sub-periods is 0.26, which is slightly higher than the r^2 of 0.21 for the model calibrated for the long period (1963--2000).

Snow

Measured weekly data of water storage in snow are available from Žďár nad Sázavou, Stržanov. These data are used to verify the snow routine of HBV model. Observed and simulated data are shown in Figure B.16 for the long calibration period ($var.US\_GWsnow0$, 1963--2000). The general pattern agrees well, although the correlation coefficient is not higher than 0.57. According to CHMI (2009), the measured snow storage is supposed to be underestimated. This is supported by the HBV simulation. The observed snow data are rarely above the simulated ones. The missing data for the years 1973, 1975, 1976 have no influence on r^2. Values of r^2 for sub-periods can be found in Table A.9. The average r^2 for the sub-periods is lower than the one for the longer period (1963--2000), which is different from the groundwater storage.

4.3 Low flow characteristics

The low flow characteristics of the observed and simulated streamflows in the Upper Metuje and Upper Sázava catchments are shown in Figure 4.6. The flow duration curve (FDC), annual base flow index (BFI) and annual minimum flow (AM) are defined in Section 3.3.2. Annual minimum flows were derived by using a moving average of seven preceding days as a smoothing filter. In this section we focus only on eight hydrological years (1982--1989) to enable comparison between both catchments and excluding major human influence.

Flow duration curves of the observed and simulated streamflow in the Upper Metuje correspond very well and they have a more gentle slope than the FDC for the Upper Sázava. This indicates that the streamflow variability for the Upper Metuje is lower than for the Upper Sázava. This corresponds with the nature of the catchment. The Upper Metuje is a slowly responding catchment and the Upper Sázava a flashy one (Chapter 2). FDCs of the Upper Sázava do not correspond that well. Besides some deviations in the higher flows due to the logarithmic calibration criterion (Section 3.2.2), FDCs also differ in the low flows. The main reason is the very low observed discharge in autumn of 1989 (Figure B.13). The shape of FDCs indicates good agreement within the Upper Metuje but poor with the Upper Sázava, as shown in Section 4.2.

Base flow indices were calculated according to Hisdal et al. (2004). The annual values for the Upper Metuje catchment vary between 0.6 and 0.8, which are typical values for for permeable catchments. Clearly, lower BFI values were calculated for the Upper Sázava, where the BFI even dropped below 0.4 in 1987 for the observed flow and in 1988 for the simulated streamflow.

Annual minimum flows. The AM(7) values for the Upper Metuje are approximately twice as high than those for the Upper Sázava. It is remarkable, that AM(7)s derived from the simulated time series for the Upper Sázava are nearly constant over eight year period, indicating difficulties for HBV to simulate low flows successfully.

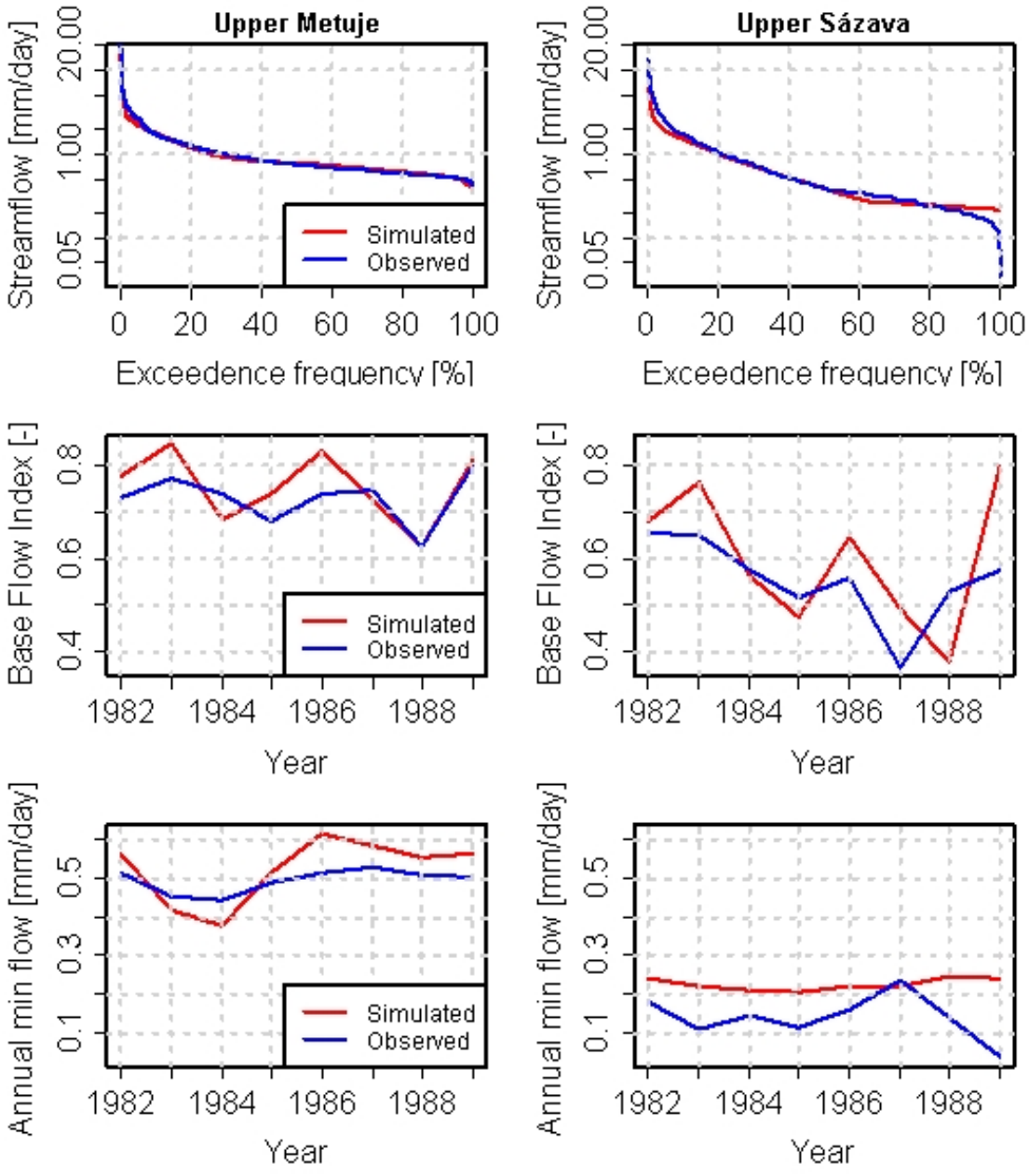

Figure 4.6: Low flow characteristics: flow duration curve, annual base flow index and annual minimum flow for the Upper Metuje and Upper Sázava catchments (1982--1989).

Chapter 5

Results of drought analysis

5.1 Meteorological drought characteristics

Meteorological drought was assessed through precipitation simulated by HBV (Psim, Section 3.2.2, Equation 3.9).

Because of the usually occurring high number of days without precipitation, we needed to transform the data by using a pooling procedure of moving average of n-days, otherwise the 80-percentile of the duration curve would be zero (MA 1 in Figure 5.1). We applied a n of 10 and 30 days to the simulated precipitation and we can observe a gradual decrease of the steepness of the duration curves (Figure 5.1), implying that the 80-percentile increases with higher n. The duration curves coincide for both the Upper Metuje and Upper Sázava catchments.

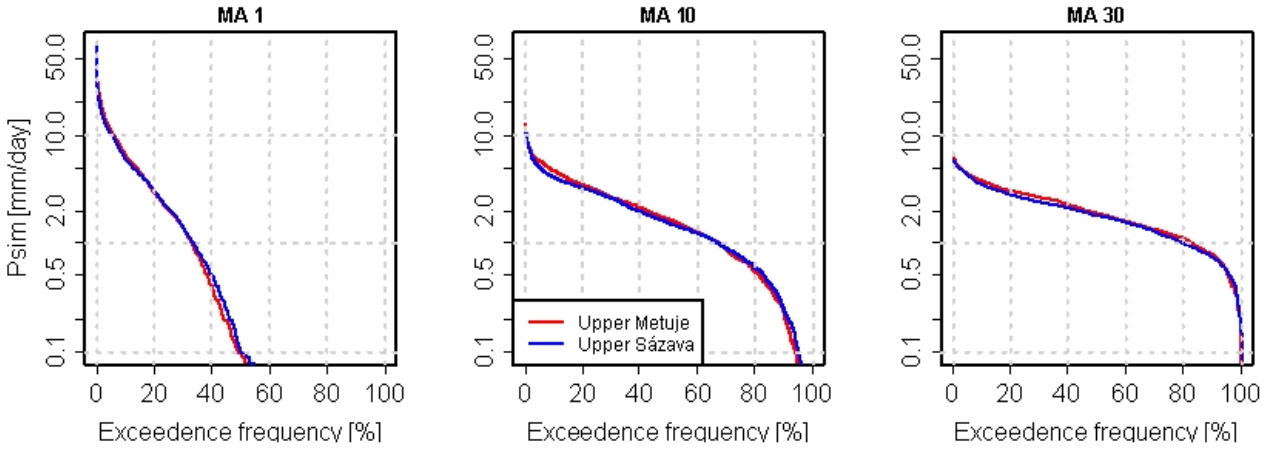

Figure 5.1: Precipitation duration curves for the Upper Metuje and Upper Sázava catchments (1982--1989).

For drought identification we applied a monthly threshold with a moving average of 30 days to the smoothed time series of simulated precipitation. We investigated, what effect the pooling has on the identified meteorological drought. We used the moving average of 10 and 30 days on a subset from the Upper Metuje (1982--1989). The results are shown in Figure 5.2. Clearly, the temporal variability of precipitation is much higher for n = 10 than for n = 30. The number of drought is also higher for precipitation based upon n = 10 (Table A.10), but the droughts are shorter and have a lower mean deficit. Since we are more interested in long-term droughts, we will use for drought identification the precipitation series based upon n = 30, which only identifies the more pronounced meteorological droughts. Note, that droughts shorter than 3 days are excluded from Table A.10.

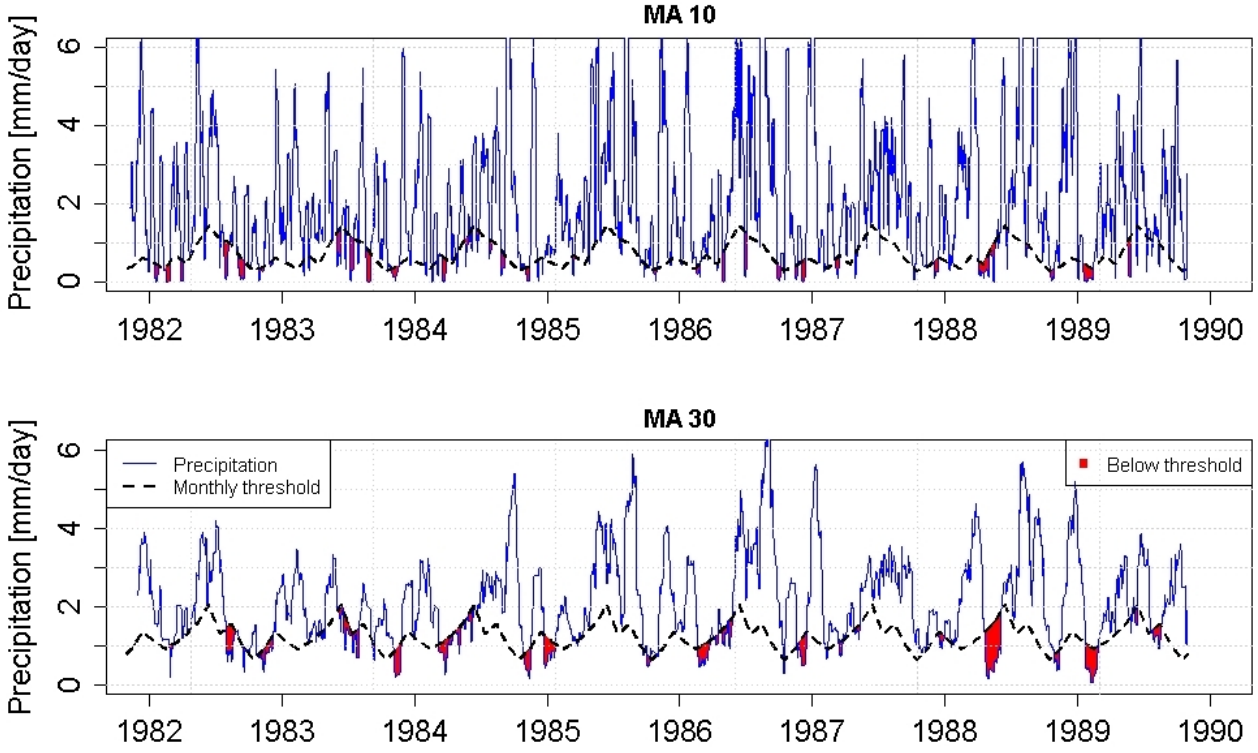

Figure 5.2: Meteorological drought for two pooled precipitation time series (MA = 10 and 30). (1982--1989) for the Upper Metuje catchment.

5.2 Upper Metuje catchment

5.2.1 Drought identification

For drought identification within the Upper Metuje we investigated the period 1982--2006, which consists of the calibration (1992--1993) (scenario 5) and the validation validation period

(1994--2006), as described in Sections 4.1.1 and 4.1.2. The threshold method (Section 3.3.3) was applied. The smoothed monthly threshold values derived for the undisturbed period (1982--1993) were also applied on the disturbed one (1994--2006). This is to identify droughts in the disturbed period and to find out, whether the drought became more frequent after the increased abstractions since 1994. The summary of characteristics of meteorological and hydrological droughts is shown in Table[1] 5.1 for the years 1982--2006, and in Tables A.11 and A.12 for the sub-periods.

Table 5.1: Characteristics of drought events for the Upper Metuje catchment (1982--2006).

Type of drought	**Number**	**Mean number of days**	**Mean deficit [mm]**	**Mean intensity [mm/day]**
Meteorological	107	15.7	6.4	0.32
Soil moisture	83	18.9	--	--
Groundwater	39	45.4	--	--
Streamflow sim.	92	18.9	1.06	0.04
Streamflow obs.	134	15.5	1.4	0.05

In the period 1982--2006, meteorological drought occurred most frequently, 107 in total. The number of soil moisture droughts was about twice as high than in groundwater. The latter lasted longer, which corresponds with a bigger persistence of the groundwater system. Drought in simulated streamflow occurred 92 times, with a average duration of almost 19 days, whereas the number of droughts in observed streamflow (134) was higher, but on average they lasted shorter (15.5 days).

The meteorological droughts with the biggest total deficit (41 mm) started in spring 1999 and lasted for 2 months, the second major drought occurred in spring 1988 with a total deficit of 33 mm (Figures B.17, B.18). The most severe soil moisture drought took place from August 1982 to January 1983 with a maximum deficit of 32 mm in December 1982 (Figure B.17). The longest multi-year groundwater drought consists of two mutually dependent droughts which were interrupted only by a break of 12 days. The groundwater drought started in July 1983 and finished in September 1984 (Figure B.17). The maximum deficit in groundwater occurred

[1]The deficit and intensity has only been calculated for fluxes (precipitation, streamflow) and not for state variables.

in March 2006 (47 mm) (Figure B.18). The biggest drought in simulated streamflow (14 mm) consists of two dependent droughts from December 2005 to March 2006, which was interrupted only by 3 days when the discharge exceeded the threshold level (Figures B.17, B.18). The reason of the interruption were two days of temperature about 1°C (17 and 18 February 2006), which caused snow melt. Another long simulated streamflow drought was identified in May 1984 for four months with a total deficit over 8 mm.

The temporal development of drought in precipitation and simulated streamflow is shown in Figure 5.3. In Figure 5.4 this was done for drought in observed streamflow. These graphs illustrate the deficit volumes of precipitation and streamflow droughts using the threshold method. The magnitude (deficit) of the drought equals the area of the rectangles, since the width stands for the duration and the height for the intensity. The colour of x-axis describes the air temperature to distinguish between summer and winter droughts.

The streamflow droughts are often mutually dependent, since we do not pool drought. The intensity within a cluster of mutually dependent droughts is increasing, e.g. in winters 1983--1984, 1993--1994, 2000--2001 and 2005--2006 (Figure 5.3). The reason for interruptions of the mutually dependent droughts seems to be caused by snow melt water, which appears in periods when air temperature exceeds 0 °C (see the x-axis in Figure 5.3).

As already mentioned more than half of the larger droughts in simulated streamflow take place in winter, which does not really correspond to lack of precipitation (i.e. snow), but the impossibility to recharge to soil moisture, groundwater and streamflow.

When we compare the droughts in simulated and observed streamflow (compare Figures 5.3 and 5.4), the simulated droughts in summer 1983 and summer 1984 did not occur in the observed ones and on the other hand, HBV completely missed the extensive 2004 drought. The year 2004 comes from the validation period, which might be a reason to miss it.

Tables A.11 and A.12 show that the mean deficits and intensities for droughts in observed and simulated streamflow are smaller for the undisturbed period compared to the disturbed period. This does not have to be exclusively related to higher groundwater abstractions but it can be simply caused by the higher precipitation deficits. A major difference occurs between the number of observed and simulated streamflow droughts (41 vs. 83) during the disturbed period. The model is not calibrated on this period, which might be a reason, in addition to the larger groundwater abstraction which is not included in the simulated series.

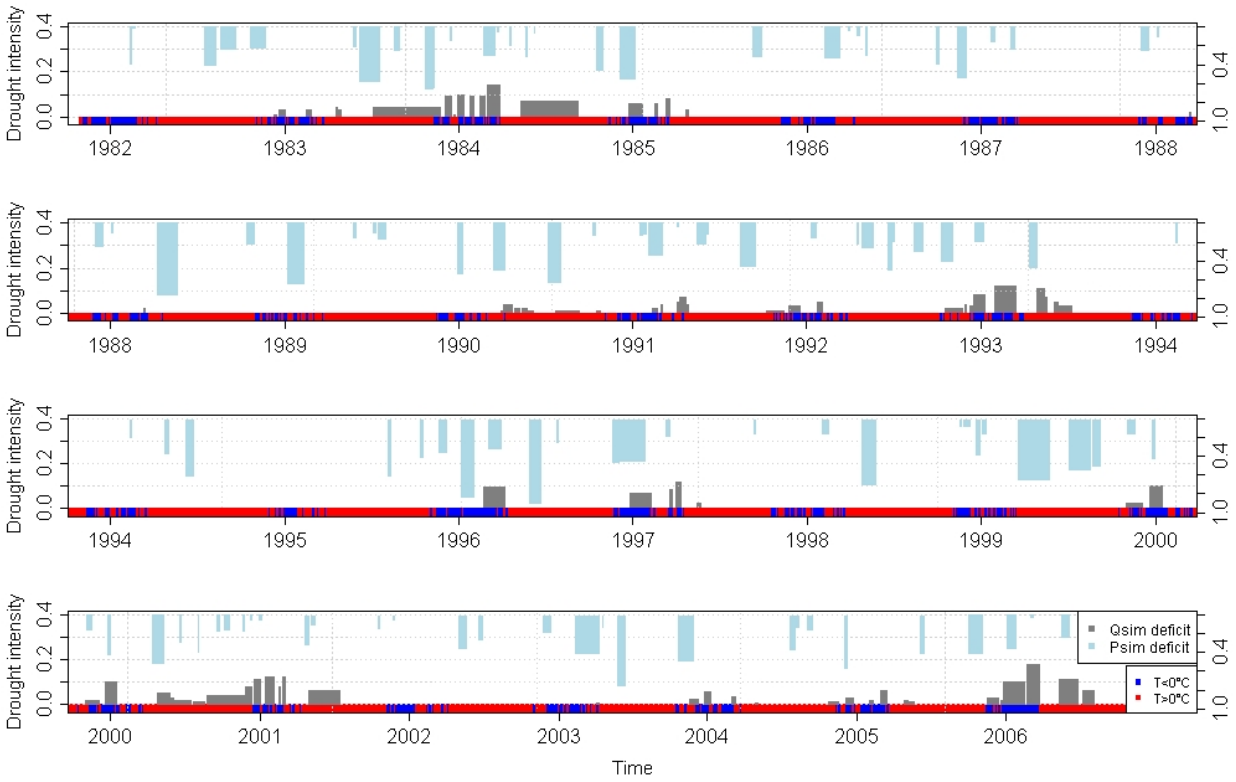

Figure 5.3: Duration and intensity of droughts in precipitation and simulated streamflow drought using a monthly threshold for the Upper Metuje catchment.

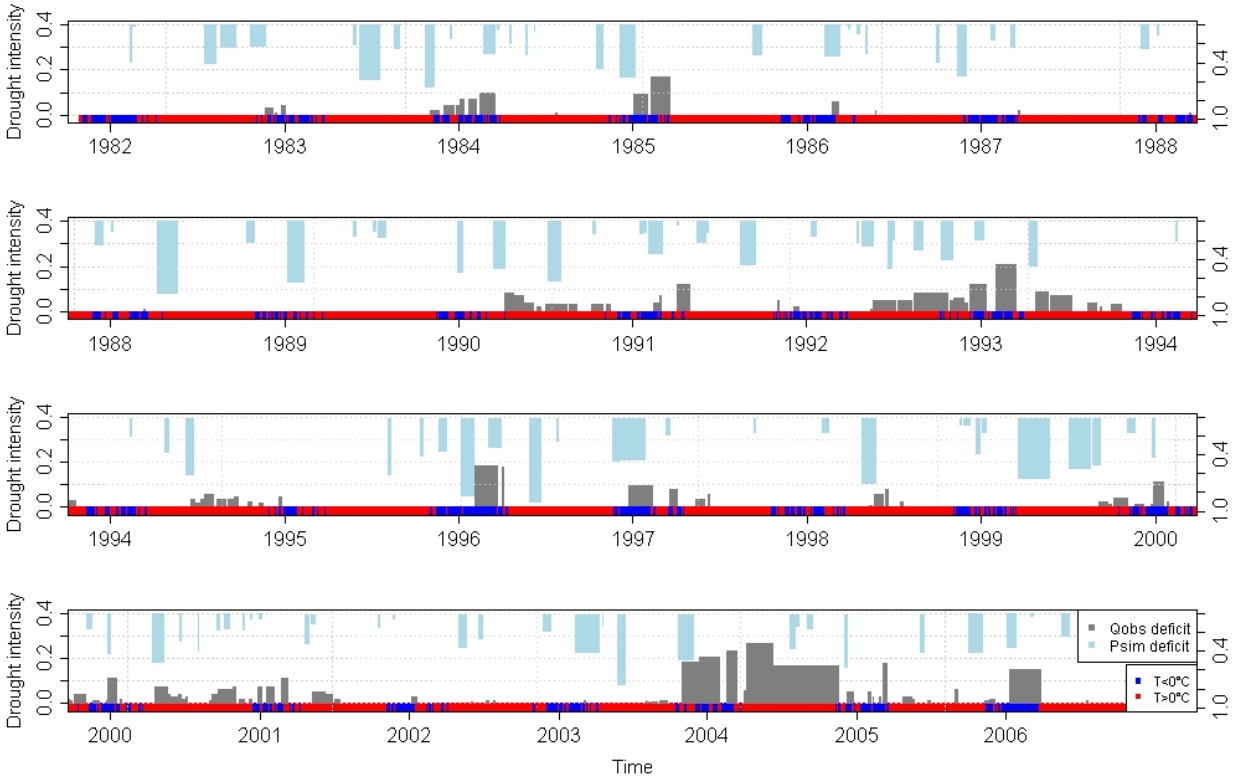

Figure 5.4: Duration and intensity of droughts in precipitation and observed streamflow drought using a monthly threshold for the Upper Metuje catchment.

5.2.2 Drought propagation

Drought propagation from a meteorological drought towards a hydrological drought is illustrated in Figures B.17 and B.18 for the whole time period (1982--2006). In this section we focus on two example periods, i.e. 1982--1984 and 1988--1990 (Figure 5.5). The droughts are identified by the threshold method, additionally the meteorological drought is also characterised by the sequent peak algorithm (SPA), which defines the end of drought when the deficit storage is completely refilled (Section 3.3.2).

The behaviour of hydrological components for the two example periods is completely different. The period 1982--1984 was very dry in terms of soil moisture, groundwater and streamflow. The period 1988--1990 did not experience any significant hydrological droughts even though in both years pronounced meteorological droughts were present. The key aspect in this is the timing of the meteorological drought.

The summer and autumn of 1982 were very dry in terms of precipitation, as indicated by the SPA in Figure 5.5 (upper left). This induced the soil moisture drought to start very quickly after the meteorological drought. However, the storage in groundwater did not drop below the threshold, because of the high storage of the preceding winter. The streamflow on its turn was still sufficiently supplied by groundwater storage. In the spring of 1983 no lack of precipitation occurred in terms of 80-percentiles of duration curves, but on the other hand there was insufficient precipitation, which could refill the soil moisture deficit of the previous dry period. Since the summer of 1983 was dry similarly to the year before repeated similarly to the year ago, the groundwater dropped below the threshold and the streamflow as well. The whole hydrological drought extended throughout the winter and spring of 1984. The whole system completely recovered in the summer of 1984 with high precipitation.

The period 1988--1990 includes one big meteorological drought in the late spring of 1988 with a deficit twice as high than for the previous example (1982--1984). Since the dry spring of 1988 was preceded by a relatively wet winter and followed by a rainy summer, no pronounced hydrological drought developed. Furthermore, the precipitation deficit in the winter of 1989 recovered due to snow melt in the following spring and hence was distinguished neither by soil moisture nor by groundwater. The consequences of the precipitation deficit in the summer of 1990 did only appear in soil moisture, because the depleted storage was soon refilled by sufficient rainfall in August and September 1990. Therefore the precipitation deficit did not propagate towards groundwater.

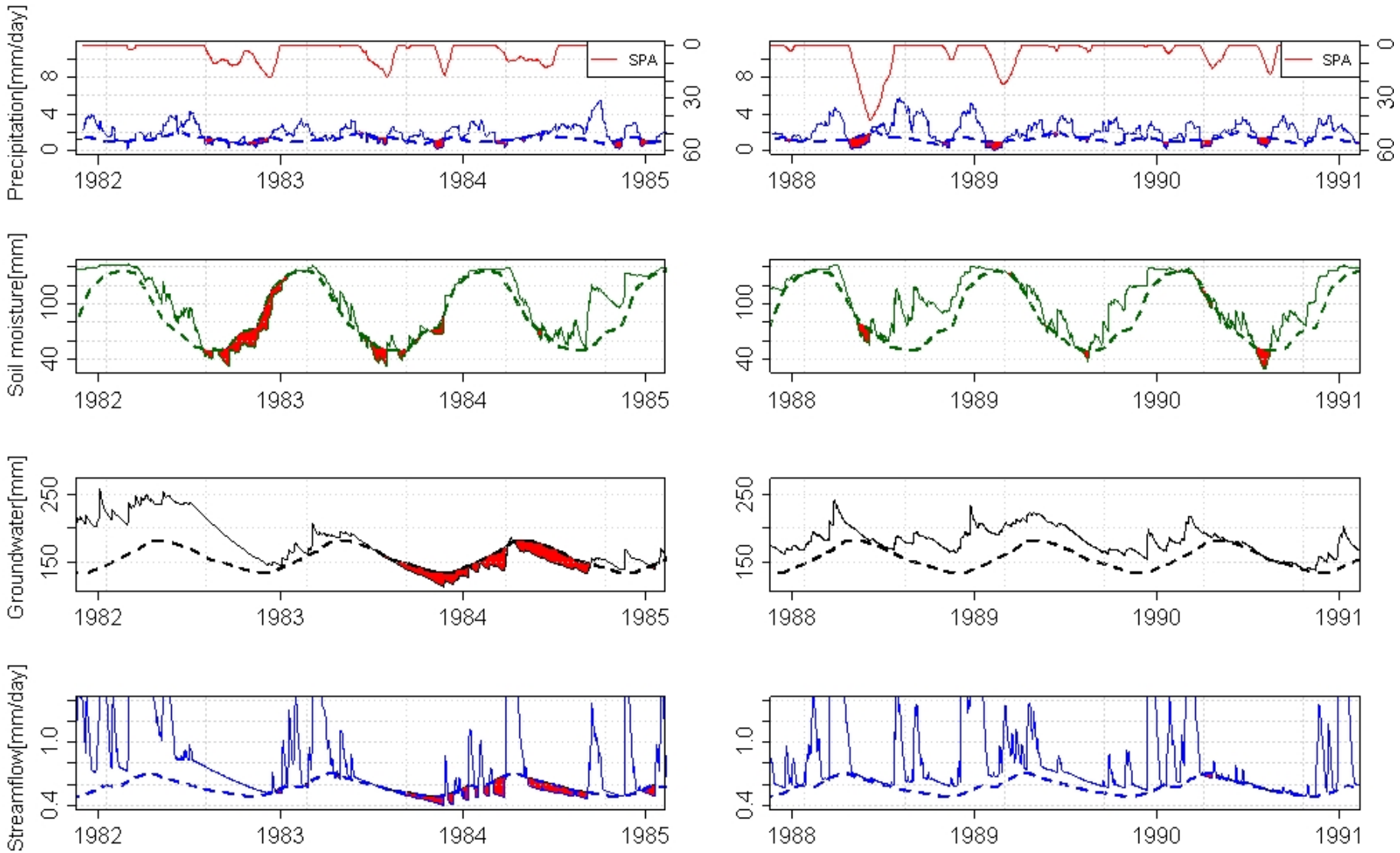

Figure 5.5: Examples of drought propagations for the Upper Metuje catchment.

5.3 Upper Sázava catchment

5.3.1 Drought identification

Meteorological and hydrological droughts within the Upper Sázava were identified using the threshold method (Section 3.3.3) over the period 1963--2000. The summary of drought characteristics is given in Table 5.2.

Meteorological drought were most frequent (179 times) with the shortest mean duration (15.1 days). Total number and duration of droughts in soil moisture and simulated streamflow are almost equal. The lowest number of drought can be found in groundwater (mean duration of 51 days). It is interesting to note that the total number of droughts in simulated flow is about 40% lower than in the observed series while the mean drought duration is about 65% higher. Since the mean deficit is identical for both, it indicates a higher mean drought intensity in the observed streamflow series.

Table 5.2: Characteristics of drought events for the Upper Sázava catchment (1963--2000).

Type of drought	**Number**	**Mean number of days**	**Mean deficit [mm]**	**Mean intensity [mm/day]**
Meteorological	179	15.1	5.7	0.27
Soil moisture	130	19.7	--	--
Groundwater	52	51.1	--	--
Streamflow sim.	130	20.7	1.2	0.04
Streamflow obs.	210	12.6	1.2	0.06

The meteorological droughts with the biggest total deficit (40 mm) can be found in the summer of 1990 and the spring of 1992 (Figure B.21), followed by 34 mm in the autumn of 1972 (Figure B.19). The most severe drought in soil moisture occurred in September 1969 and lasted over half a year with a maximum deficit of 46 mm in February 1970 (Figure B.19). The biggest groundwater drought is similar to the one in the Upper Metuje, a severe multi-year drought which consists of two dependent droughts which were interrupted by two weeks (Figure B.21). These mutual dependent groundwater droughts started in March 1990 and finished in August 1991 with a maximum deficit of 23 mm in April 1981. Droughts in the simulated streamflow showed the biggest deficit (12.6 mm) for the period May to December 1992 (Figure B.21). Another long

drought in the simulated flow started in June 1990 and lasted five months with a total deficit over 11 mm.

Temporal patters of droughts in precipitation and in simulated streamflow are shown in Figure 5.6 and for the droughts in the observed streamflow in Figure 5.7. Streamflow drought often occurs in winter season, when temperature is below zero. When we compare the droughts in the simulated and observed streamflow, the major streamflow droughts in 1990 and 1991 were simulated successfully. The model did not sufficiently capture the drought in streamflow for the summers of 1973, 1976 and 1989. On the other hand, the drought in the simulated streamflow for the summer of 1992 was not recorded at all. In general, the agreement between droughts in observed and simulated streamflow is bigger for winter droughts rather than for summer droughts.

5.3.2 Drought propagation

Drought propagation from a meteorological drought through the compartments of the hydrological system is shown in Figures B.19, B.20 and B.21. In this section we will focus on two example periods, i.e. 1982--1984 and 1988--1991 (Figure 5.8).

In the period 1982--1984, the meteorological drought developed together with the soil moisture drought in the autumn of 1982. Since the soil moisture and groundwater were recharged with high precipitation in the winter of 1982/83, the drought did not develop in groundwater and streamflow. Another big precipitation deficit (30 mm) occurred in the summer of 1983, the situation of the previous year repeated but it also propagated to the groundwater and a set of dependent streamflow droughts developed.

In the second period (1988--1990) (Figure 5.8) we can observe a fluctuating soil moisture storage due to high rainfall during the summer of 1988, which helped to overcome the deficit of 25 mm from the first half of the year. Generally, the low precipitation in the winter 1989--1990 did not recover the water deficit in the hydrological system and even though the deficit in precipitation was not so big (10 mm) related to the threshold level, severe soil moisture, groundwater and streamflow droughts developed.

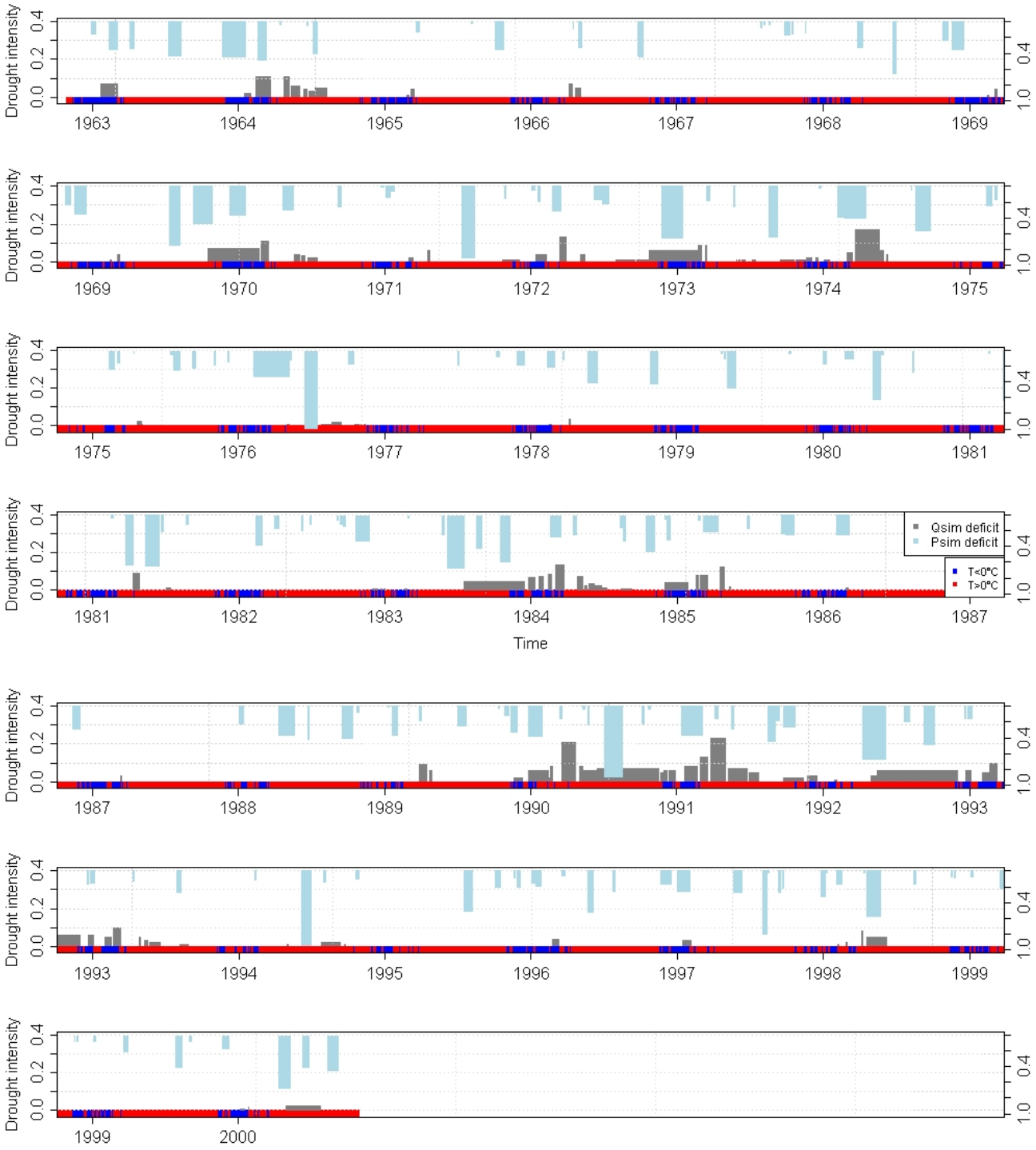

Figure 5.6: Duration and intensity of droughts in precipitation and simulated streamflow drought using a monthly threshold for the Upper Sázava catchment.

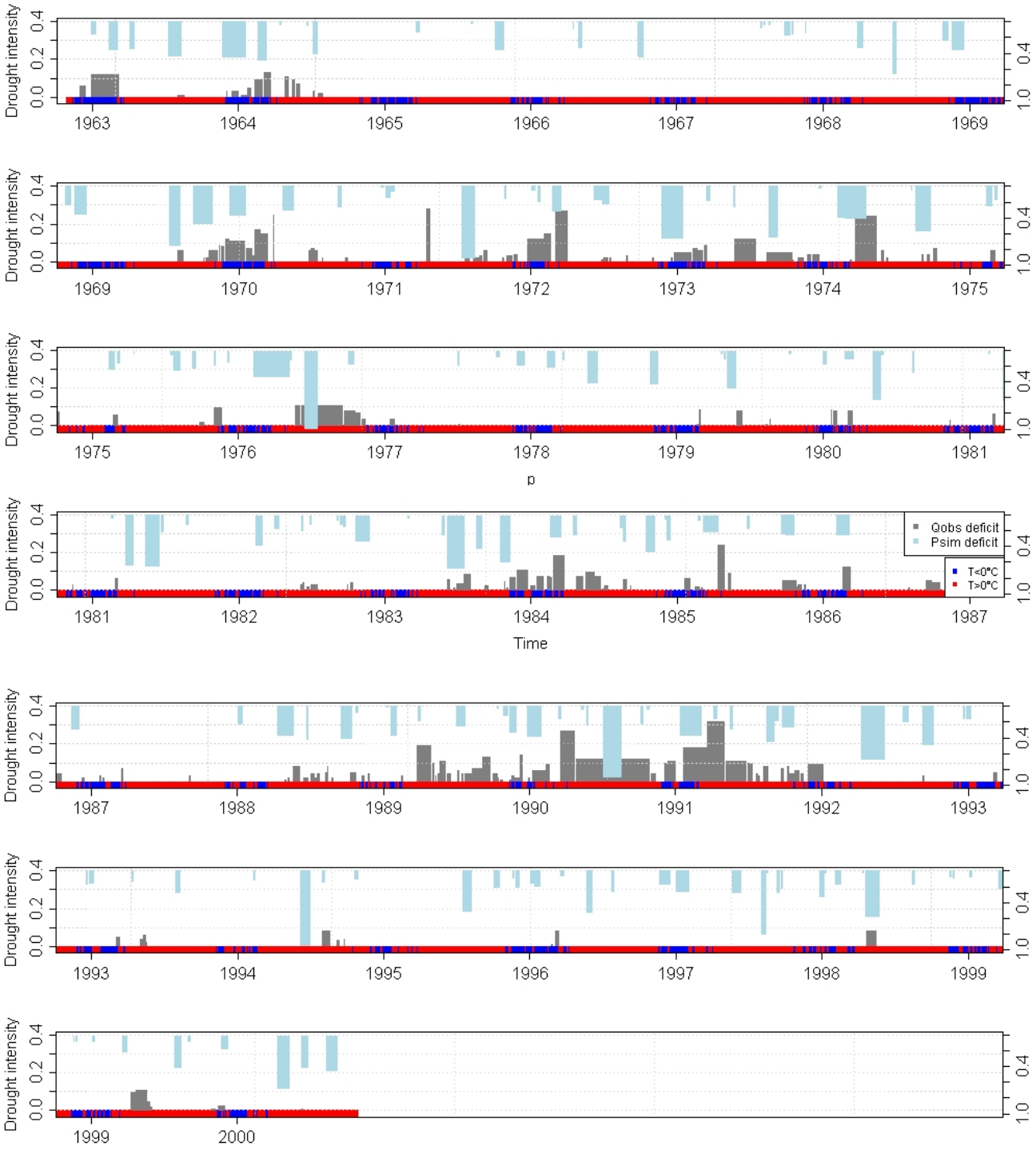

Figure 5.7: Duration and intensity of droughts in precipitation and observed streamflow drought using a monthly threshold for the Upper Sázava catchment.

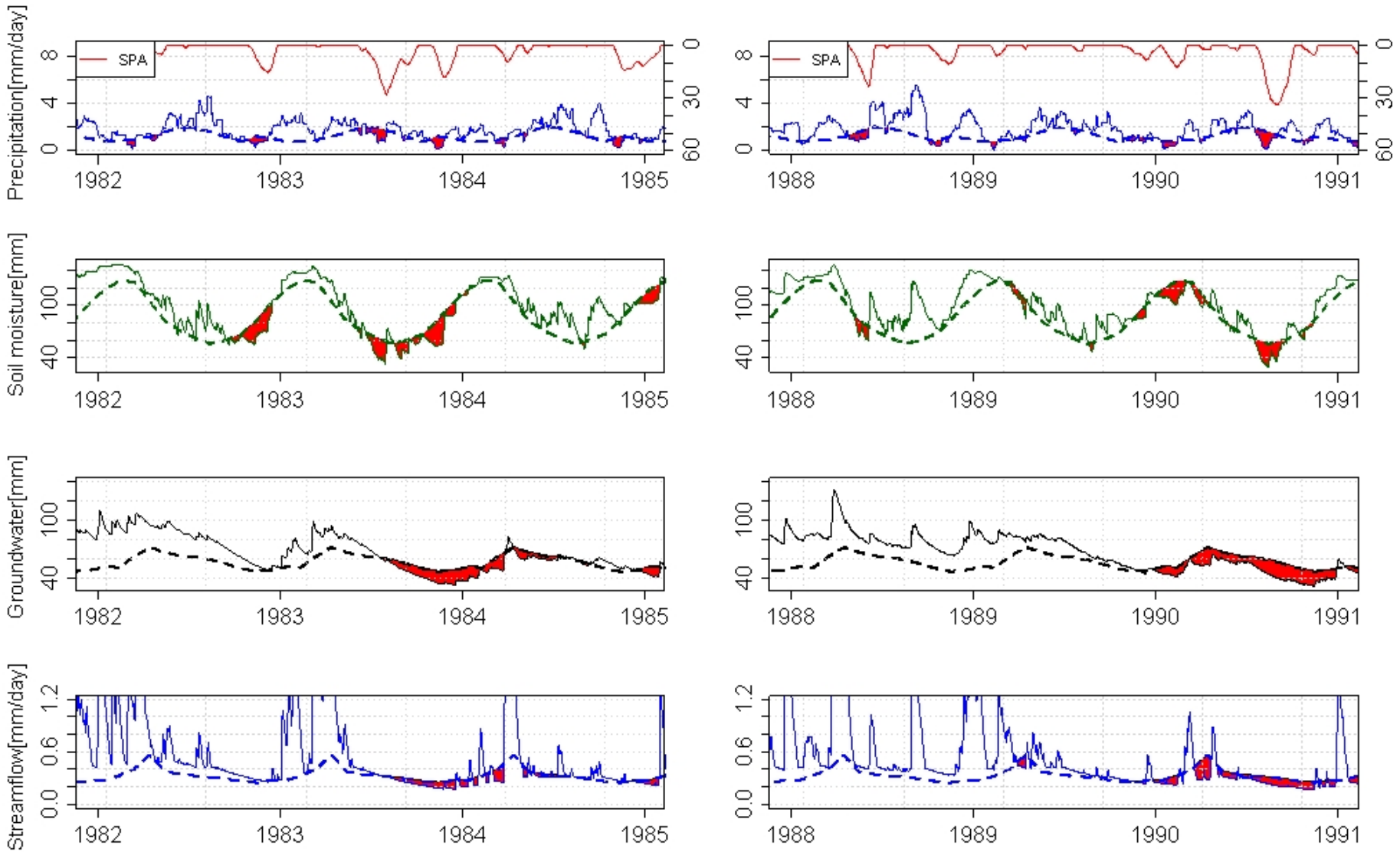

Figure 5.8: Examples of drought propagations for the Upper Sázava catchment.

5.4 Comparison of the drought propagation between the catchments

Tables 5.3 and 5.4 show the characteristics of the meteorological and hydrological droughts for the Upper Metuje and Upper Sázava. The characteristics are for the period 1982--1993, which is within the calibration period.

The number and mean duration of meteorological droughts are almost equal for both catchments.

The mean duration of soil moisture droughts is almost equal too, although they occur more often in the Upper Sázava. The maximum deficit (33 mm) in the Upper Metuje occurred in December 1982 whereas the maximum deficit was 28 mm in Upper Sázava in February 1990. Groundwater droughts developed 21 times in the Upper Metuje and 18 times in the Upper Sázava. The maximum groundwater deficit (35 mm) occurred in March 1984 and in March 1993 in the Upper Metuje. In the Upper Sázava maximum deficit was 28 mm in February 1990. The largest difference between the catchments is in the drought in the simulated streamflow. Streamflow droughts in the Upper Metuje occurred 51 times with mean duration of about 17 days, whereas in the Upper Sázava they only occurred 33 times with a higher mean duration (25 days). One would expect the opposite, such as presented for the droughts in the observed streamflow, i.e. a smaller number of streamflow droughts with a longer duration in the Upper Metuje as compared to the Upper Sázava.

Because of the inconsistency between the droughts in the simulated and observed streamflow, we decided to investigate them by the sequent peak algorithm (SPA), which enables us to pool the dependent droughts. Table A.13 shows the number of droughts for both catchments based upon the threshold method and the SPA. We can observe, that the number of droughts drops for all types of droughts when applying the SPA. However, the number of droughts in simulated streamflow in the Upper Sázava remains lower than in the Upper Metuje, even though the number of meteorological droughts is slightly higher in the Upper Sázava. Figure B.22 gives the temporal development of meteorological droughts in both catchments using SPA. Although differences in deficits occur between both catchments the pattern is similar.

Table 5.3: Characteristics of drought events for the Upper Metuje catchment (1982--1993).

Type of drought	**Number**	**Mean number of days**	**Mean deficit [mm]**	**Mean intensity [mm/day]**
Meteorological	54	15.4	5.93	0.3
Soil moisture	41	16.9	--	--
Groundwater	21	40.1	--	--
Streamflow sim.	51	16.8	0.83	0.04
Streamflow obs.	49	16.9	1.22	0.05

Table 5.4: Characteristics of drought events for the Upper Sázava catchment (1982--1993).

Type of drought	**Number**	**Mean number of days**	**Mean deficit [mm]**	**Mean intensity [mm/day]**
Meteorological	58	14.6	4.71	0.23
Soil moisture	51	16.5	--	--
Groundwater	18	46.4	--	--
Streamflow sim.	33	25.8	1.08	0.03
Streamflow obs.	66	12.2	0.74	0.04

Chapter 6

Discussion

6.1 Hydrological modelling using HBV

In the Upper Metuje (Section 4.1.1) we investigated the effect of model semi-distributivity on the objective functions (logarithmic model efficiency and volume error). We found, that breaking down of the land use and the elevation in a limited number of zones improves the model performance. That is in agreement with Uhlenbrook et al. (1999), who investigated the performance of HBV models for one and two land cover zones and for an increasing number of elevation zones.

The second scenario in Upper Metuje (Section 4.1.1) examined the importance of temporal resolution (regimes' vs. daily input) of the potential evapotranspiration input and also the selection of a suitable method. In terms of objective functions we did not find any differences between using daily and long-term mean monthly Penman-Monteith evapotranspiration. This completely agrees with Oudin et al. (2005a) who investigated the temporal resolution of Penman method for four types of conceptual models (including HBV) with different ways to calculate actual evapotranspiration in 308 catchments in different climate regions. They found that the differences between model efficiencies of both potential evaporation variants, i.e. daily versus long-term mean monthly on average did not show a significant degradation, since the drops in model performance never exceed 0.8%. Since the data demand for Penman-Monteith is rather high, we investigated also Thornthwaite method, which is based only on daily temperature. The outcome for the objective functions is identical for Thornthwaite and Penman-Monteith and also the simulated hydrographs of both variants are in the same agreement with observed data. Our results confirm the conclusions from Oudin et al. (2005b), who inspected 27 potential evapotranspiration methods for conceptual rainfall-runoff models and they found that the

McGuinness method (McGuinness and Bordne, 1972), based only on mean temperature and extraterrestrial radiation, to be the most suitable one. However, Penman-Monteith method which we applied in our study was ranked relatively high too.

Even though the model structure of the HBV delay version seems to be very suitable for the Upper Metuje, the obtained objective functions were worse than for the normal model structure. The lnReff decreased from 0.76 to 0.71 and the volume error increased from 3% to 11%, which disagrees with the results from Seibert (2000) who experienced an increased model efficiency from 0.73 to 0.76.

For the Upper Sázava we investigated scenarios of different precipitation inputs. The obtained objective functions confirm the expectations of Rakovec (2009) that the data from two professional stations outside the catchment in combination with Thiessen polygons would produce better modelling results than precipitation data only from a non-professional station in the middle of the catchment.

For the Upper Sázava we also investigated the impact of the length of the calibration period on model performance. Model performance in terms of objective functions becomes worse from many short calibration periods to one long calibration period.

It is important to address the possible human influence within both catchments. In case of th Upper Metuje we tried to eliminate it by using a period with low and constant groundwater abstraction, but in case of the Upper Sázava we struggled with the direct effluent flows from sewage disposal plants and the abstractions from surface water reservoirs. Since we did not have daily data of water releases, it was impossible to naturalise discharge (Rees et al., 2004), which was proved in scenario 4 for the Upper Metuje. Furthermore we should also address the reliability of the observed streamflow data. The low flow data from the Upper Sázava are likely to be negatively influenced by the gauging station structure that is very wide, insensitive to low flow.

6.2 Drought analysis

In our study we applied a monthly smoothed threshold for the drought analysis to detect deviations during the high as well as low flow seasons (Hisdal et al., 2004). However, you may argue, if we can still call a low flow below the monthly threshold a drought or better a streamflow anomaly, as Hisdal et al. (2004) suggest. The monthly-varying threshold level was applied only in few studies, for example, Van Lanen and Tallaksen (2007), where the authors

introduced this approach to cope with seasonality. However, from an ecological or agricultural point of view, winter droughts defined by a monthly varying threshold might not be relevant. On contrary for hydropower generation, a deviation can represent huge economic losses. That can happen, when the regular flood from snow melt does not come resulting in not filling up of the storage in the open water reservoirs.

Other studies (Hisdal et al., 2001; Hohenrainer, 2008) investigated identification of droughts by using a fixed threshold. They eliminated assessing of the seasonality by focusing only on summer droughts within a predefined summer period. Unlike those studies, we analysed droughts throughout the whole year. More pronounced droughts prevails in winter for both catchments, however, the summer droughts are more extensive.

Our approach to analyse drought propagation using simulated time series from HBV was identical to Hohenrainer (2008). Our objective to compare drought propagation between two different geological environments was infeasible, because of not fully convincing results from HBV for the Upper Sázava. The comparison of drought propagation between fast and slow responding synthetical catchments was carried out, for example, by Van Lanen and Tallaksen (2007). To make their study even more complex, the authors investigated the comparison of drought propagation for two contrasting climate regions: i.e. a humid continental and a tropical savanne one. Their results showed the expected pattern of higher number of shorter streamflow droughts in quickly-responding catchments and few but extensive droughts in slowly-responding catchments. Their success can be possibly explained by a different (coarser) data resolution and not modelling purely natural hydrological conditions.

Chapter 7

Conclusions & recommendations

Conclusions

- Hydrological modelling was successful for the Upper Metuje catchment including both streamflow calibration and streamflow and groundwater validation. The good quality streamflow data including low flows from a good gauging structure have contributed to this.

- Poorer results from the hydrological modelling were obtained for the Upper Sázava catchment, where the observed streamflow data, in particular the low flows, are strongly influenced by human activities. Without daily data of the effluent rates from sewage disposal plants we were unable to adequately naturalise daily flow.

- Drought identification for the Upper Metuje resulted in a good agreement between observed and simulated time series. In case of the Upper Sázava we cannot evaluate model performance, because we cannot assess the uncertainty in the observed streamflow record which is influenced by human activities and by a gauging station which is not designed for low flows.

- High precipitation deficits do not always lead to severe hydrological droughts. It depends on the timing of the precipitation deficit, with late summer usually being the most sensitive to lack of precipitation. The sequent peak algorithm appeared to be a useful tool to evaluate the deficit in fluxes, e.g. to investigate a meteorological drought.

- The drought signal in the Upper Metuje showed lag and attenuation when propagating through the hydrological system. Soil moisture drought still appears almost simultaneously

with the meteorological drought, but groundwater and streamflow droughts develop after extensive soil moisture deficits.

- Since no pooling of droughts was applied, droughts are often mutually dependent and within a cluster of dependent droughts, the drought intensity increases with time.

Recommendations

- For the study of man-influenced environment, daily abstraction and effluent rates should be known and it could be advisable to explore it with physically based models.
- For the investigation of droughts, the structure of the gauge station should be suitable to measure low flows with sufficient accuracy.
- In case of predominantly winter droughts, it is worthwhile to check the accuracy of discharge measurements for the winter period on ice.
- Future research should focus on:
  - the most suitable threshold and pooling procedure for meteorological drought;
  - how to evaluate mean deficit for state variables (water storage in soil and groundwater);
  - trends in observed and simulated time series;
  - a multi-model comparison.

Bibliography

References

Akhtar, M., Ahmad, N., and Booij, M. (2008). The impact of climate change on the water resources of Hindukush-Karakorum-Himalaya region under different glacier coverage scenarios. *Journal of Hydrology*, *355*(1-4), 148--163.

Allen, R., Pereira, L., Raes, D., and Smith, M. (2006). *Crop Evapotranspiration (guidelines for computing crop water requirements).* Retrieved March 24, 2009, from `http://www.fao.org/docrep/X0490E/X0490E00.htm`

BBC. (2009). *Desperation as Ethiopia's hunger grows.* Retrieved April 22, 2009, from `http://news.bbc.co.uk/2/hi/africa/7444753.stm`

Bergstrom, S., and Graham, L. (1998). On the scale problem in hydrological modelling. *Journal of Hydrology*, *211*(1--4), 253--265.

Bergstrom, S., and Sandberg, G. (1983). Simulation of Groundwater Response by Conceptual models. *Nordic Hydrology*, , 71--84.

Braun, L., and Renner, C. (1992). Application of a conceptual runoff model in different physiographic regions of Switzerland. *Hydrological Sciences -Journal- des Sciences Hydrologiques,*, *37*(3), 217--231.

Cech, L., Šumpich, J., and Zabloudil, V. (2002). *Jihlavsko.* Agency for nature conservation and landscape protection of the Czech Republic and Eco-centre Brno, Prague. In: *Protected Areas of Czech Republic, vol. VII.* (eds. Mackovčin P. and Sedláček M.), 528pp.

CENIA. (2008). IMS *map service.* Retrieved October 24, 2008, from `http://geoportal.cenia.cz`

CHMI. (2009). *Meteorological data online.* Retrieved February 24, 2009, from `http://www.chmu.cz/PR/praha/grafy/hk/grafy-ams.htm`

CHMI. (2009). *personal communication.*

Czech Geological Survey. (1995). *Geological map of Czech Republic, sheet: 04-31 Meziměstí.*

(scale 1:50,000.)

Dingman, S. (2004). *Physical Hydrology.* Prentice-Hall Inc., 646 pp.

Dratva, A. (1943). *Normální srážky 1876-1925 v povodí horního Labe (in Czech).* Ústav hydrologický a hydrotechnický v Praze.

Eckhardt, P. (1995). *Nížkov – final report of hydrogeological survey* (Tech. Rep.). GEMKO, Chrudim. (authorial copy)

Eckhardt, P. (2009). *personal communication.*

Faltysová, H., Mackovčin, P., and Sedláček, M. (2002). *Královehradecko.* Agency for nature conservation and landscape protection of the Czech Republic and Eco-centre Brno, Prague. In: *Protected Areas of Czech Republic, vol. V.* (eds. Mackovčin P. and Sedláček M.), 410pp.

Fleig, A., Tallaksen, L. M., Hisdal, H., and Demuth, S. (2006). A global evaluation of streamflow drought characteristics. *Hydrology and Earth System Sciences*, *10* , 535–-552.

Graham, L. (1999). Modeling Runoff to the Baltic Sea. *Ambio*, *28*(4), 328--334.

Heim, R. J. (2002). A Review of Twentieth- Century Drought Indices Used in the United States. *American Meteorological Society*, *83* (8), 1149--1165.

Hisdal, H., Stahl, K., Tallaksen, L. M., and Demuth, S. (2001). Have streamflow drought in Europe become more severe or frequent? *International Journal of Climatology*, *21* , 317--333.

Hisdal, H., Tallaksen, L. M., Clausen, B., Peters, E., and Gustard, A. (2004). *Hydrological Drought Characteristics. In Tallaksen, L.M. and Van Lanen, H A J. (Eds.) Hydrological Drought -– Processes and Estimation Methods for Streamflow and Groundwater.* Developments in Water Sciences, Elsevier BV, the Netherlands, 139--188pp.

Hohenrainer, J. (2008). *Propagation of drought through the hydrological cycle in two different climatic regions.* Unpublished master's thesis, Freiburg University.

Johst, M., Uhlenbrook, S., Tilch, N., Zillgens, B., Didszun, J., and Kirnbauer, R. (2008). An attempt of process-oriented rainfall-runoff modeling using multiple-response data in an alpine catchment, Loehnersbach, Austria. *Hydrology Research*, *39*(1), 1--16.

Kašpárek, L. (2009). *personal communication.*

Kašpárek, L., Kněžek, V., Nowacki, F., Procházková, J., Uhlík, J., Tyralski, M., and Serafin, R. (2006). *Water Resources of the Intra-Sudeten Basin.* Water Research Institute in Prague T.G.M, Prague, 76pp.

Klemeš, V. (1986). Operational testing of hydrological simulation models. *Hydrological Sciences*

Journal, *31* (1), 13--24.

Liden, R., and Harlin, J. (2000). Analysis of conceptual rainfall-runoff modelling performance in different climates. *Journal of Hydrology*, *238*(3-4), 231--247.

Lindstrom, G., Johansson, B., Persson, M., Gardelin, M., and Bergstrom, S. (1997). Development and test of the distributed HBV-96 hydrological model. *Journal of Hydrology*, *201*(1--4), 272--288.

Lu, J., Sun, G., McNulty, S., and Amatya, D. (2005). A comparison of Six Potential Evapotranspiration Methods for Regional Use in the Southeastern United States. *Journal of the American Water Resources Association (JAWRA)*, *41* (3), 621--633.

McGuinness, J. L., and Bordne, E. F. (1972). *A comparison of lysimeterderived potential evapotranspiration with computed values.* Technical Bulletin 1452, Agricultural Research Service, US Department of Agriculture, Washington, DC.

Menzel, L., and Burger, G. (2002). Climate change scenarios and runoff response in the Mulde catchment (Southern Elbe, Germany). *Journal of Hydrology*, *267*(1-2), 53--64.

Nash, J., and Sutcliffe, J. (1970). River flow forecasting through conceptual models part I - A discussion of principles. *Journal of Hydrology*, *10* (3), 282--290.

NVE. (2009). *Norwegian water resources and energy directorate.* Retrieved March 26, 2009, from `http://www.nve.no/en/Floods-and-landslides/Flood-forecasting-system/`

Oudin, L., Hervieu, F., Michel, C., Perrin, C., Andreassian, V., Anctil, F., and Loumagne, C. (2005b). Which potential evapotranspiration input for a lumped rainfall-runoff model? Part 2 - Towards a simple and efficient potential evapotranspiration model for rainfall-runoff modelling. *Journal of Hydrology*, *303*(1-4), 290--306.

Oudin, L., Michel, C., and Anctil, F. (2005a). Which potential evapotranspiration input for a lumped rainfall-runoff model?: Part 1 - Can rainfall-runoff models effectively handle detailed potential evapotranspiration inputs? *Journal of Hydrology*, *303*(1-4), 275--289.

Perrin, C., Michel, C., and Andréassian, C. (2001). Does a large number of parameters enhance model performance? comparative assessment of common catchment model structures on 429 catchments. *Journal of Hydrology*, *242*(3-4), 275--301.

Rakovec, O. (2009). *Hydrological data from Upper Metuje and Upper Sázava catchments* (Tech. Rep.). T.G. Masaryk Water Research Institute and Wageningen University.

Rees, G., Marsh, T., Roald, L., Demuth, S., Van Lanen, H. A. J., and Kašpárek, L. (2004). *Hydrological Data. In Tallaksen, L.M. and Van Lanen, H.A.J. (Eds.) Hydrological Drought – Processes and Estimation Methods for Streamflow and Groundwater.* Developments in

Water Sciences, Elsevier BV, the Netherlands, 99--138pp.

Salvato, J., Nemerow, N., and Agardy, F. (2003). *Environmental engineering.* John Wiley and Sons, 1544 pp.

Seibert, J. (1997). Estimation of Parameter Uncertainty in the HBV Model. *Nordic Hydrology*, *28* (4/5), 247--262.

Seibert, J. (1999). Regionalisation of parameters for a conceptual rainfall-runoff model. *Agricultural and Forest Meteorology*, *98--99* , 279--293.

Seibert, J. (2000). Multi-criteria calibration of a conceptual runoff model using a genetic algorithm. *Hydrology and Earth System Sciences*, *4* (2), 215--224.

Seibert, J. (2003). Reliability of Model Predictions Outside Calibration Conditions. *Nordic Hydrology*, *35* (5), 477--492.

Seibert, J. (2005). *Hbv light version 2, user's manual.* Retrieved March 24, 2009, from `http://people.su.se/~jseib/HBV/HBV_manual_2005.pdf`

Seibert, J., Uhlenbrook, S., Leibundgut, C., and Halldin, S. (2000). Multiscale Calibration and Validation of a Conceptual rainfall--runoff Model. *Phys. Chem. Earth (B)*, *25* (1), 59--64.

SMHI. (2009). *Swedish Meteorological and Hydrological Institute.* Retrieved March 26, 2009, from `http://www.smhi.se/cmp/jsp/polopoly.jsp?d=6056&l=en`

Steele-Dunne, S., Lynch, P., McGrath, R., Semmler, T., Wang, S., Hanafin, J., and Nolan, P. (2008). The impacts of climate change on hydrology in Ireland. *Journal of Hydrology*, *356*(1-2), 28--45.

Tallaksen, L. M., and Van Lanen, H. A. J. (2004). *Introduction. In Tallaksen, L.M. and Van Lanen, H.A.J. (Eds.) Hydrological Drought – Processes and Estimation Methods for Streamflow and Groundwater.* Developments in Water Sciences, Elsevier BV, the Netherlands, 3--17pp.

Thornthwaite, C. W. (1948). An Approach toward a Rational Classification of Climate. Geographical Review. *American Geographical Society*, *38* (1), 55--94.

Trnka, M., Dubrovský, M., Svoboda, M., Semerádová, D., Hayes, M., Žalud, Z., and Wilhite, D. (2009). Developing a regional drought climatology for the Czech Republic. *International Journal of Climatology*, *29* , 863–-883.

Uhlenbrook, S., Seibert, J., Leibundgut, C., and Rodhe, A. (1999). Prediction uncertainty of conceptual rainfall--runoff models caused by problems to identify model parameters and structure. *Hydrological Sciences--Journal--des Sciences Hydrologiques*, *44* (5), 779--798.

Van Lanen, H. A. J., Fendeková, M., Kupczyk, E., Kasprzyk, A., and Pokojski, W. (2004).

Flow Generating Processes. In Tallaksen, L.M. and Van Lanen, H.A.J. (Eds.) Hydrological Drought –- Processes and Estimation Methods for Streamflow and Groundwater. Developments in Water Sciences, Elsevier BV, the Netherlands, 53--96pp.

Van Lanen, H. A. J., and Tallaksen, L. M. (2007). Hydrological drought, climate variability and change. In *Climate and Water. - Helsinki : [s.n.], Third International Conference on Climate and Water.*

Van Lanen, H. A. J., and Tallaksen, L. M. (2008). Drought in Europe. In *Proceedings Water Down Under 2008, Adelaide Australia.*

Van Lanen, H. A. J., Tallaksen, L. M., Candel, M., Carrera, J., Crooks, S., Engeland, K., Fendeková, M., Haddeland, I., Hisdal, H., Horáček, S., Bermúdez, J. J., Loon, A., Machlica, A., Navarro, V., Novický, O., and Prudhome, C. (2008). *Database with hydrometeorological variables for selected river basins metadata catalogue, WATCH Tech. Report no. 4.* Retrieved January 15, 2009, from `http://www.eu-watch.org/nl/25222760-TechnicalReports.html`

Vodárenská. (2009). Retrieved February 24, 2009, from `http://www.vodarenska.cz/vaszr`

Wagener, T., Wheater, H., and Gupta, H. (2004). *Rainfall-runoff modelling in gauged and ungauged catchments.* Imperial College Press, 306 pp.

Wallenfelsová, M. (1955). *Hydrologické poměry křídového příkopu z jihozápadní strany Železných hor.* (Available in WRI archive)

WHO. (2008). *World Health Organisation.* Retrieved October 1, 2008, from `http://www.who.int/water_sanitati\on_health/hygiene/emergencies/floodrought/en/index2.html`

Wikipedia. (2009). *Box plot.* Retrieved July 15, 2009, from `http://en.wikipedia.org/wiki/Box_plot`

WRI. (2008). *Bučnice meteorological station, T. G. Masaryk Water Research Institute.* Retrieved November 24, 2008, from `http://www.vuv.cz/bupre/eucel.htm`

WRI. (2009). HEIS *database, T. G. Masaryk Water Research Institute.*

List of Tables

List of Figures

Annex A

Annex Tables

Table A.1: Proportion of land cover classes within the three elevation zones for the Upper Metuje catchment.

	Land cover		
Interval of mean altitude	Agriculture	Built--up area	Forest
500 m (459--550)	20	2	5
600 m (550--650)	28	1	27
700 m (650--765)	3	0	14
Total	51	3	46

Table A.2: Proportion of land cover classes in the total catchment and within the three elevation zones for the Upper Sázava catchment.

	Land cover			
Interval of mean altitude	Agriculture	Built--up area	Forest	Water
550 m a.m.s.l. (487--600)	19	5	8	0
650 m a.m.s.l. (600--700)	29	1	24	2
750 m a.m.s.l. (700--805)	2	0	10	0
Total	50	6	42	2

Table A.3: Weights of stations for precipitation scenarios for the Upper Sázava catchment.

Station	Scenario 1	Scenario 2	Scenario 3
Přibyslav	70	3	25
Svratouch	30	0	25
Žďár nad Sázavou -- Stržanov	0	88	25
Krucemburk	0	9	25

Table A.4: Parameter set (Scenario 2, variant PET 2, 017) for the Upper Metuje catchment.

Parameter	Agriculture	Built-up area	Forest
TT	-1.164998	1.521517	0.4851092
CFMAX	2.642224	1.51253	8.159228
SFCF	1.198342	1.089446	0.9992229
CWH	9.137784E-08	2.853572E-06	1.307302E-06
CFR	3.177376E-04	6.517676E-02	3.361899E-02
FC	70.10658	79.15825	137.0662
LP	0.8001258	0.3000256	0.5085089
BETA	2.313153	5.999839	5.974701
CET	1.00255E-03		
K0	0.413711		
K1	5.483047E-02		
K2	4.554195E-03		
UZL	41.51318		
PERC	1.435713		
MAXBAS	1.575819		

Table A.5: Parameter set of the reference model for drought analysis (Scenario 5) for the Upper Metuje catchment.

Parameter	Agriculture	Built-up area	Forest
TT	-1.114998	2.497804	-0.1503137
CFMAX	4.74302	4.209238	4.901584
SFCF	1.199971	1.1994	0.9701185
CWH	2.732268E-07	6.463658E-02	2.116515E-02
CFR	2.750578E-06	7.064012E-02	1.875012E-02
FC	175.963	157.1512	106.6859
LP	0.666142	0.300006	0.814807
BETA	5.684522	5.999912	2.053791
CET	1.000229E-03		
K0	0.2110155		
K1	5.000003E-02		
K2	3.500189E-03		
UZL	32.34486		
PERC	1.144661		
MAXBAS	1.000229E-03		

Table A.6: Parameter set of the reference model for drought analysis ($var.US\_Qcal0$) for the Upper Sázava catchment.

Parameter	Agriculture	Built-up area	Forest
TT	-1.406356	1.9637	0.3702982
CFMAX	2.295087	2.560853	5.226847
SFCF	1.199995	1.199919	1.199997
CWH	2.165668E-06	2.879264E-05	1.470667E-03
CFR	2.528656E-07	2.341912E-02	9.743465E-02
FC	162.356	152.1938	132.9
LP	0.8652831	0.4449807	0.6420426
BETA	3.006721	5.999678	5.904171
CET	5.564109E-02		
K0	0.1783744		
K1	6.801556E-02		
K2	5.231766E-03		
UZL	46.78084		
PERC	0.5865237		
MAXBAS	2.019186		

Table A.7: Objective functions of streamflow validation for the Upper Sázava catchment.

Length of calibration	**Code**	**lnReff**	**Reff**	**VE**
2001--2005	$var.US\_Q.val0$	0.55	0.58	11%
1974--1981	$var.US\_Q.val1$	0.49	0.50	27%
1982--1989	$var.US\_Q.val2$	0.46	0.67	2%
1990--1997	$var.US\_Q.val3$	0.46	0.49	17%
1998--2005	$var.US\_Q.val4$	0.53	0.57	16%
average of $var.US\_Q.val1$ to $var.US\_Q.val4$		0.49	0.56	16%

Table A.8: Correlation coefficients of groundwater storage validation for the Upper Sázava catchment.

Period	$\mathbf{r^2}$
1963--2000	0.21
1966--1973	0.34
1974--1981	0.34
1982--1989	0.04
1990--1997	0.17
1998--2005	0.43
average	0.26

Table A.9: Correlation coefficients of snow water storage validation for the Upper Sázava catchment.

Period	$\mathbf{r^2}$
1963--2000	0.57
1966--1973	0.56
1974--1981	0.50
1982--1989	0.46
1990--1997	0.58
1998--2005	0.59
average	0.52

Table A.10: Number of meteorological droughts for the Upper Metuje catchment (1982--1989).

Precipitation	**Number**	**Mean number of days**	**Mean deficit [mm]**	**Mean intensity [mm/day]**
MA 10	64	8.5	3.16	0.34
MA 30	40	14.2	5.58	0.27

Table A.11: Drought events for the Upper Metuje catchment (1982--1993).

Type of drought	**Number**	**Mean number of days**	**Mean deficit [mm]**	**Mean intensity [mm/day]**
Meteorological	54	15.37	5.93	0.3
Soil moisture	41	16.88	--	--
Groundwater	21	40.14	--	--
Streamflow sim.	51	16.78	0.83	0.04
Streamflow obs.	49	16.90	1.22	0.05

Table A.12: Drought events for the Upper Metuje catchment (1994--2006).

Type of drought	**Number**	**Mean number of days**	**Mean deficit [mm]**	**Mean intensity [mm/day]**
Meteorological	53	16	6.89	0.34
Soil moisture	42	20.9	--	--
Groundwater	18	51.44	--	--
Streamflow sim.	41	21.61	1.33	0.05
Streamflow obs.	83	14.80	1.52	0.05

Table A.13: Number of droughts using the threshold and SPA methods (1982--1993).

Method	**Drought**	**Catchment**	**Number**
Threshold	Q simulated	Upper Metuje	51
		Upper Sázava	33
	Q observed	Upper Metuje	49
		Upper Sázava	66
	Meteorological	Upper Metuje	54
		Upper Sázava	58
SPA	Q simulated	Upper Metuje	32
		Upper Sázava	20
	Q observed	Upper Metuje	24
		Upper Sázava	42
	Meteorological	Upper Metuje	41
		Upper Sázava	45

Annex B

Annex Figures

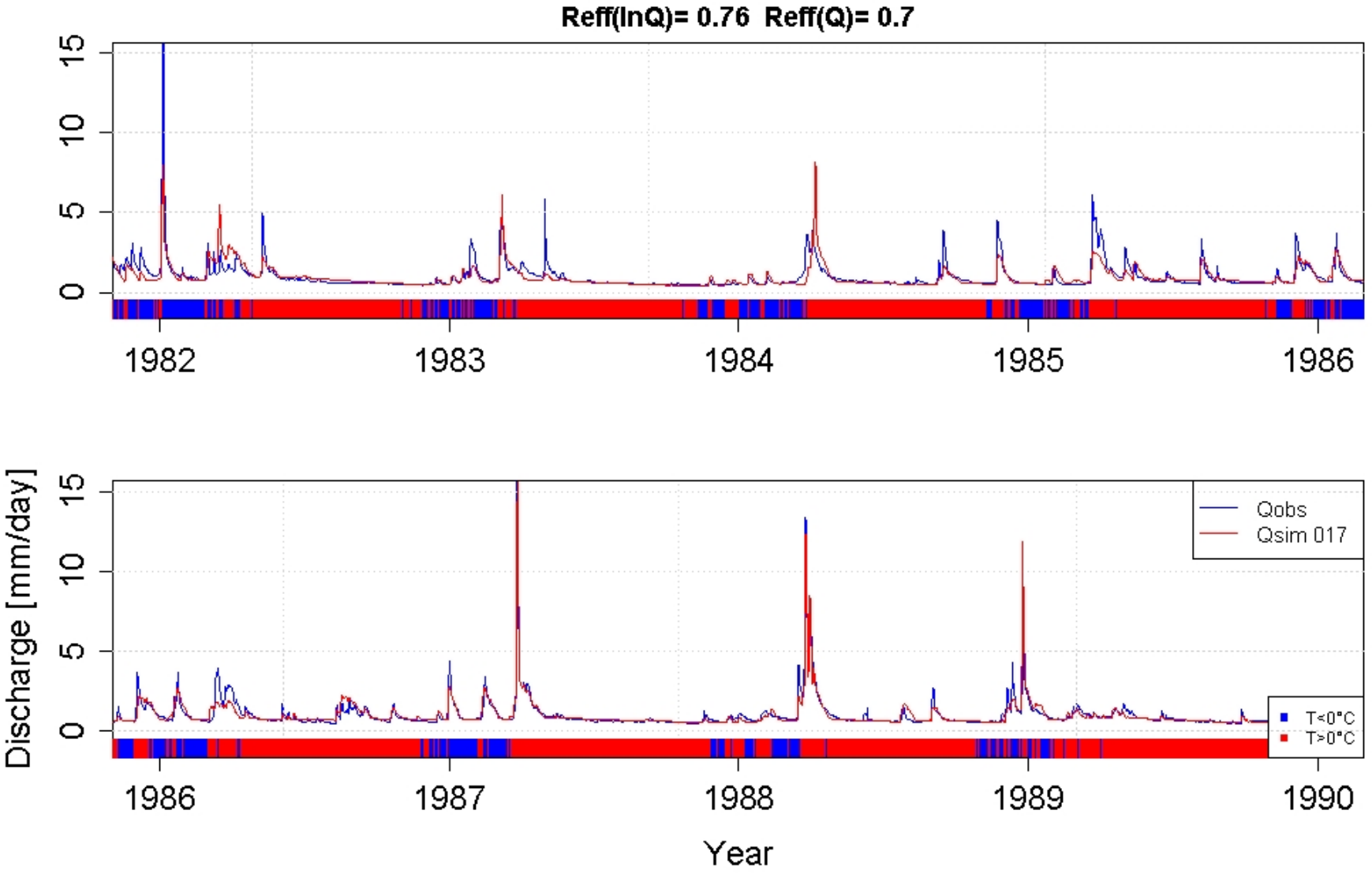

Figure B.1: Streamflow calibration of scenario 2 for the Upper Metuje catchment.

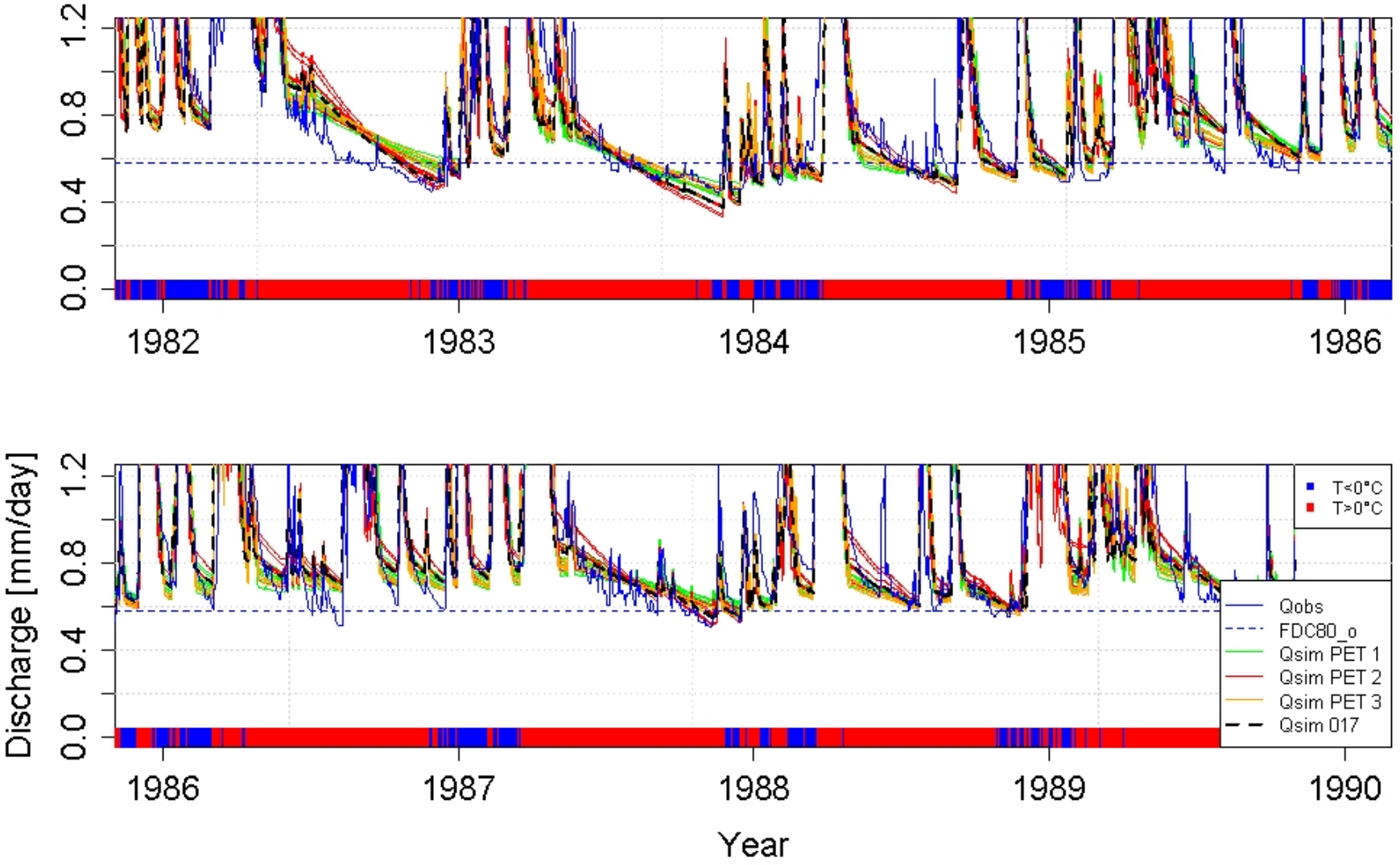

Figure B.2: Streamflow calibration of scenario 2 for the Upper Metuje catchment, zoomed to minimum flows.

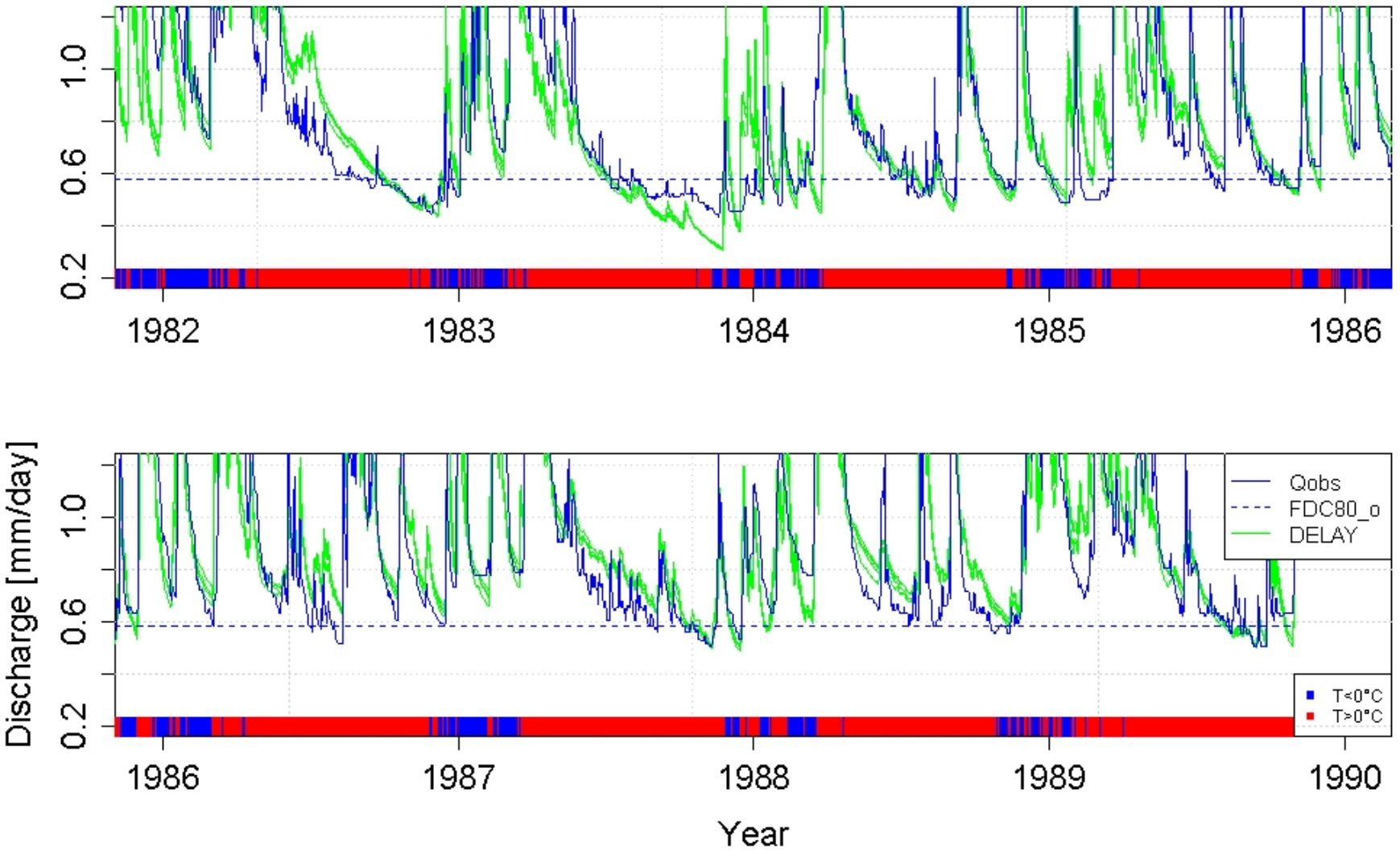

Figure B.3: Streamflow calibration of scenario 3 for the Upper Metuje catchment, zoomed to minimum flows.

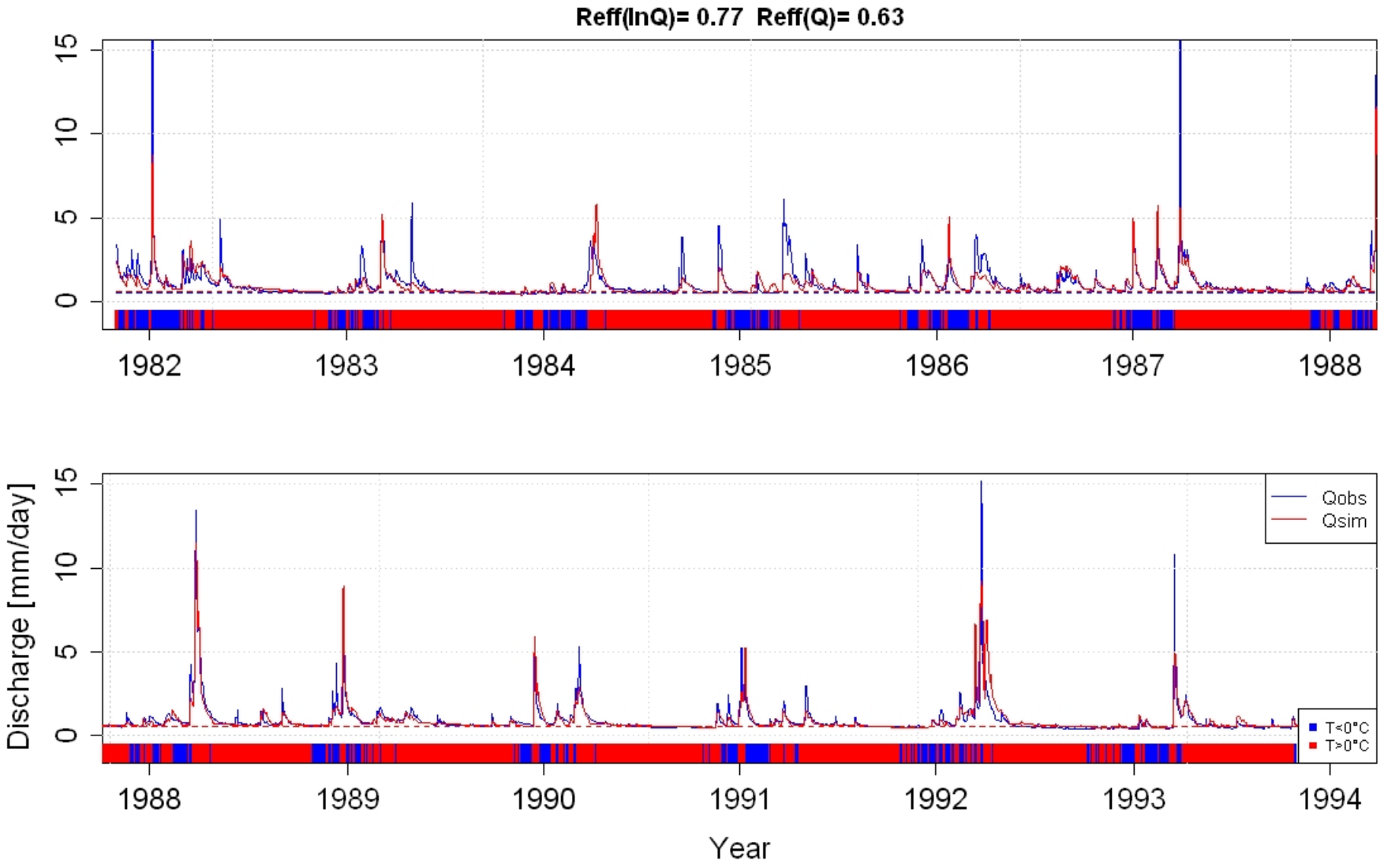

Figure B.4: Streamflow calibration of scenario 5 for the Upper Metuje catchment.

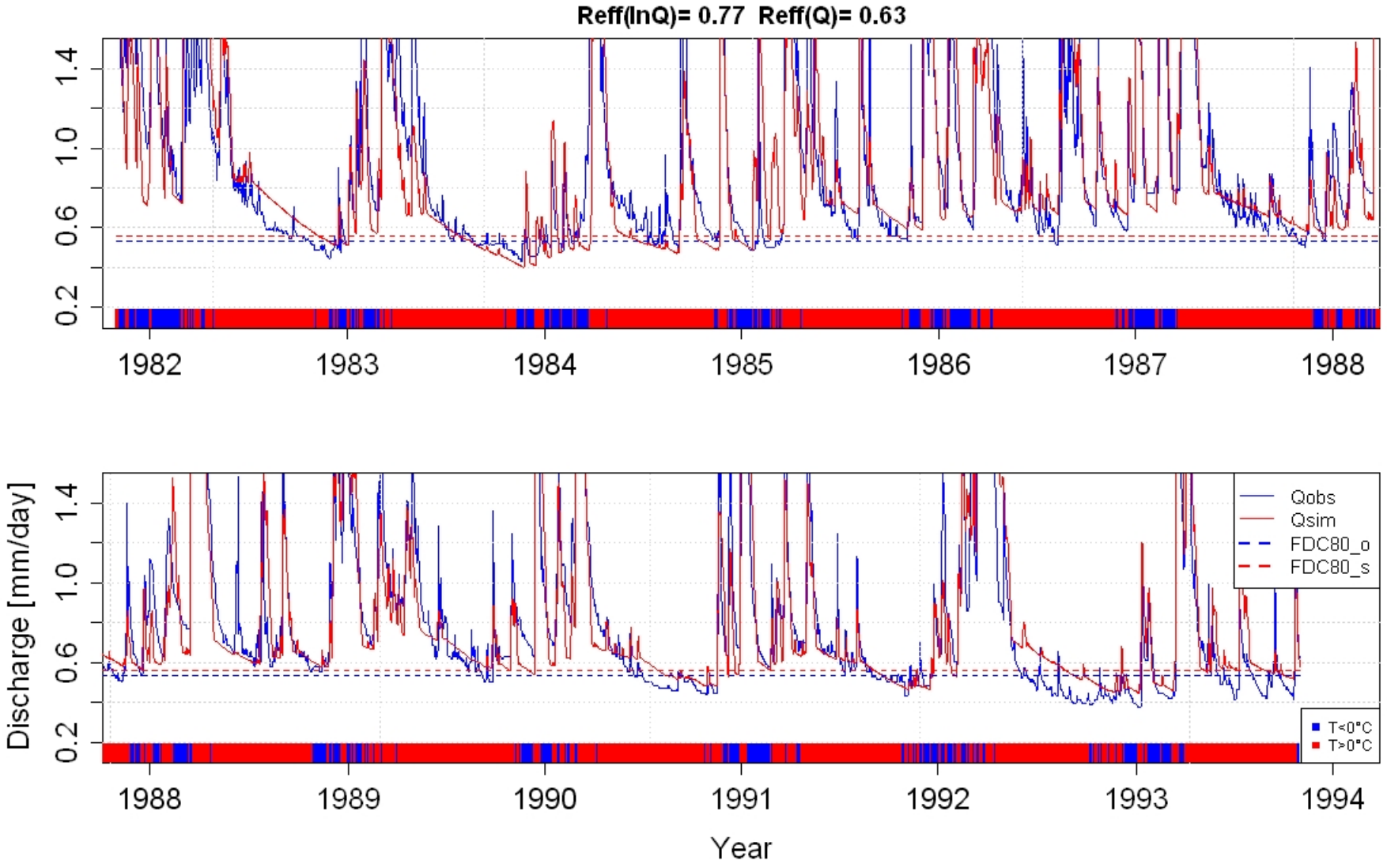

Figure B.5: Streamflow calibration of scenario 5 for the Upper Metuje catchment, zoomed to minimum flows.

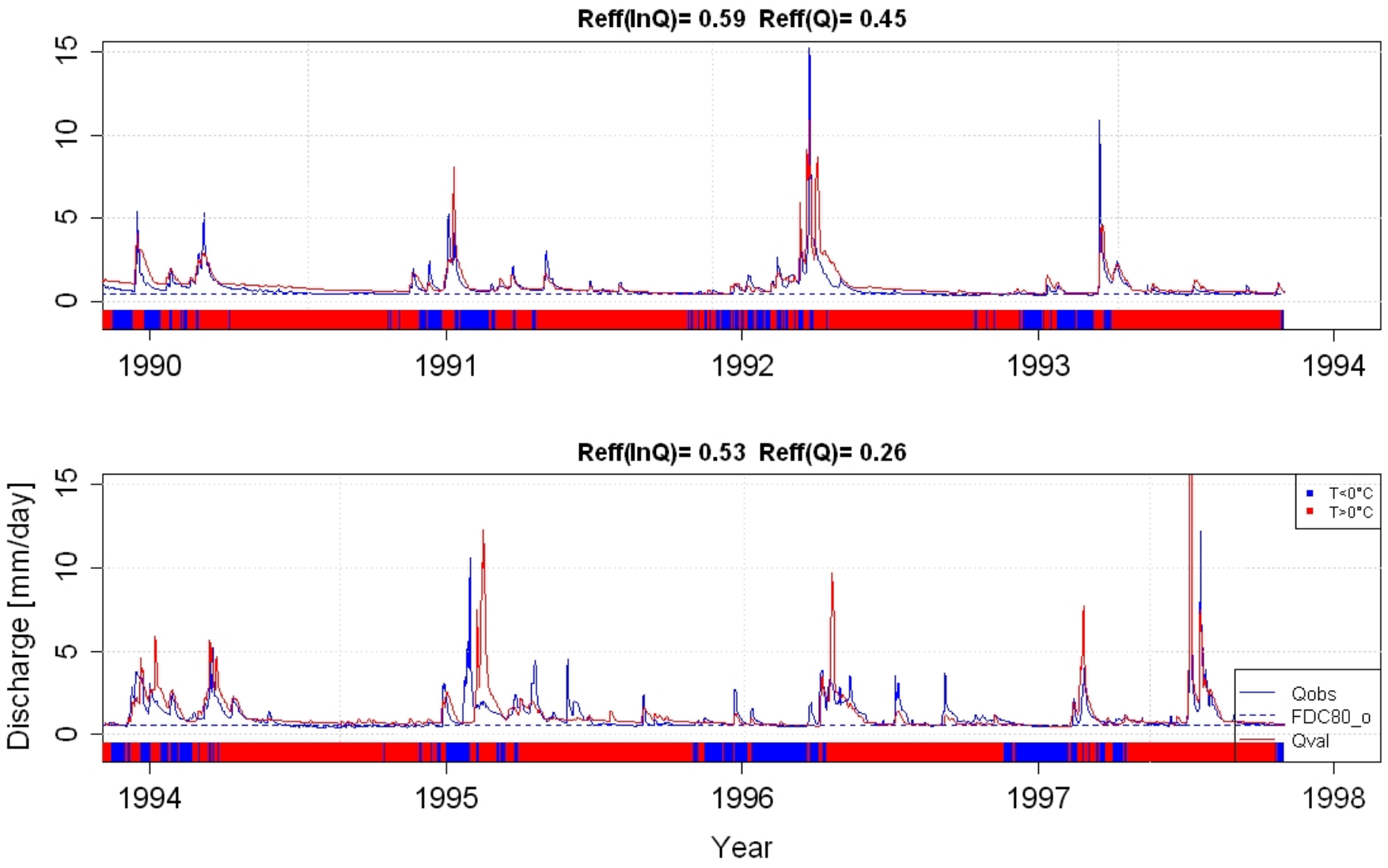

Figure B.6: Streamflow validations, undisturbed period (1990-1993) and disturbed period (1994-1997) for the Upper Metuje catchment.

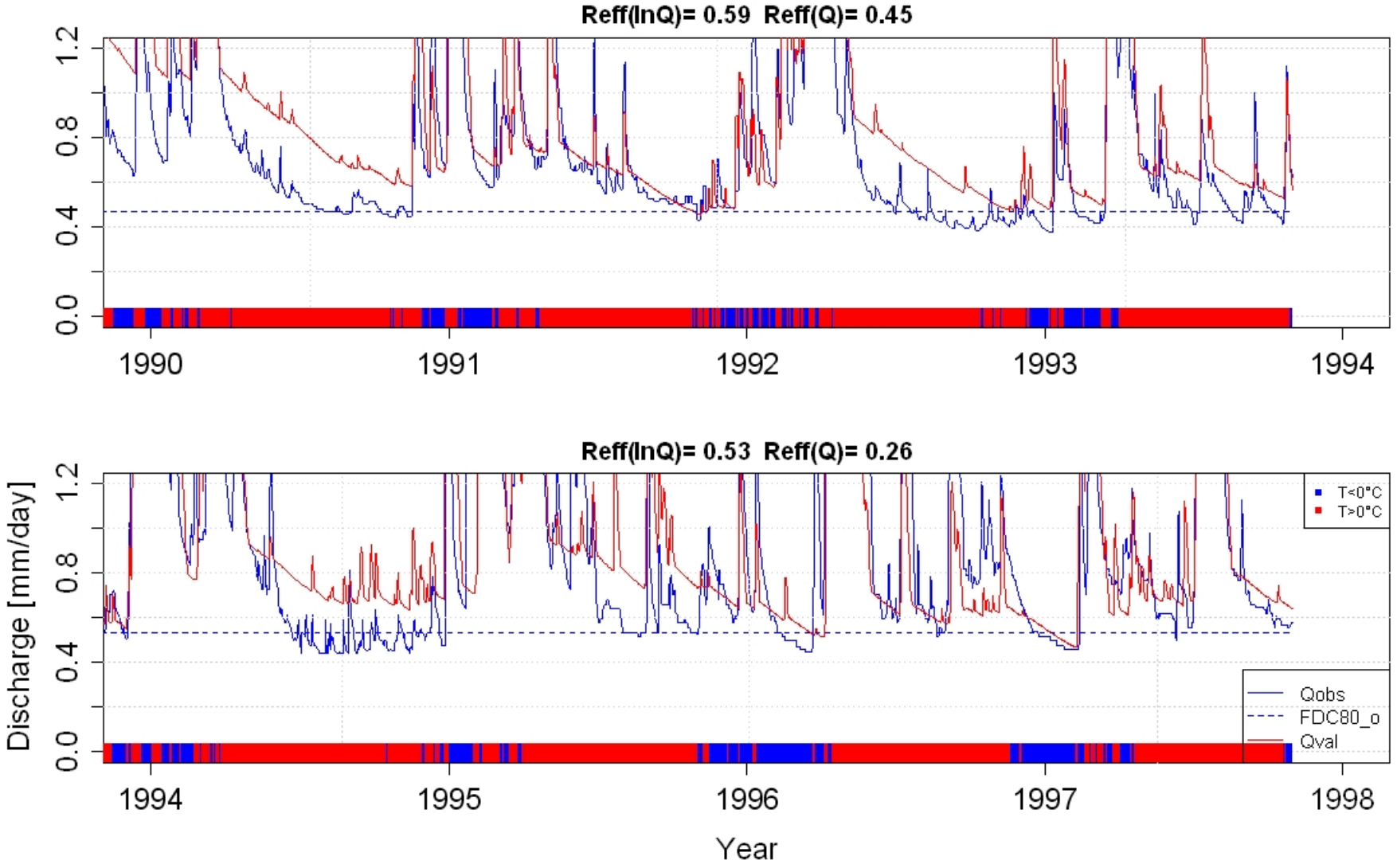

Figure B.7: Streamflow validations, undisturbed period (1990-1993) and disturbed period (1994-1997) for the Upper Metuje catchment, zoomed to minimum flows.

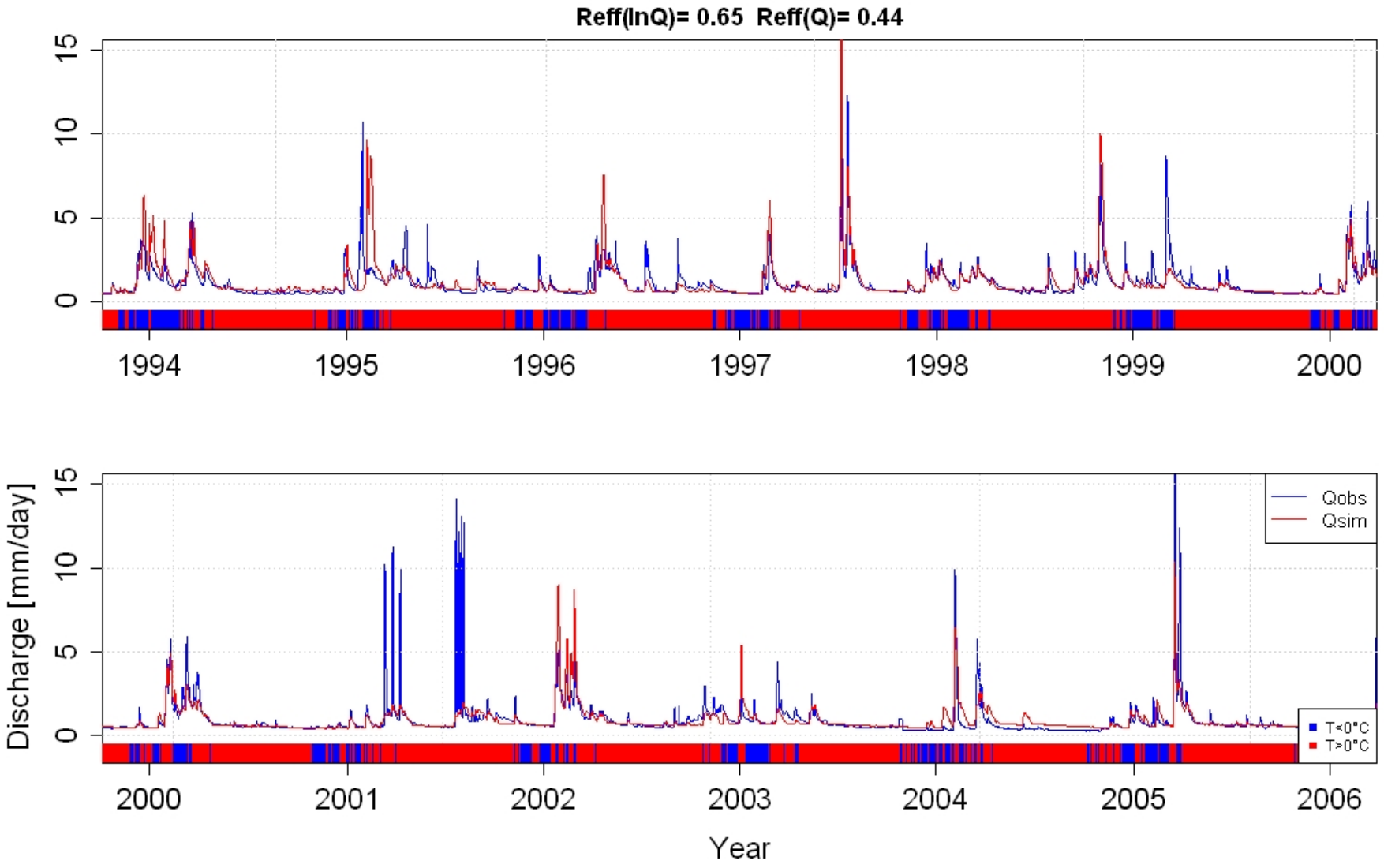

Figure B.8: Streamflow validation of scenario 5 for the Upper Metuje catchment.

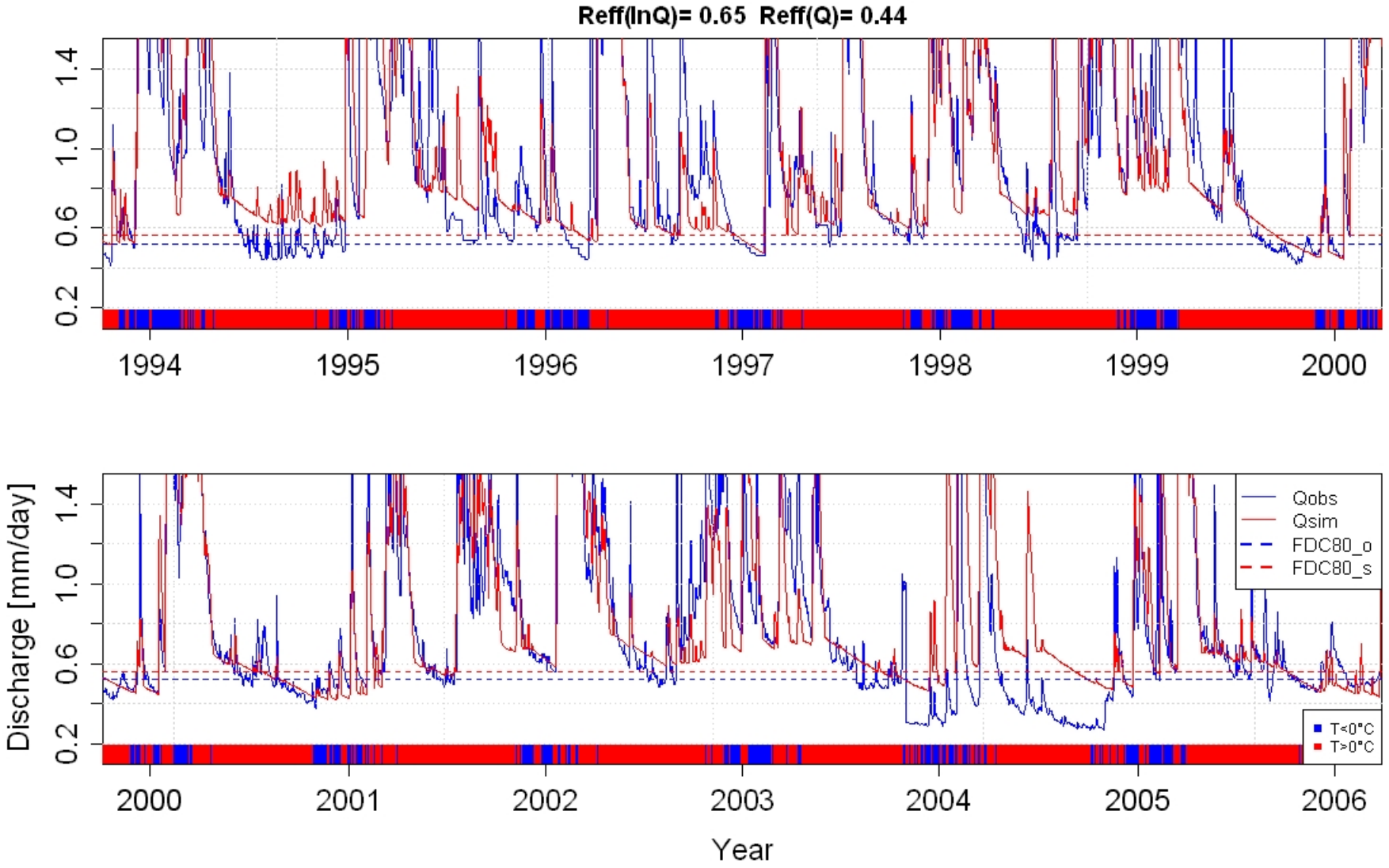

Figure B.9: Streamflow validation of scenario 5 for the Upper Metuje catchment, zoomed to minimum flows.

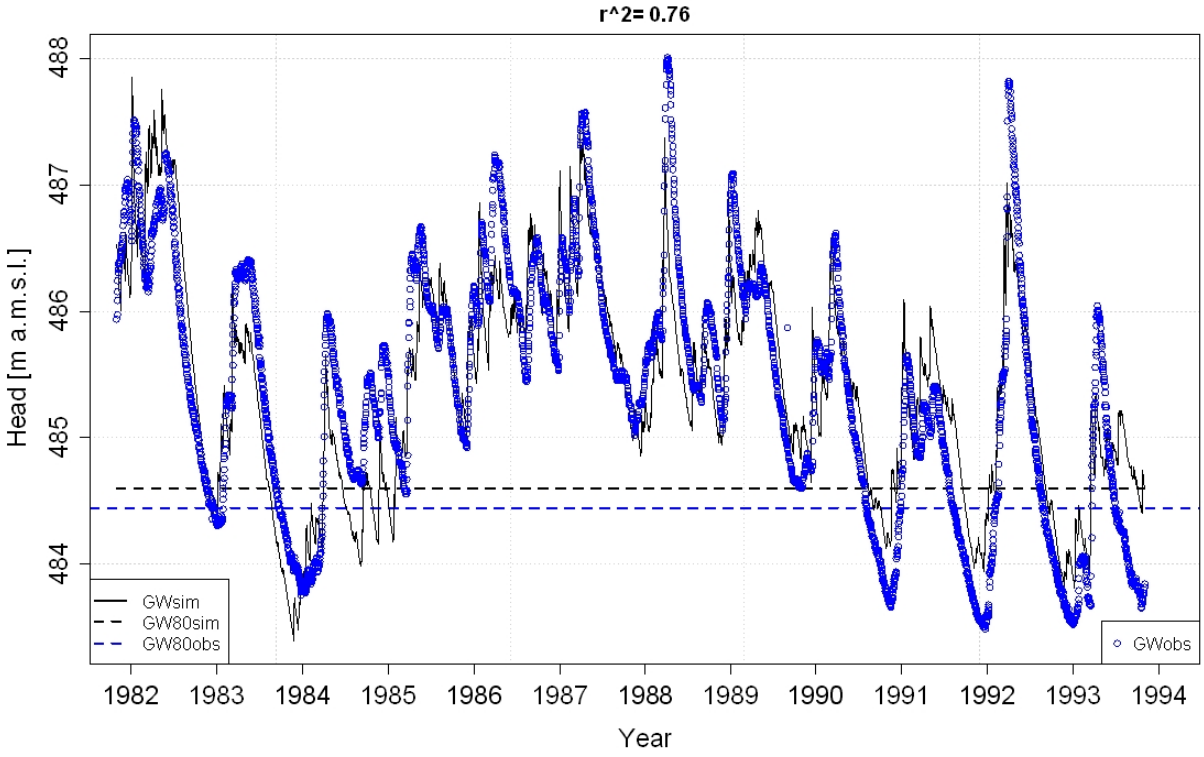

Figure B.10: Groundwater storage validation 1 for the Upper Metuje catchment, (1982-1993).

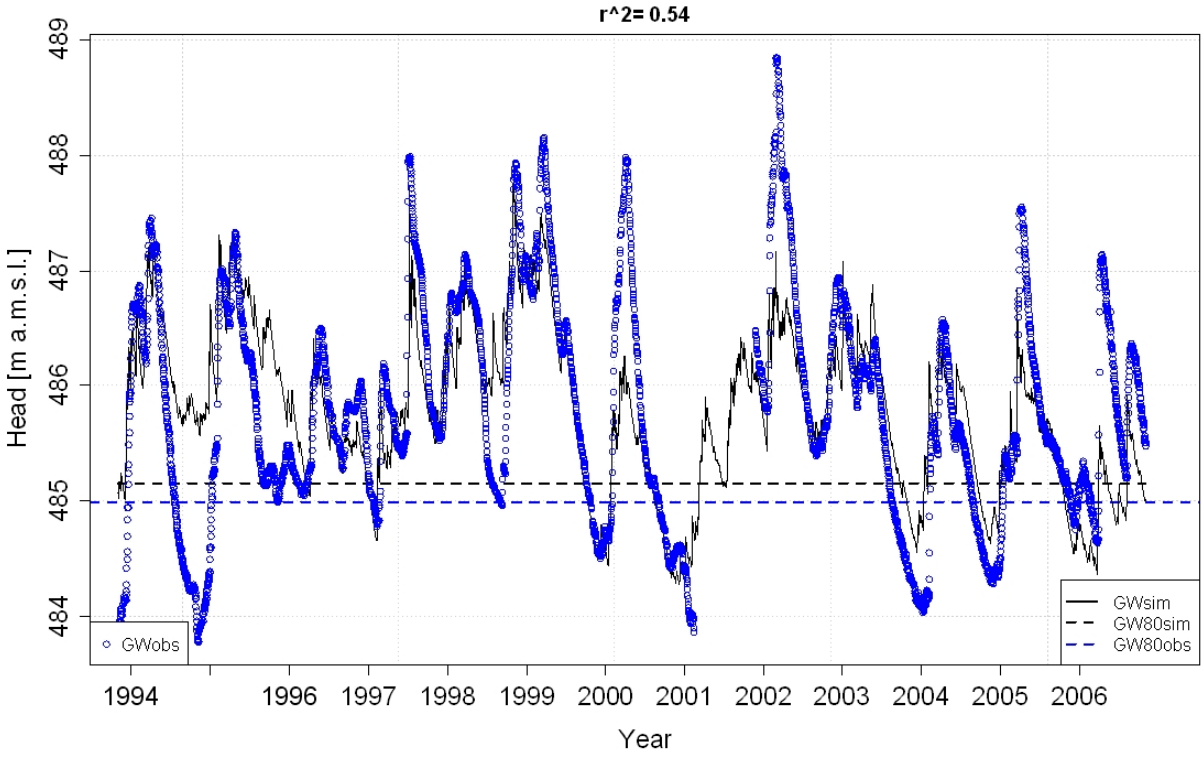

Figure B.11: Groundwater storage validation 2 for the Upper Metuje catchment, (1994-2006).

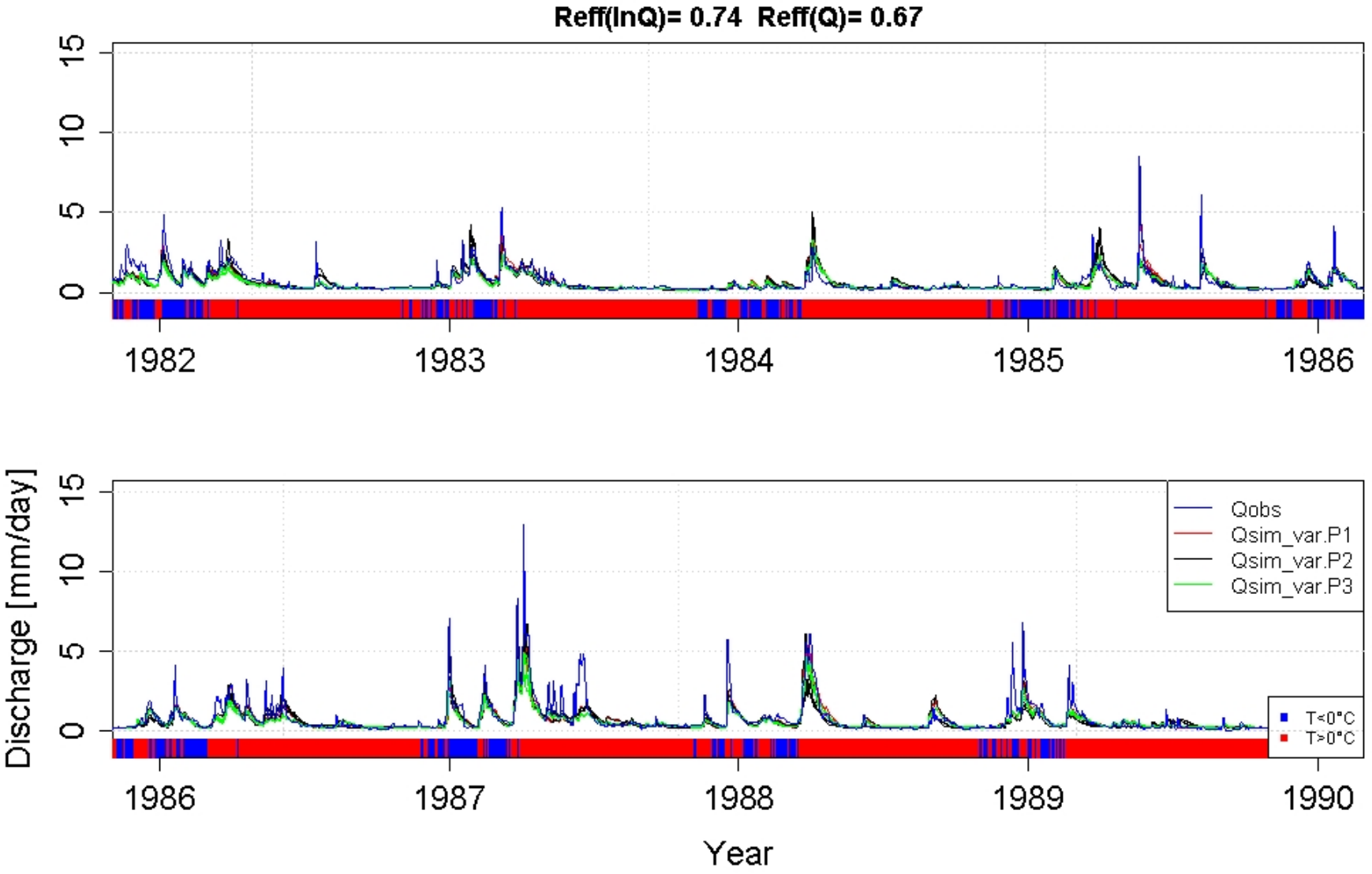

Figure B.12: Streamflow calibration of scenario 1 for the Upper Sázava catchment.

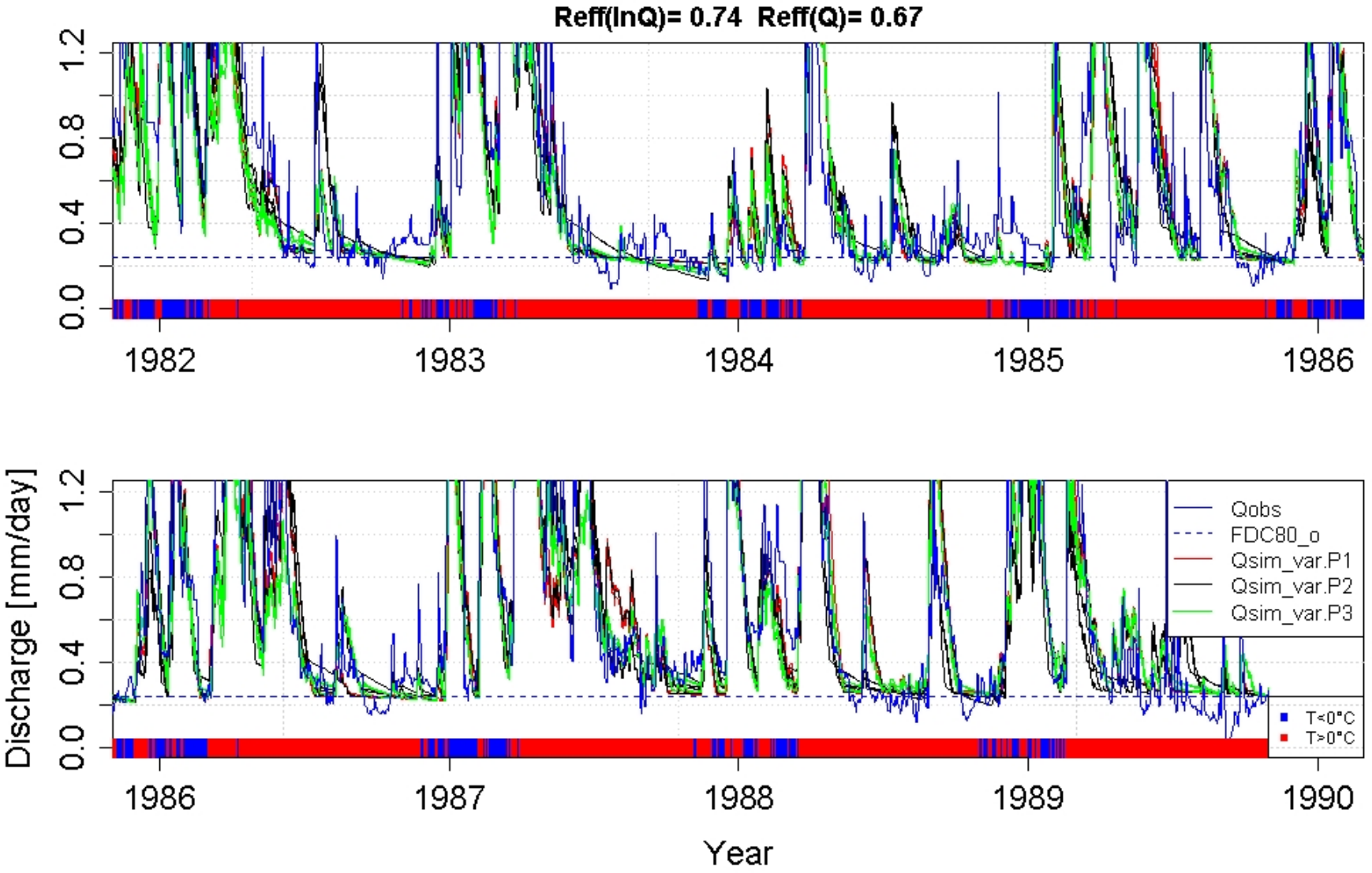

Figure B.13: Streamflow calibration of scenario 1 for the Upper Sázava catchment, zoomed to minimum flows.

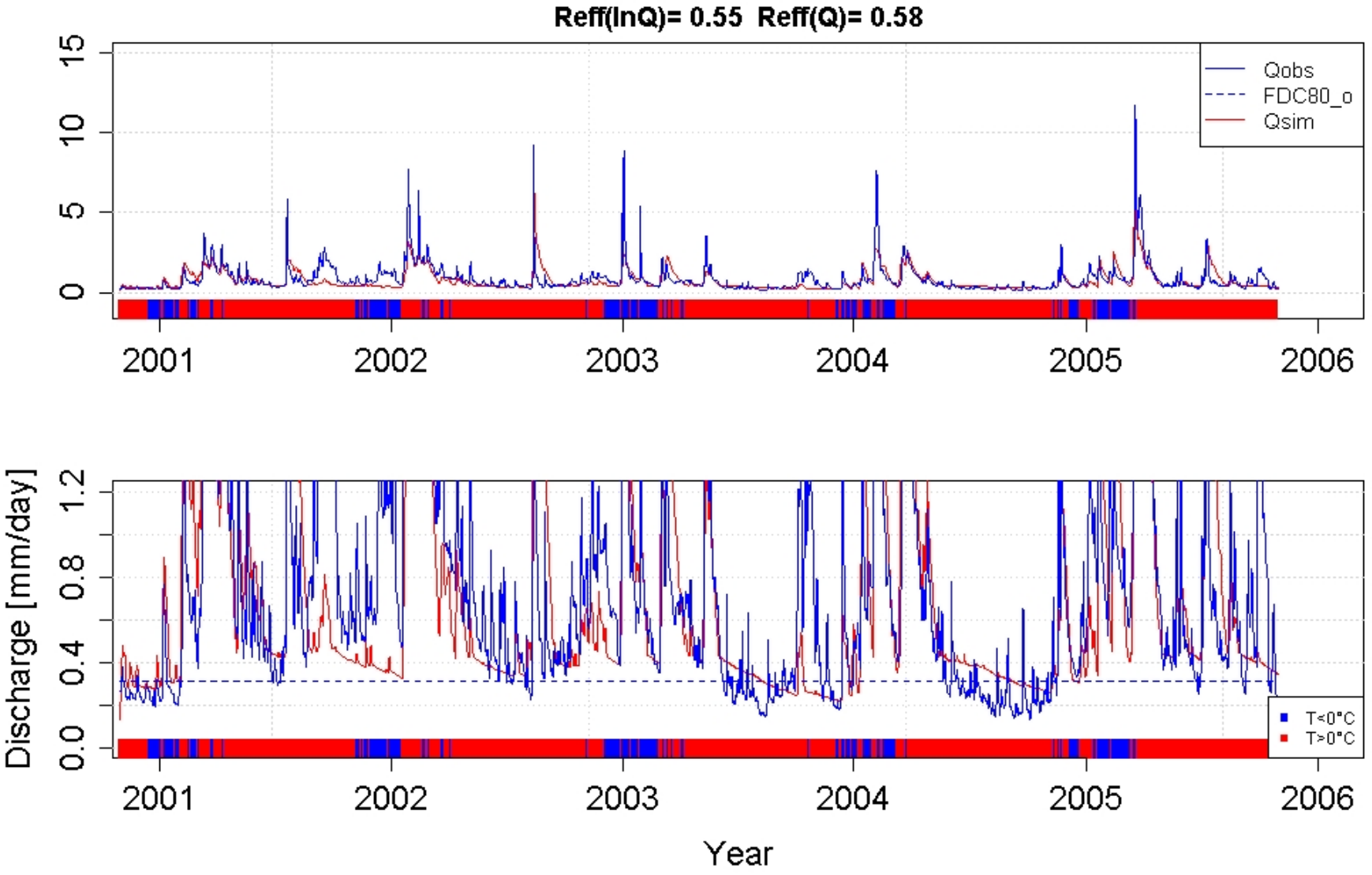

Figure B.14: Streamflow validation for (1) the full hydrograph (top) and (2) zoomed to minimum flows (bottom) for the Upper Sázava catchment.

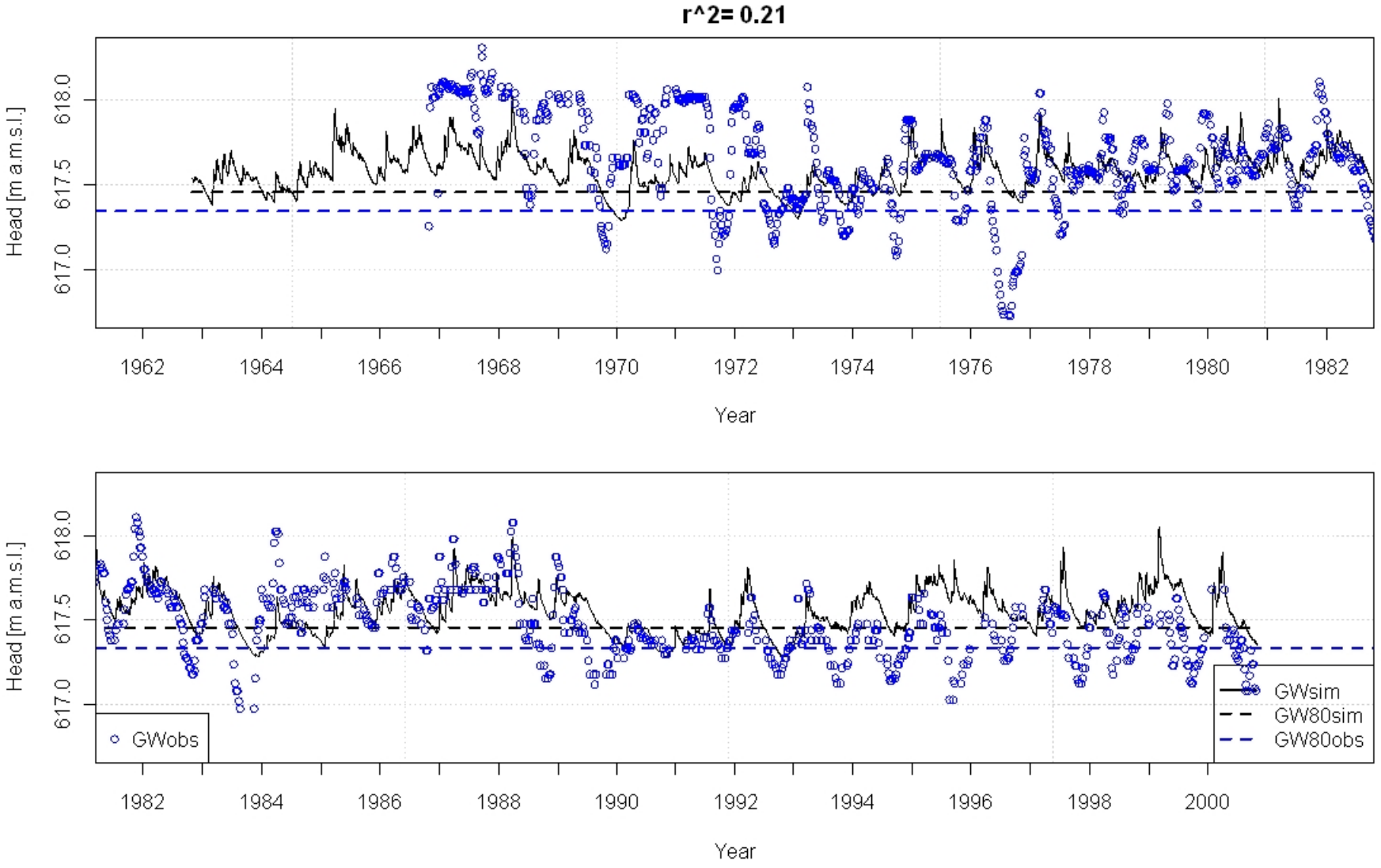

Figure B.15: Groundwater storage validation for the Upper Sázava catchment.

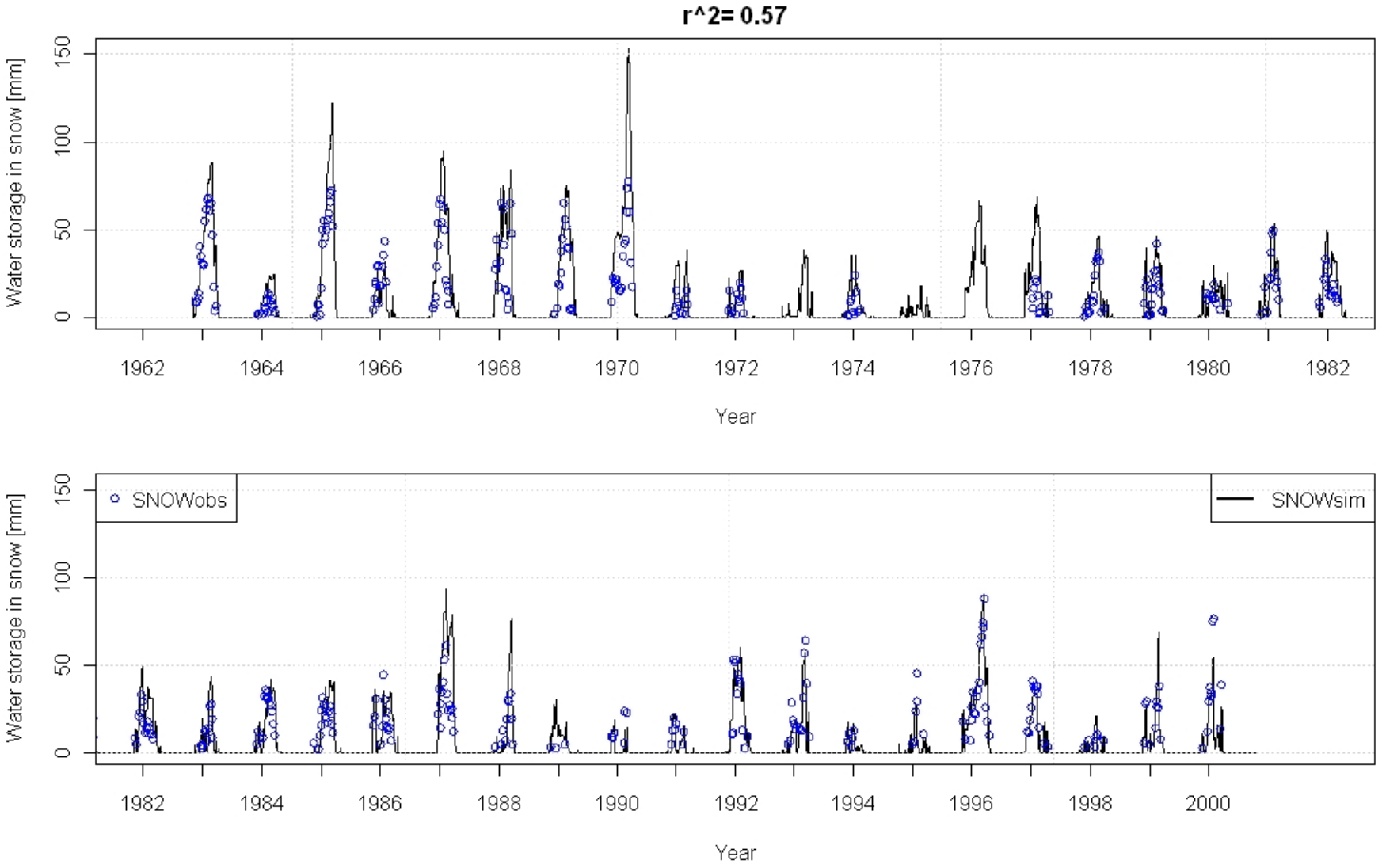

Figure B.16: Snow routine validation for the Upper Sázava catchment.

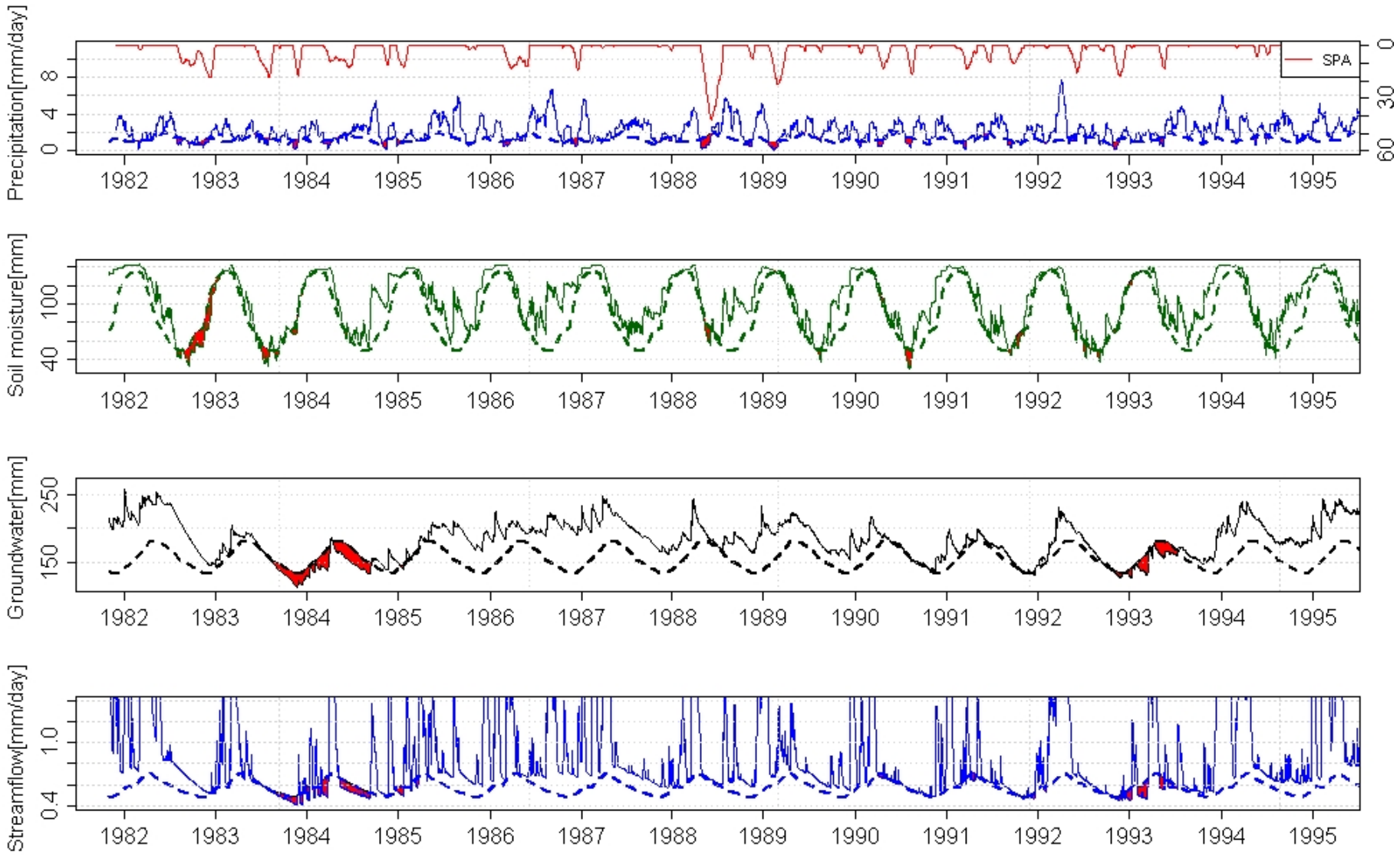

Figure B.17: Drought propagation in 1982--1995 for the Upper Metuje catchment.

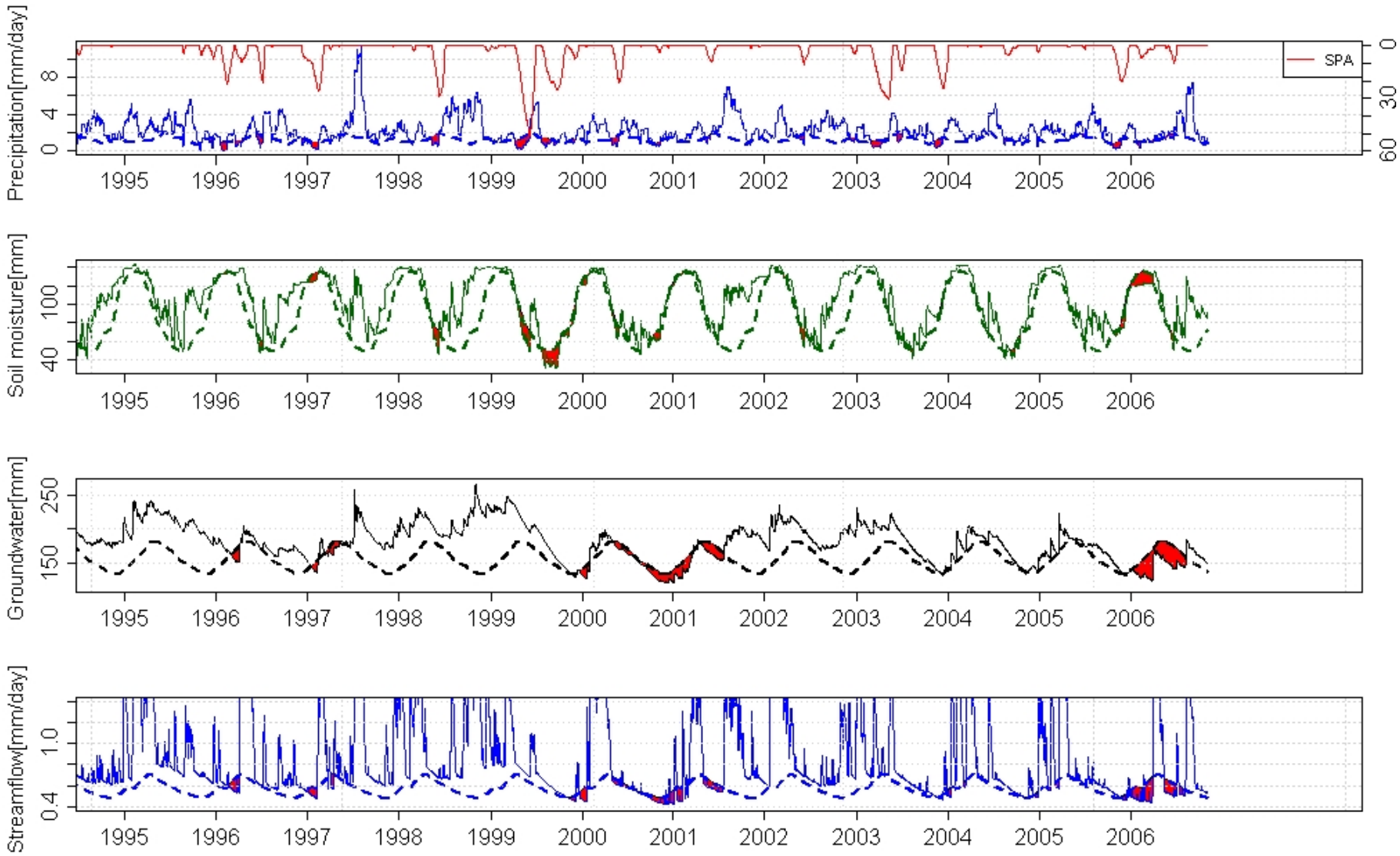

Figure B.18: Drought propagation in 1995--2006 for the Upper Metuje catchment.

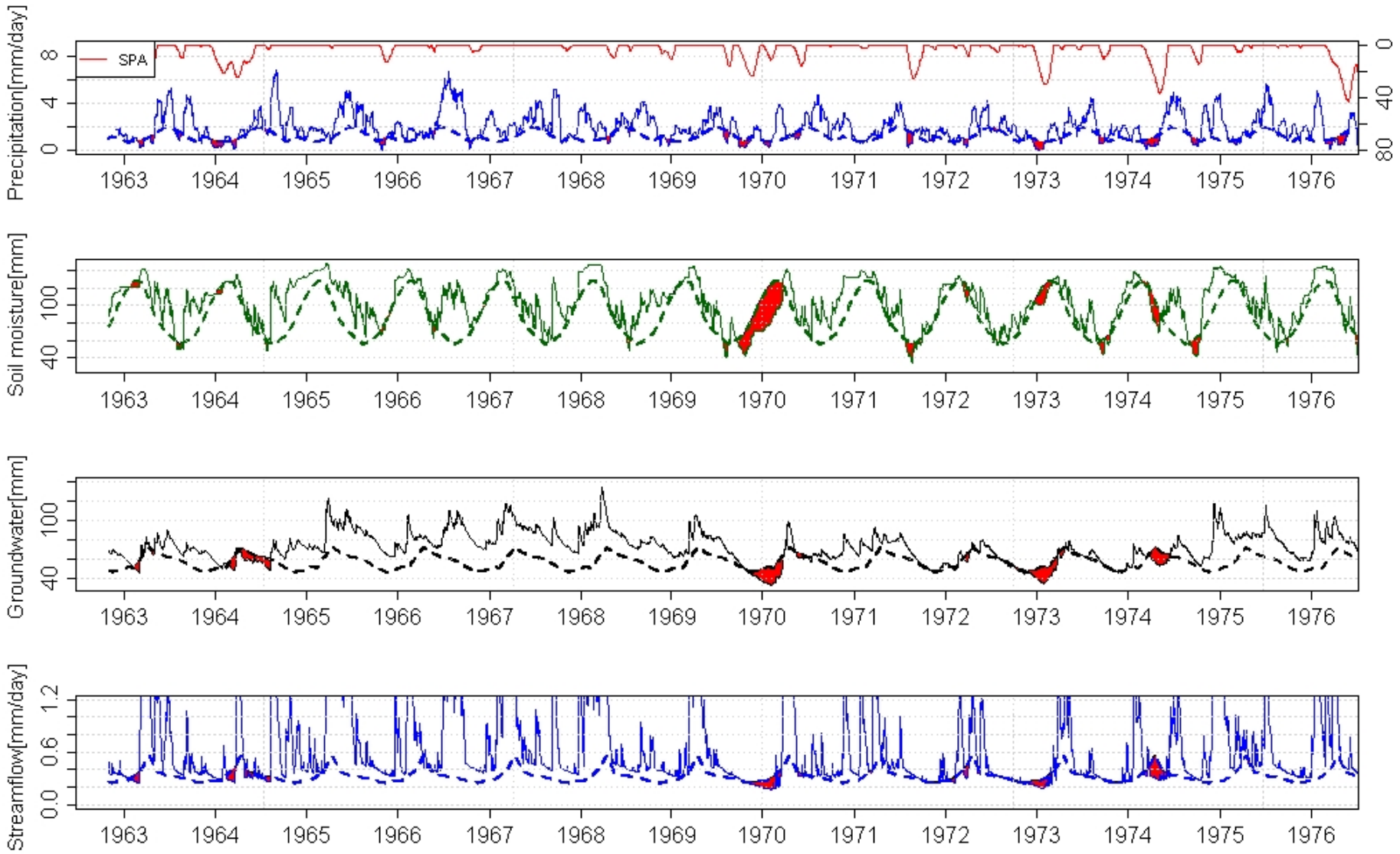

Figure B.19: Drought propagation in 1963--1976 for the Upper Sázava catchment.

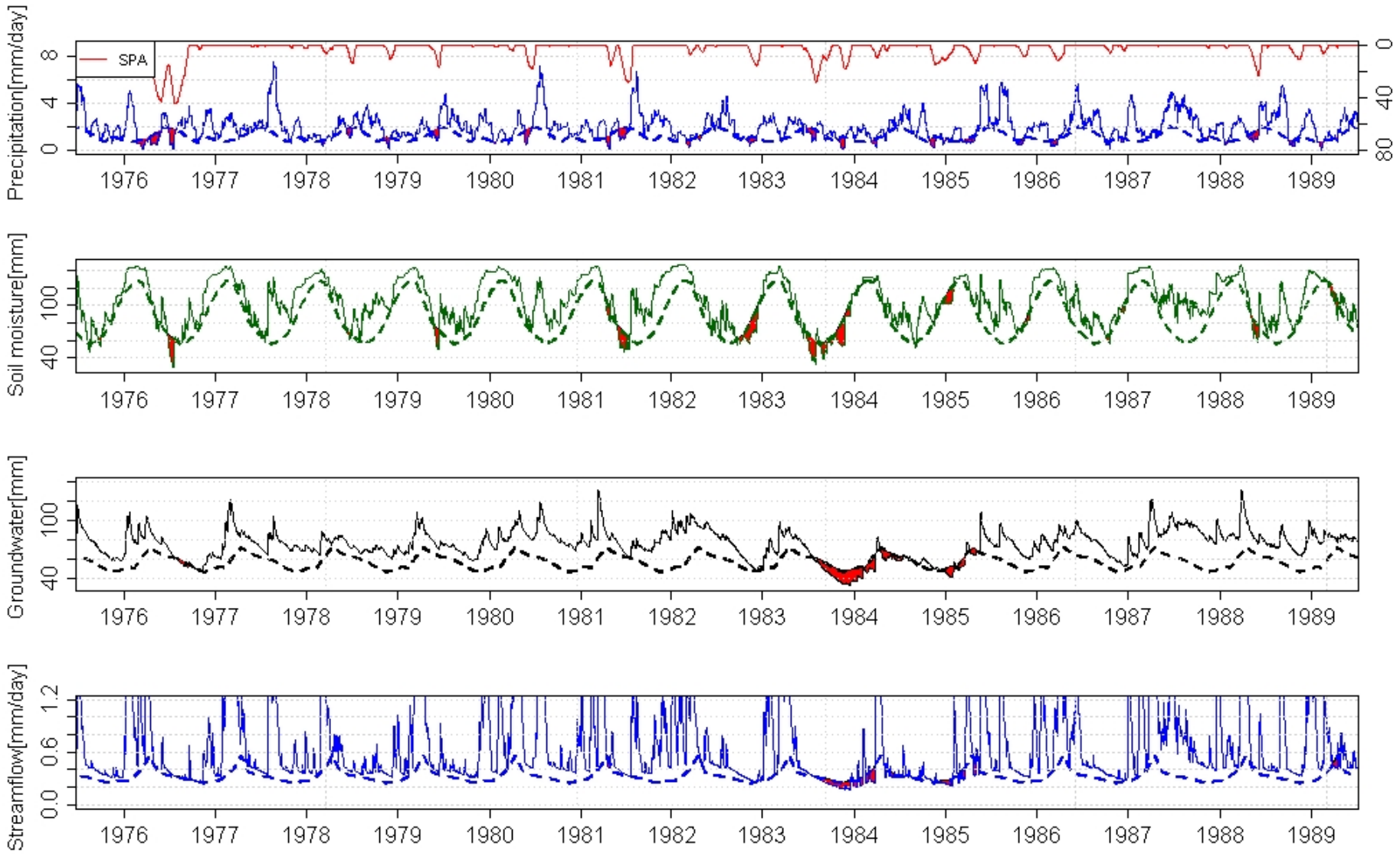

Figure B.20: Drought propagation in 1976--1989 for the Upper Sázava catchment.

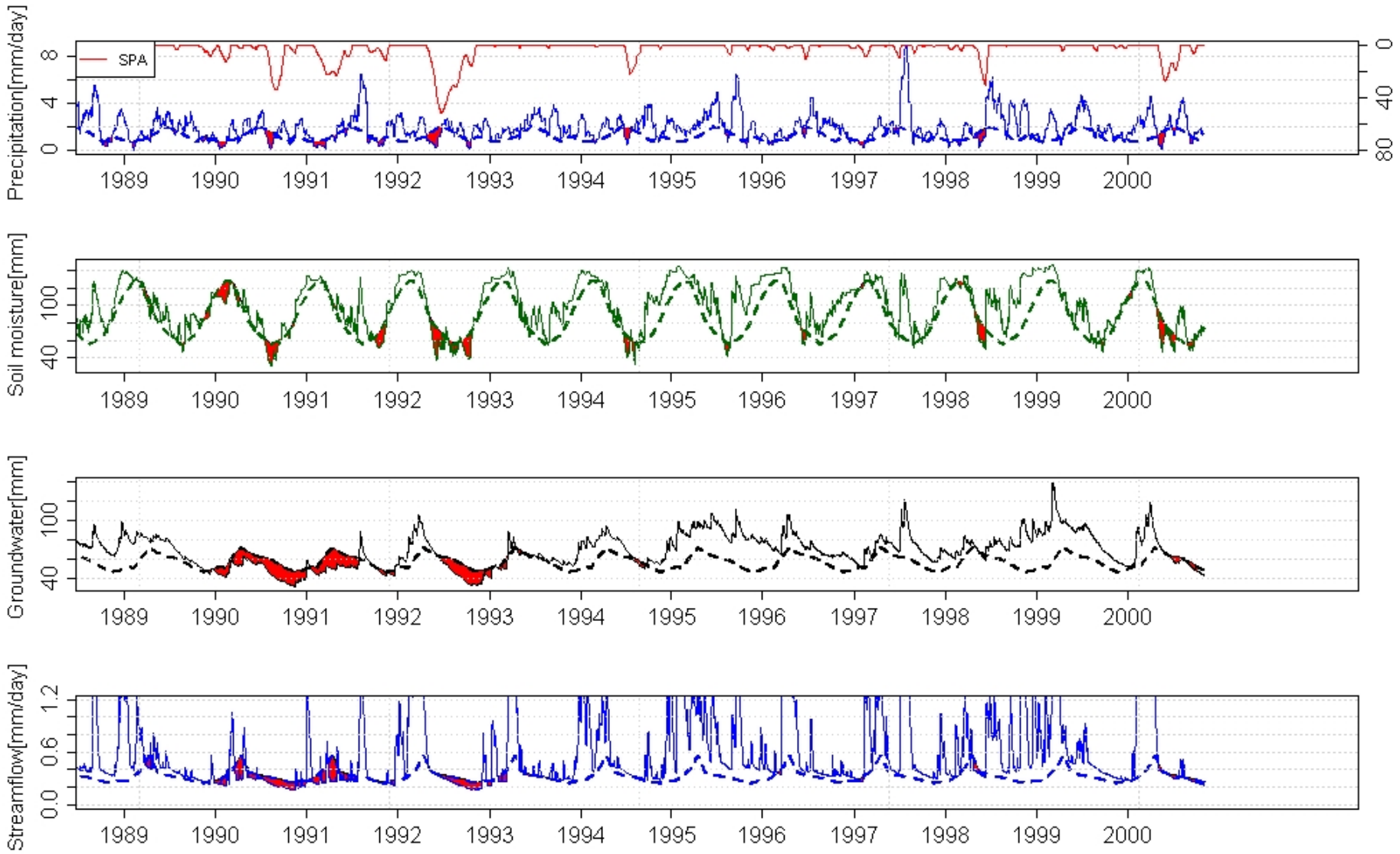

Figure B.21: Drought propagation in 1989--2000 for the Upper Sázava catchment.

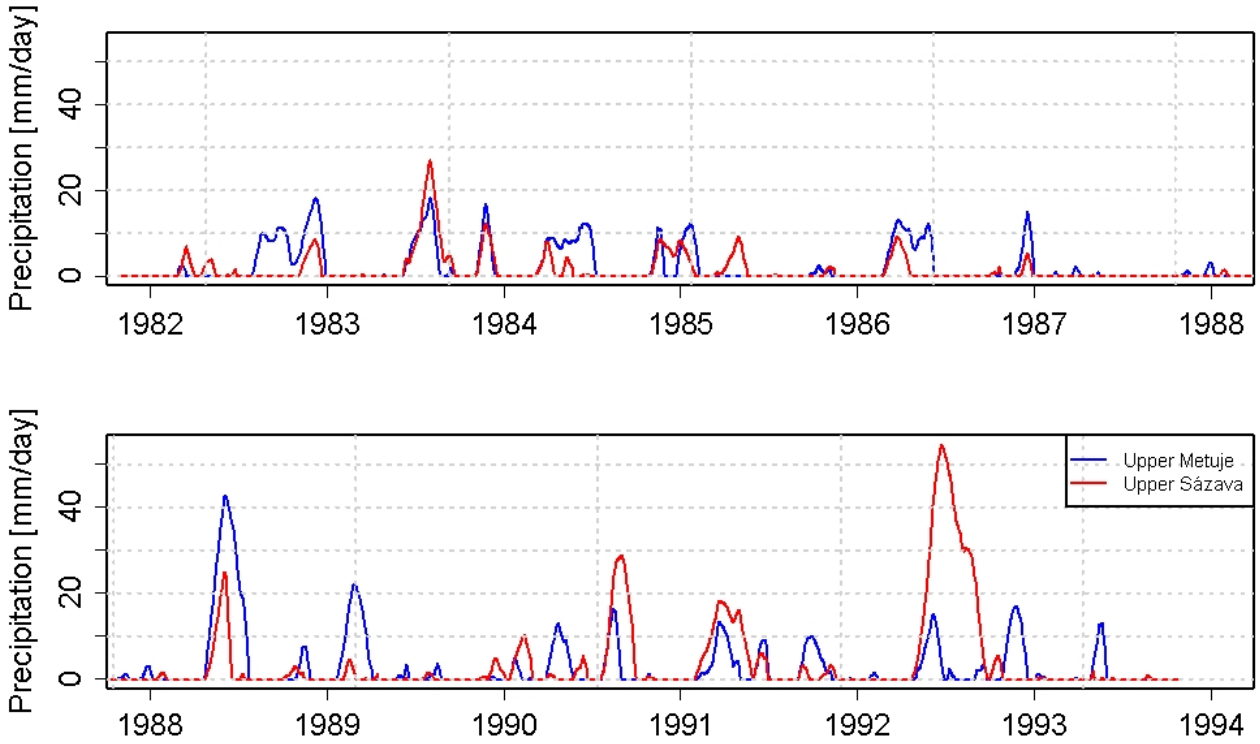

Figure B.22: Precipitation drought based upon the sequent peak algorithm for the Upper Metuje and Upper Sázava catchments, (1982--1993).